SANDIA REPORT
SAND2007-2513
Unlimited Release
Printed April 2007

Model for Resonant Plasma Probe

Larry K. Warne, William A. Johnson, Rebecca S. Coats, Roy E. Jorgenson,
and Gregory A. Hebner

Prepared by
Sandia National Laboratories
Albuquerque, New Mexico 87185 and Livermore, California 94550

Sandia is a multiprogram laboratory operated by Sandia Corporation,
a Lockheed Martin Company, for the United States Department of Energy's
National Nuclear Security Administration under Contract DE-AC04-94AL85000.

Issued by Sandia National Laboratories, operated for the United States Department of Energy by Sandia Corporation.

Available to DOE and DOE contractors from
U.S. Department of Energy
Office of Scientific and Technical Information
P.O. Box 62
Oak Ridge, TN 37831

Telephone: (865) 576-8401
Facsimile: (865) 576-5728
E-Mail: reports@adonis.osti.gov
Online ordering: http://www.osti.gov/bridge

Available to the public from
U.S. Department of Commerce
National Technical Information Service
5285 Port Royal Rd.
Springfield, VA 22161

Telephone: (800) 553-6847
Facsimile: (703) 605-6900
E-Mail: orders@ntis.fedworld.gov
Online order: http://www.ntis.gov/help/ordermethods.asp?loc=7-4-0#online

SAND2007-2513
Unlimited Release
Printed April 2007

Model for Resonant Plasma Probe

Larry K. Warne, William A. Johnson, Rebecca S. Coats, Roy E. Jorgenson
Electromagnetics and Plasma Physics Analysis Dept.

Gregory A. Hebner
Laser, Optics, and Remote Sensing Dept.

Sandia National Laboratories
P. O. Box 5800
Albuquerque, NM 87185-1152

Abstract

This report constructs simple circuit models for a hairpin shaped resonant plasma probe. Effects of the plasma sheath region surrounding the wires making up the probe are determined. Electromagnetic simulations of the probe are compared to the circuit model results. The perturbing effects of the disc cavity in which the probe operates are also found.

Intentionally Left Blank

Contents

Figures

Model for Resonant Plasma Probe

1 INTRODUCTION

A model is constructed for the quarter wave resonator probe shown in Figure 1.

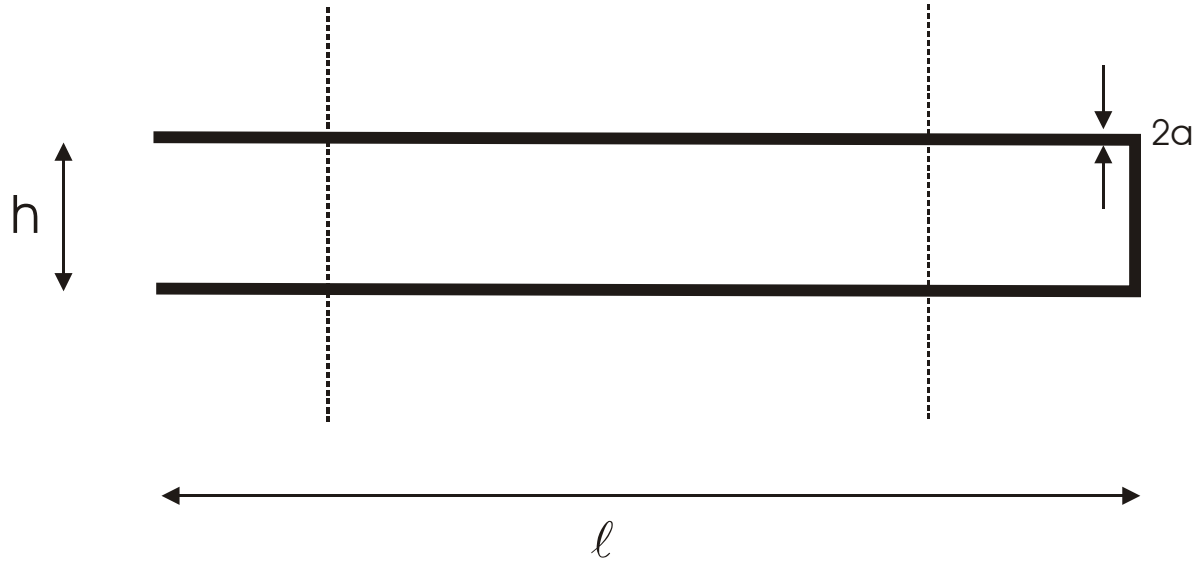

Figure 1. Geometry of quarter wave probe resonator.

2 TRANSMISSION LINE MODEL

A one dimensional transmission line model is used [1]. The transverse dimension is modeled in terms of cross sectional per unit length circuit parameters. The transmission line equations for time dependence $e^{-i\omega t}$ are

$$\frac{dV}{dz} = -ZI$$

$$Z = Z_w - i\omega L$$

$$\frac{dI}{dz} = -YV$$

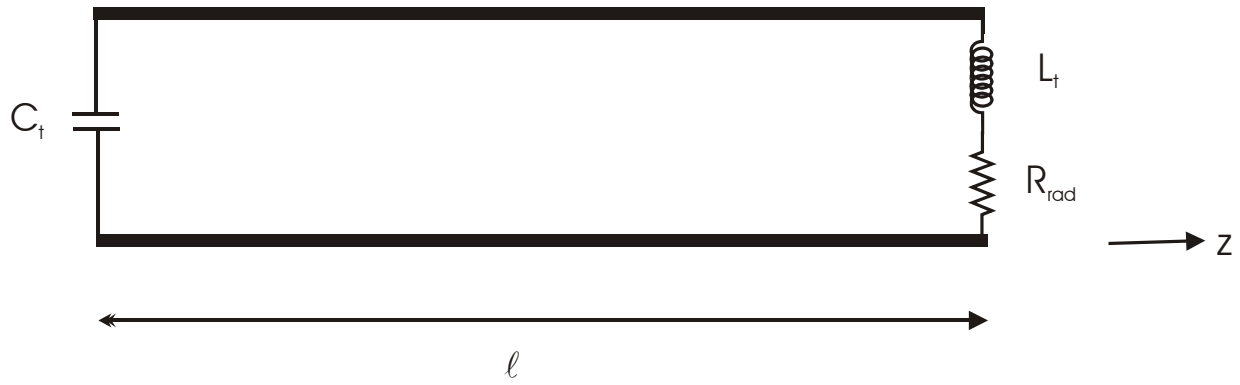

Figure 2. Transmission line circuit model for resonant probe.

$$Y = G - i\omega C$$

The transmission line parameters L and C for a two wire line can be found in the literature [1] and are given in the two sections below on the termination inductance and capacitance. The impedance per unit length of the two wires at high frequencies is

$$Z_w \sim Z_s / (\pi a)$$

$$Z_s = (1 - i) R_s$$

$$R_s = 1 / (\sigma \delta)$$

$$\delta = \sqrt{2 / (\omega \mu \sigma)}$$

The conductance per unit length of the dielectric medium (the plasma) can be found by inserting the complex permittivity

$$\varepsilon = \varepsilon' + i\varepsilon''$$

associated with the plasma collision frequency into C.

2.1 Loads

The load circuit model we have in mind is shown in Figure 2. The end load conditions are

$$I(0) = -Y_t V(0) = Y_t \frac{1}{Y} \frac{dI}{dz}(0)$$

$$Y_t = G_t - i\omega C_t$$

$$Z_t I(\ell) = V(\ell) = -\frac{1}{Y} \frac{dI}{dz}(\ell)$$

$$Z_t = Z_w h - i\omega L_t$$

The load parameters L_t and C_t represent the inductance of the "short" and the capacitance of the "open" terminations. The internal impedance $Z_w h$ accounts for the penetration of the wire at the "shorted" end. The load conductance G_t can be found by inserting the complex permittivity associated with the plasma collision frequency into C_t.

2.2 Transmission Line Solution

Elimination of the voltage in the transmission line equations gives

$$\left(\frac{d^2}{dz^2} + \gamma^2\right) I = 0$$

where the propagation constant is

$$\gamma = \sqrt{-ZY} \approx k\left(1 + \frac{i}{2}\frac{Z_w}{\omega L}\right)\left(1 + \frac{i}{2}\frac{G}{\omega C}\right)$$

and the wave number is taken as

$$k = \omega\sqrt{LC} = \omega\sqrt{\mu_0 \varepsilon'}$$

The general solution is

$$I(z) = I(0)\cos(\gamma z) + \frac{1}{\gamma}\frac{dI}{dz}(0)\sin(\gamma z)$$

The condition at the "open" end (assuming the same complex permittivity, which accounts for the loss parameters G and G_t, is used in the region surrounding the transmission line and at the "open" end) is

$$\frac{dI}{dz}(0) = \frac{Y}{Y_t} I(0) = \frac{C}{C_t} I(0)$$

and thus the current can be written as

$$I(z)/I(0) = \cos(\gamma z) + \frac{1}{\gamma}(C/C_t)\sin(\gamma z)$$

The condition at the "shorted" end

$$\frac{dI}{dz}(\ell) = -YZ_t I(\ell) = -YZ\frac{Z_t}{Z} I(\ell) = \gamma^2 \frac{Z_t}{Z} I(\ell) \approx \gamma^2 \frac{L_t}{L}\left(1 + i\frac{Z_w h}{\omega L_t} - i\frac{Z_w}{\omega L}\right) I(\ell)$$

gives

$$\frac{\cos(\gamma\ell) - \gamma(C_t/C)\sin(\gamma\ell)}{\sin(\gamma\ell) + \gamma(C_t/C)\cos(\gamma\ell)} = \gamma(Z_t/Z)$$

This is the equation for the resonant frequency.

2.3 Plasma Parameters

The dielectric parameters are given in terms of plasma frequency and collision frequency. The complex permittivity of a simple plasma is [2]

$$\varepsilon = \varepsilon_0 \left[1 - \frac{\omega_p^2/\omega^2}{1 + i\omega_{eff}/\omega} \right]$$

or in terms of the complex components

$$\varepsilon' = \varepsilon_0 \left(1 - \frac{\omega_p^2}{\omega^2 + \omega_{eff}^2} \right)$$

$$\varepsilon'' = \varepsilon_0 \left(\frac{\omega_p^2 \omega_{eff}/\omega}{\omega^2 + \omega_{eff}^2} \right)$$

where the plasma frequency is

$$\omega_p^2 = \frac{ne^2}{m\varepsilon_0}$$

and the effective collision frequency is ω_{eff}. The electron density is n, e is the electron charge, and m is the electron mass.

3 INDUCTIVE TERMINATION

The procedure is to use a formula for the static inductance of a rectangular loop. One half this value is differenced by subtraction of the inductance per unit length of a two wire transmission line times the length. This difference forms the estimate for the terminating inductance of the "shorted" end of the resonator. Using Grover [3] for the inductance of a rectangular loop of perfectly conducting wire with small radius a and dimensions 2ℓ and h

$$L_{loop} =$$

$$\frac{\mu_0}{\pi} \left[h \ln(2h/a) + 2\ell \ln(4\ell/a) + 2\sqrt{h^2 + 4\ell^2} - h\text{Arcsinh}\left(\frac{h}{2\ell}\right) - 2\ell\text{Arcsinh}(2\ell/h) - 2(h + 2\ell) \right] , \; 2\ell, h >> a$$

We approximate with $2\ell >> h$

$$L_{loop} \sim \frac{\mu_0}{\pi} \left[h \ln(2h/a) + 2\ell \ln(h/a) - 2h \right] , \; 2\ell >> h$$

Taking one half this inductance for the static resonator geometry and subtracting the transmission line inductance per unit length

$$L = \frac{\mu_0}{\pi} \text{Arccosh}\left(\frac{h}{2a}\right) \sim \frac{\mu_0}{\pi} \ln(h/a) , \; h >> 2a$$

times ℓ

$$L_t = \frac{1}{2}L_{loop} - \ell L \sim h\frac{\mu_0}{2\pi}\left[\ln\left(2h/a\right) - 2\right]$$

4 CAPACITIVE TERMINATION

The procedure is to estimate the static capacitance of a long or semi-infinite two wire line charged to a potential difference. The iterative procedure is a static version of that used to solve the problem of a thin cylindrical antenna [4]. The two conductor capacitance per unit length, times the length, is subtracted to yield the terminating capacitance of the "open" end of the resonator. The potential is (we use the thin wire kernel here)

$$\phi = \frac{1}{4\pi\varepsilon}\int_0^\ell \left[\frac{1}{\sqrt{\rho_+^2 + \left(z-z'\right)^2}} - \frac{1}{\sqrt{\rho_-^2 + \left(z-z'\right)^2}}\right] q\left(z'\right) dz'$$

where

$$\rho_\pm = \sqrt{\left(x \mp h/2\right)^2 + y^2}$$

The integral equation for the charge density is then found by setting $\phi = \pm V/2$ on the wire surface. We let $\ell \to \infty$

$$2\pi\varepsilon V = \int_0^\infty \left[\frac{1}{\sqrt{a^2 + \left(z-z'\right)^2}} - \frac{1}{\sqrt{h^2 + \left(z-z'\right)^2}}\right] q\left(z'\right) dz'$$

Now to develop an approximate solution we first write

$$2\pi\varepsilon V = q\left(z\right)\int_0^\infty \left[\frac{1}{\sqrt{a^2 + \left(z-z'\right)^2}} - \frac{1}{\sqrt{h^2 + \left(z-z'\right)^2}}\right] dz'$$

$$+ \int_0^\infty \left[\frac{1}{\sqrt{a^2 + \left(z-z'\right)^2}} - \frac{1}{\sqrt{h^2 + \left(z-z'\right)^2}}\right] \left[q\left(z'\right) - q\left(z\right)\right] dz'$$

Using

$$\int_0^\ell \frac{dz'}{\sqrt{a^2 + \left(z-z'\right)^2}} = \text{Arcsinh}\left(\frac{\ell - z}{a}\right) + \text{Arcsinh}\left(\frac{z}{a}\right)$$

gives

$$2\pi\varepsilon V = q\left(z\right)\left[\ln\left(h/a\right) - \text{Arcsinh}\left(z/h\right) + \text{Arcsinh}\left(z/a\right)\right]$$

$$+\int_0^\infty \left[\frac{1}{\sqrt{a^2+(z-z')^2}}-\frac{1}{\sqrt{h^2+(z-z')^2}}\right][q(z')-q(z)]\,dz'$$

For small a we can write this as

$$2\pi\varepsilon V \sim \Omega q(z) - q(z)\left[\ln\left(z/h+\sqrt{z^2/h^2+1}\right)-\ln(2z/h)\right]$$

$$+\int_0^\infty \left[\frac{1}{|z-z'|}-\frac{1}{\sqrt{h^2+(z-z')^2}}\right][q(z')-q(z)]\,dz'$$

where we define

$$\Omega = 2\ln(h/a)$$

An iterative solution is obtained by assuming Ω is large

$$q(z)/V \sim \frac{2\pi\varepsilon}{\Omega}\left[1+\frac{1}{\Omega}\left\{\ln\left(z/h+\sqrt{z^2/h^2+1}\right)-\ln(2z/h)\right\}\right.$$

$$+\frac{1}{\Omega^2}\left\{\ln\left(z/h+\sqrt{z^2/h^2+1}\right)-\ln(2z/h)\right\}^2$$

$$-\frac{1}{\Omega^2}\int_0^\infty\left\{\frac{1}{|z-z'|}-\frac{1}{\sqrt{h^2+(z-z')^2}}\right\}\left\{\ln\left(\frac{z'/h+\sqrt{z'^2/h^2+1}}{z/h+\sqrt{z^2/h^2+1}}\right)-\ln(z'/z)\right\}dz'$$

$$\left.+\cdots\right]$$

The leading term is the transmission line capacitance per unit length

$$q_0/V = C$$

where

$$C=\frac{\pi\varepsilon}{\text{Arccosh}\left(\frac{h}{2a}\right)}\sim\frac{\pi\varepsilon}{\ln(h/a)}\ ,\ h>>2a$$

The next term can be integrated to give the leading terminating capacitance

$$C_t \sim \frac{2\pi\varepsilon}{\Omega^2}\int_0^\infty\left\{\ln\left(z/h+\sqrt{z^2/h^2+1}\right)-\ln(2z/h)\right\}dz$$

$$\sim \frac{2\pi h\varepsilon}{\Omega^2}\int_0^\infty\left\{\ln\left(u+\sqrt{u^2+1}\right)-\ln(2u)\right\}du$$

Letting

$$u+\sqrt{u^2+1}=s$$

$$\frac{1}{2}\left(s-1/s\right)=u$$

$$du=\frac{1}{2}\left(1+1/s^2\right)ds$$

gives

$$C_t\sim\frac{2\pi h\varepsilon}{\Omega^2}\lim_{U\to\infty}\left[\frac{1}{2}\int_1^{U+\sqrt{U^2+1}}\ln\left(s\right)\left(1+1/s^2\right)ds-U\left\{\ln\left(2U\right)-1\right\}\right]$$

Using

$$\int_1^{U+\sqrt{U^2+1}}\ln\left(s\right)\left(1+1/s^2\right)ds=$$

$$\left(U+\sqrt{U^2+1}\right)\left\{\ln\left(U+\sqrt{U^2+1}\right)-1\right\}+1-\left(U+\sqrt{U^2+1}\right)^{-1}\left\{\ln\left(U+\sqrt{U^2+1}\right)+1\right\}+1$$

gives

$$C_t\sim\frac{2\pi h\varepsilon}{\Omega^2}$$

To include the next term we write it as

$$C_t\sim\frac{2\pi h\varepsilon}{\Omega^2}\left(1+C_e/\Omega\right)$$

where

$$hC_e\sim\int_0^\infty\left\{\ln\left(z/h+\sqrt{z^2/h^2+1}\right)-\ln\left(2z/h\right)\right\}^2dz$$

$$-\int_0^\infty\int_0^\infty\left\{\frac{1}{|z-z'|}-\frac{1}{\sqrt{h^2+\left(z-z'\right)^2}}\right\}\left\{\ln\left(\frac{z'/h+\sqrt{z'^2/h^2+1}}{z/h+\sqrt{z^2/h^2+1}}\right)-\ln\left(z'/z\right)\right\}dz'dz$$

or

$$C_e\sim\int_0^\infty\left\{\ln\left(u+\sqrt{u^2+1}\right)-\ln\left(2u\right)\right\}^2du$$

$$-\int_0^\infty\int_0^\infty\left\{\frac{1}{|u-u'|}-\frac{1}{\sqrt{1+\left(u-u'\right)^2}}\right\}\left\{\ln\left(\frac{u'+\sqrt{u'^2+1}}{u+\sqrt{u^2+1}}\right)-\ln\left(u'/u\right)\right\}du'du$$

Carrying the first of these out using integration by parts

$$\int_0^U \left\{\ln\left(u+\sqrt{u^2+1}\right)-\ln(2u)\right\}^2 du = \left\{\ln\left(U+\sqrt{U^2+1}\right)-\ln(2U)\right\}^2 U$$

$$-2\int_0^U \left\{\ln\left(u+\sqrt{u^2+1}\right)-\ln(2u)\right\}\left(\frac{u}{\sqrt{u^2+1}}-1\right) du$$

$$= \left\{\ln\left(U+\sqrt{U^2+1}\right)-\ln(2U)\right\}^2 U$$

$$-2\left\{\ln\left(U+\sqrt{U^2+1}\right)-\ln(2U)\right\}\left(\sqrt{U^2+1}-U-1\right)$$

$$+2\int_0^U \left(\frac{1}{\sqrt{u^2+1}}-\frac{1}{u}\right)\left(\sqrt{u^2+1}-u-1\right) du$$

$$= \left\{\ln\left(U+\sqrt{U^2+1}\right)-\ln(2U)\right\}^2 U$$

$$-2\left\{\ln\left(U+\sqrt{U^2+1}\right)-\ln(2U)\right\}\left(\sqrt{U^2+1}-U-1\right)$$

$$+2\int_0^U \left\{2-\frac{2u}{\sqrt{u^2+1}}-\frac{1}{\sqrt{u^2+1}}-\frac{1}{u\sqrt{u^2+1}}+\frac{1}{u}\right\} du$$

$$= \left\{\ln\left(U+\sqrt{U^2+1}\right)-\ln(2U)\right\}^2 U$$

$$-2\left\{\ln\left(U+\sqrt{U^2+1}\right)-\ln(2U)\right\}\left(\sqrt{U^2+1}-U-1\right)$$

$$+2\left\{2U-2\sqrt{U^2+1}-\operatorname{Arcsinh}(U)+\ln\left(1+\sqrt{U^2+1}\right)+2-\ln 2\right\}$$

In the limit $U \to \infty$

$$\int_0^\infty \left\{\ln\left(u+\sqrt{u^2+1}\right)-\ln(2u)\right\}^2 du = 4(1-\ln 2)$$

Using the symmetry

$$\int_0^\infty \int_0^\infty \left\{\frac{1}{\sqrt{\nu^2+(u-u')^2}}-\frac{1}{\sqrt{1+(u-u')^2}}\right\}\left\{\ln\left(u'+\sqrt{u'^2+1}\right)-\ln(2u')\right\} du'du$$

$$= \int_0^\infty \int_0^\infty \left\{\frac{1}{\sqrt{\nu^2+(u-u')^2}}-\frac{1}{\sqrt{1+(u-u')^2}}\right\}\left\{\ln\left(u+\sqrt{u^2+1}\right)-\ln(2u)\right\} du'du$$

and noting that

$$\int_0^U \left\{ \frac{1}{\sqrt{\nu^2 + (u-u')^2}} - \frac{1}{\sqrt{1 + (u-u')^2}} \right\} du'$$

$$= \text{Arcsinh}\left(\frac{U-u}{\nu}\right) + \text{Arcsinh}\left(\frac{u}{\nu}\right) - \text{Arcsinh}\,(U-u) + \text{Arcsinh}\,(u)$$

$$\int_0^\infty \left\{ \frac{1}{\sqrt{\nu^2 + (u-u')^2}} - \frac{1}{\sqrt{1 + (u-u')^2}} \right\} du' = -\ln\nu + \text{Arcsinh}\left(\frac{u}{\nu}\right) + \text{Arcsinh}\,(u)$$

$$\sim 2\ln(2u/\nu)\ ,\ u \to \infty$$

we see that the integrals are convergent. The difference of the two sides shows that the second integral vanishes. Note that the limit $\nu \to 0$, after the difference of the two sides is taken, produces the required absolute value. Thus

$$C_e = 4\,(1 - \ln 2)$$

and finally

$$C_t \sim hC\frac{1}{\Omega}\left[1 + 4\,(1-\ln 2)\,/\Omega\right]$$

$$C \sim 2\pi\varepsilon/\Omega$$

$$\Omega = 2\ln(h/a)$$

A numerical calculation with $\ell = 5$ cm, $h = 3$ mm, $a = 0.3$ mm gives $C_t = \varepsilon\,(1.10\text{ mm})$ whereas the formula gives $C_t = \varepsilon\,(1.1257\text{ mm})$. This is an error of only 2.3%.

5 RESONANT FREQUENCY

Now we assume that

$$C_t/C << \ell$$

$$\gamma C_t/C << 1$$

and take

$$\ell_t = \ell + C_t/C$$

The resonant condition then can approximately be written as

$$\cot(\gamma\ell_t) \approx \gamma(Z_t/Z) \approx \gamma\frac{L_t}{L}\left[1 + i\frac{Z_w}{\omega L}\left(\frac{hL}{L_t} - 1\right)\right]$$

The preceding termination parameters are

$$L_t/L = \frac{h}{2}\left[1 - \frac{2}{\Omega}(2 - \ln 2)\right]$$

$$L = \frac{\mu_0}{2\pi}\Omega$$

$$C_t/C = \frac{h}{\Omega}\left[1 + \frac{4}{\Omega}(1 - \ln 2)\right]$$

$$C = 2\pi\varepsilon/\Omega$$

$$\Omega = 2\ln(h/a)$$

For the moment we ignore the loss terms $\gamma \to k$ and find

$$\cot(k\ell_t) \approx k\frac{L_t}{L} \approx k\frac{h}{2}\left[1 - \frac{2}{\Omega}(2 - \ln 2)\right]$$

$$\ell_t = \ell + \frac{h}{\Omega}\left[1 + \frac{4}{\Omega}(1 - \ln 2)\right]$$

If we take $a = 0.125$ mm, $h = 3$ mm, and $\ell = 25$ mm we find

$$\ell_t = 25.56 \text{ mm}$$

$$\cot(k\ell_t) \approx kL_t/L \approx k\,(0.88 \text{ mm})$$

$$k = k_0 - \Delta k$$

$$k_0\ell_t = \pi/2$$

$$\cot(k\ell_t) \approx \Delta k\ell_t \approx (k_0 - \Delta k)\,L_t/L$$

$$\Delta k\,(\ell_t + 0.88 \text{ mm}) \approx k_0\,(0.88 \text{ mm}) = \frac{\pi}{2}\,(0.88 \text{ mm})\,/\ell_t$$

$$\Delta k \approx \frac{k_0 L_t/L}{\ell_t + L_t/L}$$

$$k_r \approx \frac{k_0 \ell_t}{\ell_t + L_t/L} \approx \frac{\pi/2}{\ell + C_t/C + L_t/L}$$

Thus the effect of both loads is a simple lengthening of the structure.

$$f = 2.8346 \text{ GHz}$$

Without loads

$$k\ell = \pi/2$$

$$f = 2.9979 \text{ GHz}$$

equal to a 5.4% downshift in frequency. Note that L_t alone would give 2.89237 GHz and C_t alone would give 2.9322 GHz. Now we need to add the loss terms and the shift due to the plasma.

6 RADIATION LOSSES

The radiation losses are estimated by first finding the magnetic vector potential from the current distribution [5]

$$\underline{A}\left(\underline{r}\right) = \mu_0 \int_V \underline{J}\left(\underline{r}'\right) \frac{e^{ik\left|\underline{r}-\underline{r}'\right|}}{4\pi\left|\underline{r}-\underline{r}'\right|} dV'$$

Here we neglect the small loss part of the plasma permittivity and take

$$k = \omega\sqrt{\mu_0 \varepsilon'}$$

We note that collision losses are included in the transmission line admittance per unit length (as well as the "open" terminating admittance) in ε''. If the imaginary part of the permittivity becomes sizable compared to the real part we would expect the collisional losses to dominate over the radiation. On the other hand, if collisional losses and radiation losses are both small perturbational effects, we would expect that the two loss contributions can be added separately.

Thus there are two components of the vector potential

$$A_z\left(x,y,z\right) = \frac{\mu_0}{4\pi}\int_0^\ell I\left(z'\right)\left[\frac{e^{ik\sqrt{(x-h/2)^2+y^2+(z-z')^2}}}{\sqrt{\left(x-h/2\right)^2+y^2+\left(z-z'\right)^2}} - \frac{e^{ik\sqrt{(x+h/2)^2+y^2+(z-z')^2}}}{\sqrt{\left(x+h/2\right)^2+y^2+\left(z-z'\right)^2}}\right] dz'$$

$$A_x\left(x,y,z\right) = -\frac{\mu_0}{4\pi} I\left(\ell\right)\int_{-h/2}^{h/2} \frac{e^{ik\sqrt{(x-x')^2+y^2+(z-\ell)^2}}}{\sqrt{\left(x-x'\right)^2+y^2+\left(z-\ell\right)^2}} dx'$$

where we have approximated the "shorted" end as having constant current and taken the load current $I\left(\ell\right)$ to be directed toward the $-x$ direction. Now we will approximate the current distribution along the transmission line to be the quarter wave form

$$I(z)/I(0) = \cos(\gamma z) + \frac{1}{\gamma}(C/C_t)\sin(\gamma z)$$

$$I(z)/I(\ell) = \left[\cos(k_0 z) + \frac{1}{k_0}(C/C_t)\sin(k_0 z)\right] I(0)/I(\ell)$$

$$I(z') \approx I(\ell)\sin(k_0 z') = I(\ell)\sin\left(\frac{\pi z'}{2\ell}\right)$$

We are interested in the far zone field. Thus we approximate the potentials as

$$A_z \sim \frac{\mu_0}{4\pi r} I(\ell)\int_0^\ell \sin(k_0 z')\left[e^{ik\left(r-(h/2)\sin\theta\cos\varphi - z'\cos\theta\right)} - e^{ik\left(r+(h/2)\sin\theta\cos\varphi - z'\cos\theta\right)}\right] dz'$$

$$\sim -i\frac{\mu_0 e^{ikr}}{2\pi r} I(\ell)\sin\{k(h/2)\sin\theta\cos\varphi\}\int_0^\ell \sin(k_0 z')\, e^{-ikz'\cos\theta} dz'$$

$$\sim -\frac{\mu_0 e^{ikr}}{4\pi r} I(\ell)\sin\{k(h/2)\sin\theta\cos\varphi\}\int_0^\ell \left[e^{i(k_0 - k\cos\theta)z'} - e^{-i(k_0+k\cos\theta)z'}\right] dz'$$

$$\sim i\frac{\mu_0 e^{ikr}}{4\pi r} I(\ell)\sin\{k(h/2)\sin\theta\cos\varphi\}\left[\frac{e^{i(k_0-k\cos\theta)\ell}-1}{(k_0-k\cos\theta)} + \frac{e^{-i(k_0+k\cos\theta)\ell}-1}{(k_0+k\cos\theta)}\right]$$

Now taking $k_0 \to k$ and subsequently $k \to \pi/(2\ell)$ *(if the plasma sheath is large enough to substantially change the propagation constant along the transmission line, then we need to carry this radiation integral out without this further approximation, which can be done in terms of sine and cosine integrals)*

$$A_z \sim i\frac{\mu_0 e^{ikr}}{4\pi r} I(\ell)(h/2)\sin\theta\cos\varphi\left[\frac{e^{ik\ell(1-\cos\theta)}-1}{(1-\cos\theta)} + \frac{e^{-ik\ell(1+\cos\theta)}-1}{(1+\cos\theta)}\right]$$

Similarly

$$A_x \sim -\frac{\mu_0}{4\pi r} I(\ell)\int_{-h/2}^{h/2} e^{ik\left(r - x'\sin\theta\cos\varphi - \ell\cos\theta\right)} dx'$$

$$\sim -\frac{\mu_0 e^{ik(r-\ell\cos\theta)}}{4\pi r} I(\ell)\int_{-h/2}^{h/2} e^{-ikx'\sin\theta\cos\varphi} dx'$$

$$\sim -\frac{\mu_0 e^{ik(r-\ell\cos\theta)}}{2\pi r} I(\ell)\frac{\sin\{k(h/2)\sin\theta\cos\varphi\}}{k\sin\theta\cos\varphi} \sim -\frac{\mu_0 e^{ik(r-\ell\cos\theta)}}{2\pi r} I(\ell)\frac{h}{2}$$

where we have assumed that $kh/2 << 1$ and the final form is that associated with a small dipole. The far zone fields are found from

$$\underline{H} = \frac{1}{\mu_0}\nabla\times\underline{A} \sim i\frac{k}{\mu_0}\underline{e}_r\times\underline{A}$$

$$\underline{E} = \frac{i}{\omega\varepsilon}\nabla\times\underline{H} \sim -\frac{k}{\omega\varepsilon}\underline{e}_r\times\underline{H} \sim -i\omega\underline{e}_r\times\underline{e}_r\times\underline{A} = i\omega\underline{A}_t$$

where $\underline{A}_t$ denotes transverse components. The Poynting vector is

$$\underline{S} = \frac{1}{2}\underline{E} \times \underline{H}^*$$

and in the far zone

$$S_r \sim \frac{1}{2\mu_0}\omega k \underline{e}_r \cdot [\underline{A}_t \times (\underline{e}_r \times \underline{A}_t^*)] = \frac{1}{2\mu_0}\omega k \left|\underline{A}_t\right|^2 = \frac{1}{2\mu_0}\omega k \left(|A_\theta|^2 + |A_\varphi|^2\right)$$

Using the unit vector relations

$$\underline{e}_x = \underline{e}_r \sin\theta\cos\varphi + \underline{e}_\theta \cos\theta\cos\varphi - \underline{e}_\varphi \sin\varphi$$

$$\underline{e}_z = \underline{e}_r \cos\theta - \underline{e}_\theta \sin\theta$$

the spherical form of the potential (ignoring A_r) is

$$A_\theta \sim A_x \cos\theta\cos\varphi - A_z \sin\theta$$

$$\sim -\frac{\mu_0 e^{ik(r-\ell\cos\theta)}}{2\pi r} I(\ell)\frac{h}{2}\cos\theta\cos\varphi - i\frac{\mu_0 e^{ikr}}{4\pi r} I(\ell)(h/2)\sin^2\theta\cos\varphi\left\{\frac{e^{ik\ell(1-\cos\theta)}-1}{(1-\cos\theta)} + \frac{e^{-ik\ell(1+\cos\theta)}-1}{(1+\cos\theta)}\right\}$$

$$\sim -\frac{\mu_0 e^{ik(r-\ell\cos\theta)}}{2\pi r} I(\ell)\frac{h}{2}\cos\theta\cos\varphi$$

$$-i\frac{\mu_0 e^{ikr}}{4\pi r} I(\ell)(h/2)\cos\varphi\left\{e^{ik\ell(1-\cos\theta)}(1+\cos\theta) + e^{-ik\ell(1+\cos\theta)}(1-\cos\theta) - 2\right\}$$

$$\sim -\frac{\mu_0 e^{ik(r-\ell\cos\theta)}}{2\pi r} I(\ell)\frac{h}{2}\cos\theta\cos\varphi - i\frac{\mu_0 e^{ik(r-\ell\cos\theta)}}{2\pi r} I(\ell)(h/2)\cos\varphi\left\{\cos(k\ell) + i\sin(k\ell)\cos\theta - e^{ik\ell\cos\theta}\right\}$$

$$\sim \frac{e^{ik(r-\ell\cos\theta)}}{2\pi r}(h/2)\mu_0 I(\ell)\left[(-1+\sin(k\ell))\cos\theta - i\cos(k\ell) + ie^{ik\ell\cos\theta}\right]\cos\varphi$$

$$A_\varphi \sim -A_x \sin\varphi \sim \frac{\mu_0 e^{ik(r-\ell\cos\theta)}}{2\pi r} I(\ell)\frac{h}{2}\sin\varphi$$

The power radiated is now found by integrating over the sphere at infinity

$$P = \int_0^{2\pi}\int_0^{\pi} S_r r^2 \sin\theta d\theta d\varphi$$

$$= \frac{1}{2\mu_0}\omega k \int_0^{2\pi}\int_0^{\pi} |A_\theta|^2 r^2 \sin\theta d\theta d\varphi + \frac{1}{2\mu_0}\omega k \int_0^{2\pi}\int_0^{\pi} |A_\varphi|^2 r^2 \sin\theta d\theta d\varphi$$

$$= \frac{1}{8\pi}\omega\mu_0 k \left|I\left(\ell\right)\right|^2 \left(h/2\right)^2 \int_{-1}^{1} \left|\left(-1+\sin\left(k\ell\right)\right)u - i\cos\left(k\ell\right) + ie^{ik\ell u}\right|^2 du$$

$$+\frac{1}{8\pi}\omega\mu_0 k \left|I\left(\ell\right)\right|^2 \left(h/2\right)^2 \int_{-1}^{1} du$$

$$= \frac{1}{8\pi}\omega\mu_0 k \left|I\left(\ell\right)\right|^2 \left(h/2\right)^2$$

$$\int_{-1}^{1} \left[\left(-1+\sin\left(k\ell\right)\right)^2 u^2 - 2\left(-1+\sin\left(k\ell\right)\right)u\sin\left(k\ell u\right) + 1 + \cos^2\left(k\ell\right) - 2\cos\left(k\ell u\right)\cos\left(k\ell\right)\right] du$$

$$+\frac{1}{4\pi}\omega\mu_0 k \left|I\left(\ell\right)\right|^2 \left(h/2\right)^2$$

$$= \frac{1}{4\pi}\omega\mu_0 k \left|I\left(\ell\right)\right|^2 \left(h/2\right)^2$$

$$\left[1 + \frac{1}{3}\left(-1+\sin\left(k\ell\right)\right)^2 - 2\left(-1+\sin\left(k\ell\right)\right)\left\{-\frac{1}{k\ell}\cos\left(k\ell\right) + \frac{1}{k^2\ell^2}\sin\left(k\ell\right)\right\} + 1 + \cos^2\left(k\ell\right) - \frac{2}{k\ell}\sin\left(k\ell\right)\cos\left(k\ell\right)\right]$$

Letting $k\ell = \pi/2 - v$

$$P = \frac{1}{4\pi}\omega\mu_0 k \left|I\left(\ell\right)\right|^2 \left(h/2\right)^2$$

$$\left[\frac{1}{3}4\sin^4\left(v/2\right) + 4\sin^2\left(v/2\right)\left\{-\frac{1}{\left(\pi/2-v\right)}\sin v + \frac{1}{\left(\pi/2-v\right)^2}\cos v\right\} + 2 + \sin^2 v - \frac{1}{\left(\pi/2-v\right)}\sin\left(2v\right)\right]$$

$$\sim \frac{1}{2\pi}\omega\mu_0 k \left|I\left(\ell\right)\right|^2 \left(h/2\right)^2 \left(1 - \frac{2}{\pi}v\right) \ , \ v << 1$$

Using the approximation $v = \pi/2 - k\ell << 1$

$$P \sim \frac{1}{2\pi}\omega\mu_0 k \left|I\left(\ell\right)\right|^2 \left(h/2\right)^2 \frac{2}{\pi}k\ell$$

This is then used to find the quality factor or can be included in the circuit model as a lossy element. For example, we could set

$$P = \frac{1}{2}R_{rad}\left|I\left(\ell\right)\right|^2$$

to obtain

$$R_{rad} \sim \frac{1}{\pi}\sqrt{\mu_0/\varepsilon'}\left(kh/2\right)^2 \frac{2}{\pi}k\ell$$

This can be inserted as a perturbing series element at $z = \ell$ to account for radiation.

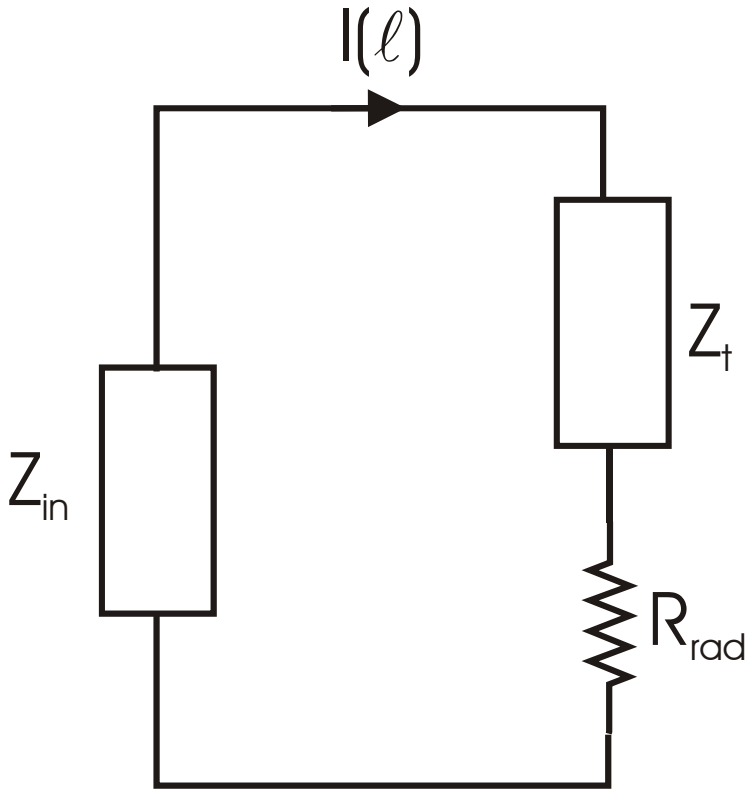

Figure 3. Lumped circuit model at "shorted" termination.

7 CIRCUIT MODEL

It is convenient to derive the circuit model at the "shorted" end of the resonator, as shown in Figure 3. The capacitance C_t at the end $z = 0$ can be transformed to the position $z = \ell$ by means of the distributions

$$I(z) = I(0)\left[\cos(\gamma z) + \frac{1}{\gamma}(Y/Y_t)\sin(\gamma z)\right]$$

$$V(z) = -\frac{1}{Y}\frac{dI}{dz} = I(0)\frac{1}{Y}\left[\gamma\sin(\gamma z) - (Y/Y_t)\cos(\gamma z)\right]$$

$$\gamma = \sqrt{-ZY}$$

to give the input impedance element

$$Z_{in} = -V(\ell)/I(\ell) = \frac{\gamma}{Y}\frac{\cos(\gamma\ell) - \gamma(Y_t/Y)\sin(\gamma\ell)}{\sin(\gamma\ell) + \gamma(Y_t/Y)\cos(\gamma\ell)} = -\frac{Z}{\gamma}\frac{\cos(\gamma\ell) - \gamma(Y_t/Y)\sin(\gamma\ell)}{\sin(\gamma\ell) + \gamma(Y_t/Y)\cos(\gamma\ell)}$$

This impedance element is in series with R_{rad} and Z_t. Resonance is achieved when

$$\mathrm{Im}\left[Z_{in}(\omega_r) + Z_t(\omega_r)\right] = 0$$

An approximation to this condition, ignoring losses, was discussed previously. The quality factor can be

found by setting

$$|\mathrm{Im}\left[Z_{in}\left(\omega_r+\Delta\omega_r\right)+Z_t\left(\omega_r+\Delta\omega_r\right)\right]|=\mathrm{Re}\left[Z_{in}\left(\omega_r\right)+Z_t\left(\omega_r\right)+R_{rad}\left(\omega_r\right)\right]$$

where

$$Q=\frac{\omega_r}{2\Delta\omega_r}$$

Using a Taylor approximation

$$|\mathrm{Im}\left[Z_{in}\left(\omega_r+\Delta\omega_r\right)+Z_t\left(\omega_r+\Delta\omega_r\right)\right]|\approx|\mathrm{Im}\left[Z'_{in}\left(\omega_r\right)+Z'_t\left(\omega_r\right)\right]|\,\Delta\omega_r$$

Let us ignore all loss terms on the right side of this equation so that we can write

$$Z_{in}\rightarrow i\frac{k}{\omega C}\frac{\cos\left(k\ell\right)-k\left(C_t/C\right)\sin\left(k\ell\right)}{\sin\left(k\ell\right)+k\left(C_t/C\right)\cos\left(k\ell\right)}\approx i\sqrt{L/C}\cot\left(k\ell_t\right)$$

where

$$\ell_t=\ell+C_t/C$$

$$Z_t\rightarrow-i\omega L_t$$

so that

$$\mathrm{Im}\left[Z'_{in}\left(\omega_r\right)+Z'_t\left(\omega_r\right)\right]\approx\mathrm{Im}\left[i\sqrt{L/C}\frac{d}{d\omega}\cot\left(\omega\sqrt{LC}\ell_t\right)-iL_t\right]_{\omega_r}=-L\ell_t\csc^2\left(\omega_r\sqrt{LC}\ell_t\right)-L_t$$

Using the resonant condition

$$\cot\left(\omega_r\sqrt{LC}\ell_t\right)\approx\omega_r\sqrt{LC}\frac{L_t}{L}$$

this can be written as

$$-\mathrm{Im}\left[Z'_{in}\left(\omega_r\right)+Z'_t\left(\omega_r\right)\right]\approx\left\{1+\left(\frac{\omega_r L_t}{\sqrt{L/C}}\right)^2\right\}L\ell_t+L_t$$

The real parts are (we are ignoring all terms that are quadratic in the loss elements)

$$\gamma=\sqrt{-ZY}\approx k\left(1+\frac{i}{2}\frac{Z_w}{\omega L}\right)\left(1+\frac{i}{2}\frac{G}{\omega C}\right)\approx k\left(1+\frac{i}{2}\frac{R_s}{\pi a\omega L}+\frac{i}{2}\frac{\varepsilon''}{\varepsilon'}\right)$$

$$\cos\left(\gamma\ell\right)\approx\cos\left[\frac{\pi}{2}\left(1+\frac{i}{2}\frac{R_s}{\pi a\omega L}+\frac{i}{2}\frac{\varepsilon''}{\varepsilon'}\right)\right]\approx-i\frac{\pi}{4}\left(\frac{R_s}{\pi a\omega L}+\frac{\varepsilon''}{\varepsilon'}\right)$$

$$\sin\left(\gamma\ell\right)\approx\sin\left[\frac{\pi}{2}\left(1+\frac{i}{2}\frac{R_s}{\pi a\omega L}+\frac{i}{2}\frac{\varepsilon''}{\varepsilon'}\right)\right]\approx1+O\left[\left(\frac{i}{2}\frac{R_s}{\pi a\omega L}+\frac{i}{2}\frac{\varepsilon''}{\varepsilon'}\right)^2\right]$$

$$Y = -i\omega C\left(1 + i\frac{G}{\omega C}\right) = -i\omega C\left(1 + i\frac{\varepsilon''}{\varepsilon'}\right)$$

$$\mathrm{Re}\left[Z_{in}\right] = \mathrm{Re}\left[\frac{\gamma}{Y}\frac{\cos\left(\gamma\ell\right) - \gamma\left(Y_t/Y\right)\sin\left(\gamma\ell\right)}{\sin\left(\gamma\ell\right) + \gamma\left(Y_t/Y\right)\cos\left(\gamma\ell\right)}\right]$$

$$\mathrm{Re}\left[Z_{in}\left(\omega_r\right) + Z_t\left(\omega_r\right) + R_{rad}\left(\omega_r\right)\right] \approx R_s\left(\omega_r\right)\frac{h}{\pi a} + R_{rad}\left(\omega_r\right) +$$

$$\mathrm{Re}\left[i\sqrt{L/C}\left(1 + \frac{i}{2}\frac{R_s}{\pi a\omega L} - \frac{i}{2}\frac{\varepsilon''}{\varepsilon'}\right)\frac{-i\frac{\pi}{4}\left(\frac{R_s}{\pi a\omega L} + \frac{\varepsilon''}{\varepsilon'}\right) - \left(1 + \frac{i}{2}\frac{R_s}{\pi a\omega L} + \frac{i}{2}\frac{\varepsilon''}{\varepsilon'}\right)\left(kC_t/C\right)}{1 - i\left(kC_t/C\right)\frac{\pi}{4}\left(\frac{R_s}{\pi a\omega L} + \frac{\varepsilon''}{\varepsilon'}\right)}\right]_{\omega_r}$$

$$\approx R_s\left(\omega_r\right)\frac{h}{\pi a}\left(1 + \frac{C_t}{hC}\right) + R_{rad}\left(\omega_r\right) +$$

$$\frac{\pi}{4}\left\{1 + \left(k_r C_t/C\right)^2\right\}\left\{\frac{R_s\left(\omega_r\right)}{\pi a k_r} + \frac{\varepsilon''}{\varepsilon'}\sqrt{L/C}\right\}$$

If we ignore terms that are quadratic in $C_t/\left(hC\right)$

$$\mathrm{Re}\left[Z_{in}\left(\omega_r\right) + Z_t\left(\omega_r\right) + R_{rad}\left(\omega_r\right)\right] \approx \frac{\pi}{4}\left\{\frac{R_s\left(\omega_r\right)}{\pi a k_r} + \frac{\varepsilon''}{\varepsilon'}\sqrt{L/C}\right\} + R_s\left(\omega_r\right)\frac{h}{\pi a} + R_{rad}\left(\omega_r\right)$$

The first term in the braces is the wire loss along the transmission line, the second term in braces is the dielectric loss in the plasma along the transmission line, the third term is the wire loss along the "short", and the final term is radiation loss. The frequency shift is then

$$\Delta\omega_r \approx \frac{\frac{\pi}{4}\left\{\frac{R_s(\omega_r)}{\pi a k_r} + \frac{\varepsilon''}{\varepsilon'}\sqrt{L/C}\right\} + R_s\left(\omega_r\right)\frac{h}{\pi a} + R_{rad}\left(\omega_r\right)}{\left\{1 + \left(\omega_r\sqrt{LC}L_t/L\right)^2\right\}L\ell_t + L_t}$$

The resonant frequency is approximately

$$k_r = \omega_r\sqrt{LC} = \omega_r\sqrt{\mu_0\varepsilon'} \approx \frac{\pi/2}{\ell + C_t/C + L_t/L}$$

and the quality factor is

$$Q = \frac{\frac{\pi}{4}\sqrt{L/C}\left[1 + \left(\omega_r\sqrt{LC}L_t/L\right)^2\right]}{\frac{\pi}{4}\left\{\frac{R_s(\omega_r)}{\pi a k_r} + \frac{\varepsilon''}{\varepsilon'}\sqrt{L/C}\right\} + R_s\left(\omega_r\right)\frac{h}{\pi a} + R_{rad}\left(\omega_r\right)}$$

Dropping the small quadratic term in the short inductance finally gives

$$Q = \frac{\frac{\pi}{4}\sqrt{L/C}}{\frac{\pi}{4}\left\{\frac{R_s(\omega_r)}{\pi a k_r} + \frac{\varepsilon''}{\varepsilon'}\sqrt{L/C}\right\} + R_s\left(\omega_r\right)\frac{h}{\pi a} + R_{rad}\left(\omega_r\right)}$$

Note that the transmission line characteristic impedance (without the loss terms) is

$$\sqrt{L/C} \approx \sqrt{\mu_0/\varepsilon'}\frac{1}{\pi}\ln(h/a)$$

The first term of the denominator is the loss along the wires of the transmission line, the second term is the loss resulting from plasma collisions along the transmission line, the third term is the loss along the wire at the short and the final term is the radiation loss.

8 THIN PLASMA SHEATH

Now if there is a thin layer of radius b surrounding the wire, for which the medium is nearly free space, the effect can be included by modifying the capacitance per unit length of the transmission line

$$1/C \approx \frac{\ln(h/b)}{\pi\varepsilon'} + \frac{\ln(b/a)}{\pi\varepsilon_0}$$

where ε_0 is the permittivity of free space. To include the plasma losses we define the admittance per unit length by

$$1/Y \approx \frac{\ln(h/b)}{-i\omega\pi\varepsilon} + \frac{\ln(b/a)}{-i\omega\pi\varepsilon_0}$$

When the excitation frequency is high compared to the plasma and collision frequencies the effect is quite small.

We ignore this sheath at the "shorted" end since the voltage and electric field are small in this region. At the "open" circuit end the electric field is large and we modify the terminating capacitance to

$$C_t \sim C\frac{h}{\Omega'}\left[1 + 4\left(1 - \ln 2\right)/\Omega'\right]$$

$$\Omega' = 2\left[\ln(h/b) + \frac{\varepsilon'}{\varepsilon_0}\ln(b/a)\right]$$

In terms of the admittance

$$Y_t \sim Y\frac{h}{\Omega'}\left[1 + 4\left(1 - \ln 2\right)/\Omega'\right]$$

8.1 Multipole Moment Solution

A check can be easily made regarding the use of the approximate formula

$$1/C \approx \frac{1}{\pi\varepsilon'}\mathrm{Arccosh}\left(\frac{h}{2b}\right) + \frac{\ln(b/a)}{\pi\varepsilon_0} \approx \frac{\ln(h/b)}{\pi\varepsilon'} + \frac{\ln(b/a)}{\pi\varepsilon_0} \tag{1}$$

when the plasma is lossless. A multipole approach was previously used to model a dielectric coated wire above a ground plane [8]. Symmetry can be used to relate the case of a wire above a ground plane to the two wire line problem discussed here. Multipoles are used to represent the potential function with unknowns g_n and $\widehat{g}_n$

$$\phi = -\frac{q}{2\pi\varepsilon'}\ln(\rho) + \sum_{n=1}^{\infty}\frac{(b/\rho)^n g_n}{2\pi\varepsilon'}\cos(n\varphi)$$

$$+\frac{q}{2\pi\varepsilon'}\ln(\rho') - \sum_{n=1}^{\infty}\frac{(-b/\rho')^n g_n}{2\pi\varepsilon'}\cos(n\varphi')\ ,\ \rho > b$$

$$= -\frac{q^{dr}}{2\pi\varepsilon'}\ln(b) + \sum_{n=1}^{\infty}\frac{g_n^{dr}}{2\pi\varepsilon'(b/\rho)^n}\cos(n\varphi) - \frac{\widehat{q}}{2\pi\varepsilon'}\ln(\rho) + \sum_{n=1}^{\infty}\frac{(b/\rho)^n \widehat{g}_n}{2\pi\varepsilon'}\cos(n\varphi)$$

$$+\frac{q}{2\pi\varepsilon'}\ln(\rho') - \sum_{n=1}^{\infty}\frac{(-b/\rho')^n g_n}{2\pi\varepsilon'}\cos(n\varphi')\ ,\ \rho < b$$

where

$$-\pi < \varphi \leq \pi$$

$$\rho' = \sqrt{(x-h)^2 + y^2} = \sqrt{\rho^2 - 2h\rho\cos\varphi + h^2}$$

$$\varphi' = \arctan\left(\frac{y}{x-h}\right) = \arctan\left(\frac{\rho\sin\varphi}{\rho\cos\varphi - h}\right)$$

$$= \left[\pi - \arctan\left(\frac{\rho|\sin\varphi|}{h - \rho\cos\varphi}\right)\right]\operatorname{sgn}(\varphi)$$

where the arctan in the final equation is taken to lie between 0 and $+\pi/2$ (if $\varphi = 0$ or π we take $\varphi' = \pi$)

$$\pi/2 < \varphi' \leq \pi \text{ or } -\pi < \varphi' < -\pi/2$$

Note that the potential on the ground plane is zero. Now setting the voltage equal to $\phi = V$ on $\rho = a < b$ gives

$$V = -\frac{q^{dr}}{2\pi\varepsilon'}\ln(b) + \sum_{n=1}^{\infty}\frac{g_n^{dr}}{2\pi\varepsilon'(b/a)^n}\cos(n\varphi) - \frac{\widehat{q}}{2\pi\varepsilon'}\ln(a) + \sum_{n=1}^{\infty}\frac{(b/a)^n \widehat{g}_n}{2\pi\varepsilon'}\cos(n\varphi) \tag{2}$$

$$+\frac{q}{2\pi\varepsilon'}\ln(\rho') - \sum_{n=1}^{\infty}\frac{(-b/\rho')^n g_n}{2\pi\varepsilon'}\cos(n\varphi')$$

where

$$\rho' = \sqrt{a^2 - 2ha\cos\varphi + h^2}$$

$$\varphi' = \arctan\left(\frac{a\sin\varphi}{a\cos\varphi - h}\right) = \left[\pi - \arctan\left(\frac{a|\sin\varphi|}{h - a\cos\varphi}\right)\right]\operatorname{sgn}(\varphi)$$

Continuity of the potential at $\rho = b$ gives

$$-\frac{q}{2\pi\varepsilon'}\ln(b)+\sum_{n=1}^{\infty}\frac{g_n}{2\pi\varepsilon'}\cos(n\varphi)=-\frac{q^{dr}}{2\pi\varepsilon'}\ln(b)+\sum_{n=1}^{\infty}\frac{g_n^{dr}}{2\pi\varepsilon'}\cos(n\varphi)-\frac{\widehat{q}}{2\pi\varepsilon'}\ln(b)+\sum_{n=1}^{\infty}\frac{\widehat{g}_n}{2\pi\varepsilon'}\cos(n\varphi)$$

Because this must hold over the entire circumference we can equate the summands

$$q=q^{dr}+\widehat{q}$$

$$g_n=g_n^{dr}+\widehat{g}_n$$

Next we equate the normal component of the displacement at $\rho=b$

$$-q-\sum_{n=1}^{\infty}ng_n\cos(n\varphi)$$

$$+q\frac{b}{\rho'}\frac{\partial\rho'}{\partial\rho}+\sum_{n=1}^{\infty}n\left(-b/\rho'\right)^n g_n\left[\frac{b}{\rho'}\frac{\partial\rho'}{\partial\rho}\cos(n\varphi')+b\frac{\partial\varphi'}{\partial\rho}\sin(n\varphi')\right]$$

$$=\sum_{n=1}^{\infty}n\left(\varepsilon_0/\varepsilon'\right)g_n^{dr}\cos(n\varphi)-\left(\varepsilon_0/\varepsilon'\right)\widehat{q}-\sum_{n=1}^{\infty}n\left(\varepsilon_0/\varepsilon'\right)\widehat{g}_n\cos(n\varphi)$$

$$+q\left(\varepsilon_0/\varepsilon'\right)\frac{b}{\rho'}\frac{\partial\rho'}{\partial\rho}+\sum_{n=1}^{\infty}n\left(-b/\rho'\right)^n g_n\left(\varepsilon_0/\varepsilon'\right)\left[\frac{b}{\rho'}\frac{\partial\rho'}{\partial\rho}\cos(n\varphi')+b\frac{\partial\varphi'}{\partial\rho}\sin(n\varphi')\right] \tag{3}$$

where

$$\frac{\partial\rho'}{\partial\rho}=\left(\rho-h\cos\varphi\right)/\sqrt{\rho^2-2h\rho\cos\varphi+h^2}$$

$$\frac{\partial\varphi'}{\partial\rho}=\frac{-h\sin\varphi}{\rho^2-2h\rho\cos\varphi+h^2}$$

and on $\rho=b$

$$\rho'=\sqrt{b^2-2hb\cos\varphi+h^2}$$

$$\varphi'=\arctan\left(\frac{b\sin\varphi}{b\cos\varphi-h}\right)=\left[\pi-\arctan\left(\frac{b\left|\sin\varphi\right|}{h-b\cos\varphi}\right)\right]\operatorname{sgn}(\varphi)$$

$$\frac{\partial\rho'}{\partial\rho}=\left(b-h\cos\varphi\right)/\sqrt{b^2-2hb\cos\varphi+h^2}$$

$$b\frac{\partial\varphi'}{\partial\rho}=\frac{-hb\sin\varphi}{b^2-2hb\cos\varphi+h^2}$$

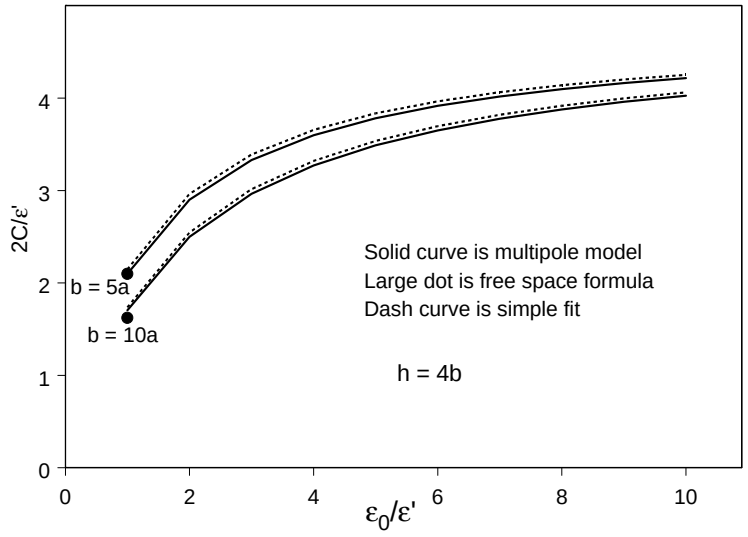

Figure 4. Calculation for proximity effect between cylindrical arms on the capacitance per unit length of the resonator as a function of the normalized permittivity ε' of the plasma. The solid curve includes a series of multipole moments, yielding an exact (two-dimensional) representation for the cylindrical arms, the dashed curve is the simple series combination of the symmetrical homogeneous plasma sheath (free space permittivity) and the exterior plasma dielectric, and the large dot is the free space plasma value. The center-to-center spacing between arms is h, the sheath has radius b, and the perfect conductor has radius a.

$$\frac{b}{\rho'}\frac{\partial \rho'}{\partial \rho} = \frac{b\,(b - h\cos\varphi)}{b^2 - 2hb\cos\varphi + h^2}$$

If we truncate the series at $n = N$ we have $2N + 2$ unknowns (q^{dr}, q, g_n, and g_n^{dr}). The constant V is set and $\widehat{q}$ and $\widehat{g}_n$ are related by the above equations. If we match (2) and (3) at the points

$$\varphi = m\pi/N\ ,\ m = 0, 1, ..., N$$

we then have $2N + 2$ equations in $2N + 2$ unknowns. The capacitance per unit length in the two wire line problem is found from

$$2C = q/V$$

Figures 4 and 5 show a comparison of the multipole model (solid curves), the first equality on the right of the simple series combination (1) (dash curves), and the formula $C/\varepsilon' = \pi/\mathrm{Arccosh}\left(\frac{h}{2a}\right)$ (for $\varepsilon' = \varepsilon_0$) (shown as the large dots).

Notice that the series form (1) (the dashed curves in the graphs) is an accurate approximation throughout the graph. It turns out that for $\varepsilon' \to \varepsilon_0$ and $h > 2b$ the second equality in (1) is even closer to the multipole solution than the first equality, shown in the figures (indeed for the homogeneous sheath with $a = 0.0625$ mm, $b = 0.3625$ mm, $h = 3$ mm, and $\varepsilon'/\varepsilon_0 = 0.95$ the ratio of the capacitance found from the multipole solution to the second formula in (1) is 1.0002). Note in the first graph that if $a = 0.0625$ mm,

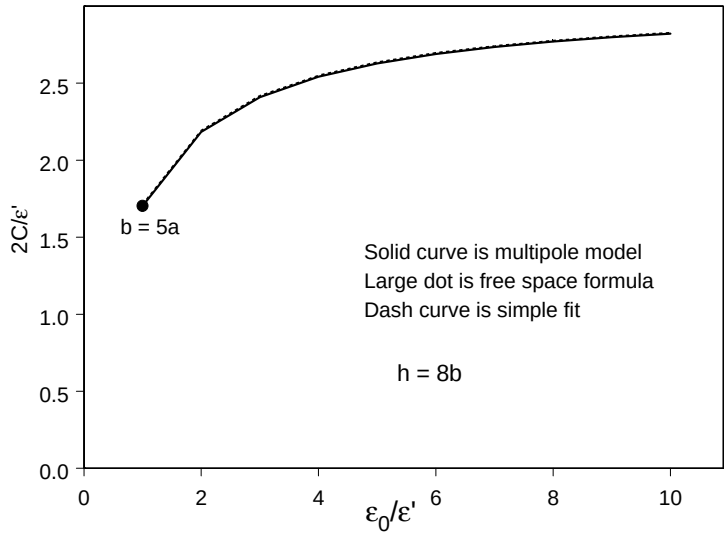

Figure 5. Comparison of the multipole capacitance per unit length and the simple series combination of the homogeneous sheath and plasma regions for a wider spacing.

$b = 10a = 0.625$ mm, $h = 4b = 2.5$ mm, which is near the dimensions of the resonator, replacing the linear profile sheath by a homogeneous sheath. Also in the second graph $b = 5a = 0.3125$ mm, and $h = 8b = 2.5$ mm, also near the dimensions of the resonator. We conclude from this comparison that the series form (1) which has been used in both the sheath circuit models above, and the thin wire algorithm for the simulations below, is a very accurate approximation in these resonators.

8.2 Inhomogeneous Sheath

If the plasma density is assumed to have a continuous radial profile centered about the wire we can easily derive an effective capacitance. The radial electric field is taken locally as minus the gradient of the scalar potential

$$E_\rho = -\frac{\partial \phi}{\partial \rho}$$

where the divergence of the electric displacement $D_\rho = \varepsilon E_\rho$ vanishes

$$\frac{1}{\rho}\frac{\partial}{\partial \rho}\left[\rho \varepsilon(\rho)\frac{\partial \phi}{\partial \rho}\right] = 0$$

Thus integration gives

$$\phi = -\frac{q}{2\pi}\int_a^\rho \frac{d\rho'}{\rho' \varepsilon(\rho')}$$

where we have chosen the integration constants to produce zero potential on the wire and to represent a total charge per unit length on the wire q. Let us assume that the radial sheath profile becomes the homogeneous plasma beyond radius b from the wire. Then the voltage at radius b is negative and equal to $\phi(b)$. If the plasma is lossless with real permittivity $\varepsilon = \varepsilon'(\rho)$, then the local capacitance per unit length C_b is the ratio of the charge to the potential difference

$$1/C_b = \frac{1}{2\pi}\int_a^b \frac{d\rho}{\rho \varepsilon'(\rho)}$$

and the capacitance per unit length is then

$$1/C \approx \frac{\ln(h/b)}{\pi \varepsilon'(b)} + 1/C_b$$

If collisional losses are present then we take the local admittance per unit length to be

$$1/Y_b = \frac{1}{\pi}\int_a^b \frac{d\rho/\rho}{-i\omega\varepsilon(\rho)}$$

and the admittance per unit length

$$1/Y = \frac{\ln(h/b)}{-i\omega\varepsilon(b)\pi} + 1/Y_b$$

At the "open" circuit end the terminating capacitance is modified to

$$C_t \sim C\frac{h}{\Omega'}\left[1+4\left(1-\ln 2\right)/\Omega'\right]$$

$$\Omega' = 2\left[\ln\left(h/b\right)+\varepsilon'\left(b\right)\int_a^b \frac{d\rho}{\rho\varepsilon'\left(\rho\right)}\right]$$

In terms of the admittance

$$Y_t \sim Y\frac{h}{\Omega'}\left[1+4\left(1-\ln 2\right)/\Omega'\right]$$

8.2.1 linear profile

A linear profile $\varepsilon\left(\rho\right)=\varepsilon_0+\left\{\varepsilon\left(b\right)-\varepsilon_0\right\}\left(\rho-a\right)/\left(b-a\right)$ gives

$$1/Y_b = \frac{-1}{-i\omega\pi\left\{b\varepsilon_0-a\varepsilon\left(b\right)\right\}/\left(b-a\right)}a_s\int_a^b\frac{d\rho/\rho}{\rho-a_s} = \frac{-1}{-i\omega\pi\left\{b\varepsilon_0-a\varepsilon\left(b\right)\right\}/\left(b-a\right)}\int_a^b\left[\frac{1}{\rho-a_s}-\frac{1}{\rho}\right]d\rho$$

$$= \frac{\ln\left(b/a\right)-\ln\left(b-a_s\right)+\ln\left(a-a_s\right)}{-i\omega\pi\left\{b\varepsilon_0-a\varepsilon\left(b\right)\right\}/\left(b-a\right)}$$

where

$$a_s = \left\{b\varepsilon_0-a\varepsilon\left(b\right)\right\}/\left\{\varepsilon_0-\varepsilon\left(b\right)\right\}$$

and proper care must be taken about the branch of the logarithm when a_s is complex (absolute values can be used when a_s is real).

Note that in the lossless case we can equate $1/C$ to $\ln\left(h/b_e\right)/\left(\pi\varepsilon'\right)+\ln\left(b_e/a\right)/\left(\pi\varepsilon_0\right)$ or

$$\ln\left(h/b\right)/\left(\pi\varepsilon'\right)+\frac{\ln\left(b/a\right)-\ln\left|b-a_s\right|+\ln\left|a-a_s\right|}{\pi\left(b\varepsilon_0-a\varepsilon'\right)/\left(b-a\right)} = \ln\left(h/b_e\right)/\left(\pi\varepsilon'\right)+\ln\left(b_e/a\right)/\left(\pi\varepsilon_0\right)$$

or

$$\frac{\ln\left(b/a\right)-\ln\left|b-a_s\right|+\ln\left|a-a_s\right|}{\pi\left(b\varepsilon_0-a\varepsilon'\right)/\left(b-a\right)} = \ln\left(b/a\right)/\left(\pi\varepsilon_0\right)+\frac{1}{\pi}\left(\frac{1}{\varepsilon'}-\frac{1}{\varepsilon_0}\right)\ln\left(b/b_e\right)\approx 2.400/\left(\pi\varepsilon_0\right)$$

$$\varepsilon' = 0.95\varepsilon_0$$

$$a_s = \left(b\varepsilon_0-a\varepsilon'\right)/\left(\varepsilon_0-\varepsilon'\right)\approx 12.0625$$

to determine an equivalent homogeneous layer radius $b_e\approx b/2.1\approx 0.315$ mm. This is only slightly smaller than the average that was used 0.3625 mm and accounts for the slight downward shift observed for the homogeneous sheath relative to the linear profile sheath.

9 RECEIVING CIRCUIT

The receiving circuit also causes changes in resonant frequency and quality factor. Suppose we take the resonator to be connected to the measurement circuit by attaching a loop along the "shorted" end which feeds into a coax connection to the measurement device. Let us assume that the coax and measurement device (which is matched to the coax) have a $R_m = 50$ ohm input impedance. The coupling mechanism is inductive. We assume that the effective radius of the joined wires is a_e. The terminating self inductance of the resonator is thus modified to

$$L_t \to L_1 \approx h\frac{\mu_0}{2\pi}\left[\ln\left(2h/a_e\right) - 2\right]$$

The mutual inductance of the receiving circuit is approximately

$$M \approx h\frac{\mu_0}{2\pi}\ln\left(c/a_e\right)$$

The voltage at the load is then

$$V\left(\ell\right) = -i\omega\left[L_1 I\left(\ell\right) + MI_2\right]$$

where I_2 is the current in the measurement circuit. In the measurement circuit we can write

$$\left(R_m - i\omega L_2\right) I_2 - i\omega M I\left(\ell\right) = 0$$

where L_2 is the self inductance of the measurement loop. For a rectangular measurement loop, the self inductance L_2 can be estimated by using the formula for L_{loop} in the preceding inductance section, where the loop dimensions 2ℓ and h, and wire radius a are modified for the measurement loop. To correct this formula for different wire radii on the measurement loop, we choose the radius a in L_{loop} to match, say, the top and bottom legs, and then add a term $\ell_{wire}\mu_0 \ln\left(a_{wire}/a\right)/\left(2\pi\right)$ for each leg that has a different radius, where ℓ_{wire} is the length of the leg and a_{wire} is the corresponding radius. Using this to eliminate I_2 we find

$$Z_t \to V\left(\ell\right)/I\left(\ell\right) = -i\omega L_1 + \frac{\omega^2 M^2}{R_m - i\omega L_2}$$

9.1 Voltage Drive

One of the simplest excitations of the resonator is a voltage source located at the center of the short circuit. We now summarize all the preceding formulas for the calculations in this case.

Suppose we take this drive to be V_0 so that the end condition becomes

$$V\left(\ell\right) = -\frac{1}{Y}\frac{dI}{dz}\left(\ell\right) = V_0 + \left(R_{rad} + h\frac{Z_s}{2\pi a} - i\omega L_t\right) I\left(\ell\right)$$

$$I\left(\ell\right)/I\left(0\right) = \cos\left(\gamma\ell\right) + \frac{1}{\gamma}\left(C/C_t\right)\sin\left(\gamma\ell\right)$$

$$\frac{dI}{dz}\left(\ell\right)/I\left(0\right) = -\gamma\sin\left(\gamma\ell\right) + \left(C/C_t\right)\cos\left(\gamma\ell\right)$$

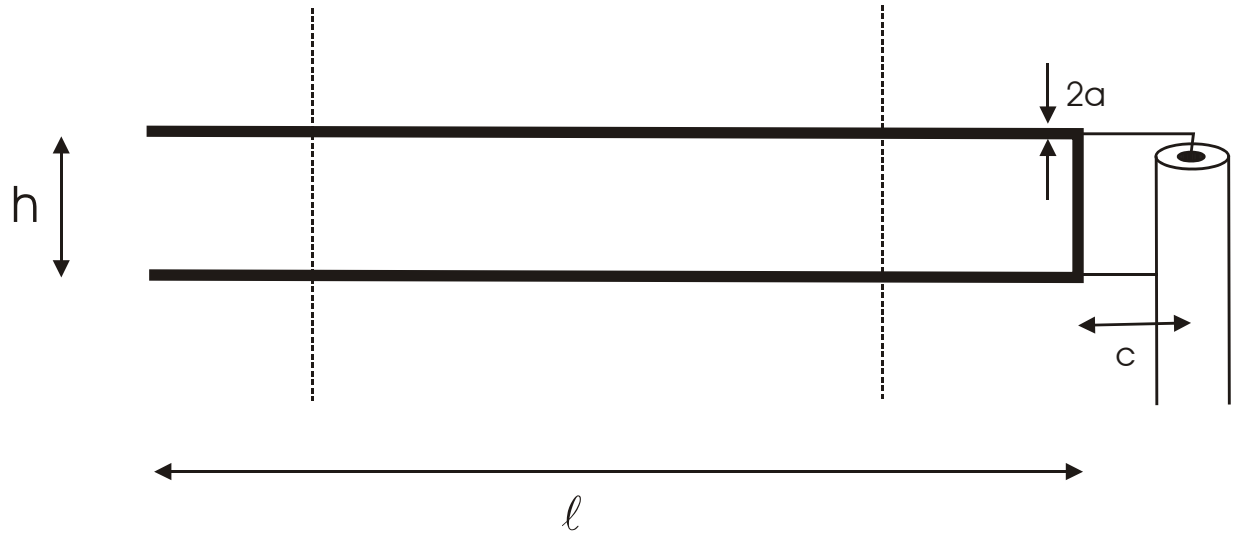

Figure 6. Illustration of a coaxial inductive pickoff of resonator current.

where we have added the internal impedance of the short section of wire. Thus

$$R_{rad} + h\frac{Z_s}{2\pi a} - i\omega L_t + \frac{\gamma}{Y}\left[\frac{-\gamma \sin(\gamma\ell) + (C/C_t)\cos(\gamma\ell)}{\gamma\cos(\gamma\ell) + (C/C_t)\sin(\gamma\ell)}\right] = -V_0/I(\ell)$$

$$Z = Z_w - i\omega L$$

$$Y = G - i\omega C$$

The transmission line parameters L and C have already been given. The impedance per unit length of the two wires at high frequencies is

$$Z_w \sim Z_s/(\pi a)$$

$$Z_s = (1-i)R_s$$

$$R_s = 1/(\sigma\delta)$$

$$\delta = \sqrt{2/(\omega\mu\sigma)}$$

The conductance per unit length of the dielectric medium (the plasma) can be found by inserting the complex permittivity

$$\varepsilon = \varepsilon' + i\varepsilon''$$

$$\gamma = \sqrt{-ZY}$$

$$\varepsilon = \varepsilon_0\left[1 - \frac{\omega_p^2/\omega^2}{1 + i\omega_{eff}/\omega}\right]$$

$$\varepsilon' = \varepsilon_0\left(1 - \frac{\omega_p^2}{\omega^2 + \omega_{eff}^2}\right)$$

$$\varepsilon'' = \varepsilon_0\left(\frac{\omega_p^2\omega_{eff}/\omega}{\omega^2 + \omega_{eff}^2}\right)$$

$$\omega_p^2 = \frac{ne^2}{m\varepsilon_0}$$

$$L \sim \frac{\mu_0}{\pi}\ln(h/a)\ ,\ h >> 2a$$

$$L_t \sim h\frac{\mu_0}{2\pi}\left[\ln(2h/a) - 2\right]$$

$$C_t \sim hC\frac{1}{\Omega}\left[1 + 4(1 - \ln 2)/\Omega\right]$$

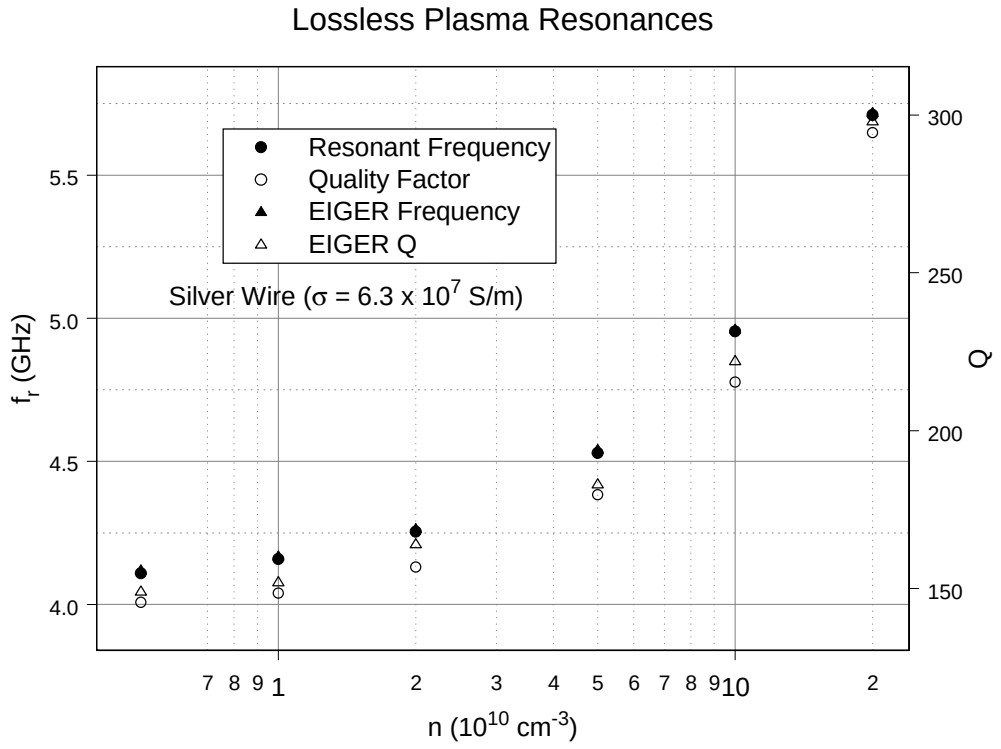

Figure 7. Eamples of resonant frequency and quality factor from circuit model, and from EIGER simulations, as a function of plasma electron density. The plasma is lossless but the resonator wire is silver.

$$C \sim 2\pi\varepsilon/\Omega$$

$$\Omega = 2\ln\left(h/a\right)$$

$$k = \omega\sqrt{\mu_0\varepsilon'}$$

$$R_{rad} = \frac{1}{2\pi}\sqrt{\mu_0/\varepsilon'}\left(kh/2\right)^2$$

$$\left[1 + \frac{1}{3}\left(-1+\sin\left(k\ell\right)\right)^2 - 2\left(-1+\sin\left(k\ell\right)\right)\left\{-\frac{1}{k\ell}\cos\left(k\ell\right) + \frac{1}{k^2\ell^2}\sin\left(k\ell\right)\right\} + 1 + \cos^2\left(k\ell\right) - \frac{2}{k\ell}\sin\left(k\ell\right)\cos\left(k\ell\right)\right]$$

$$\sim \frac{1}{\pi}\sqrt{\mu_0/\varepsilon'}\left(kh/2\right)^2\frac{2}{\pi}k\ell\ ,\ k\ell \to \pi/2$$

This can be inserted as a perturbing series element at $z = \ell$ to account for radiation.

The metal conductivities were take from linear interpolation of the resistivity tables in [6] to 20^o C. The magnetic permeability of Nickel for small amplitude signals was taken from [7] near 4 GHz.

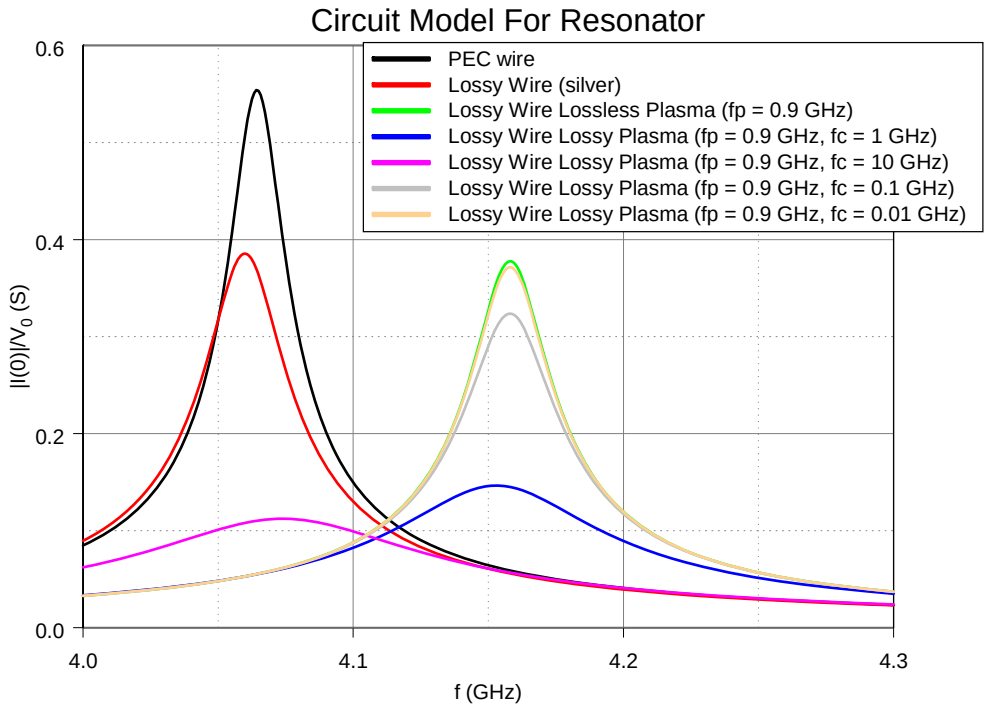

Figure 8. Variation of drive current divided by drive voltage with frequency near the resonance for various plasma collision frequencies and a silver resonator. The case of a perfectly conducting wire without a plasma and the case of a silver wire without a plasma are also shown.

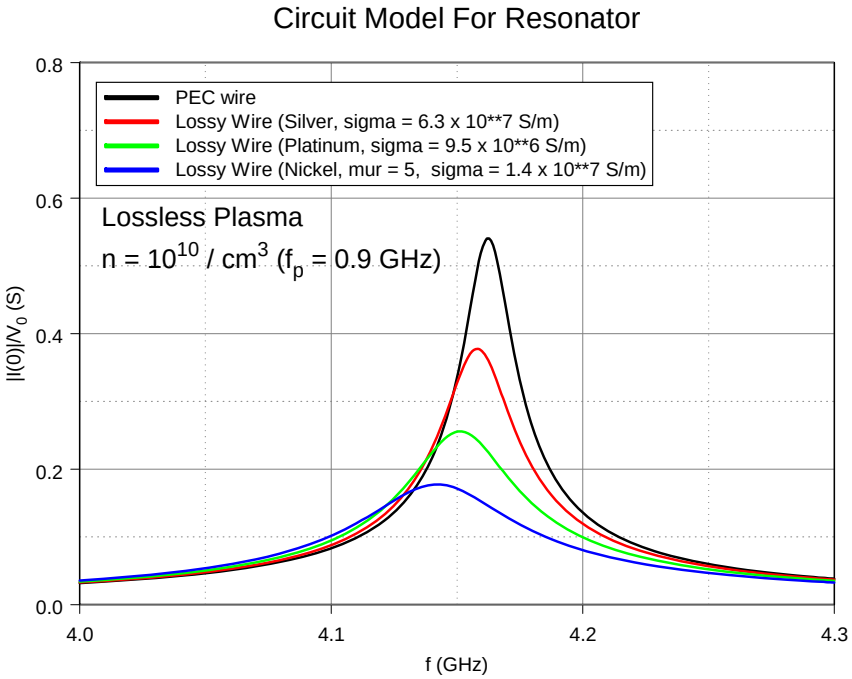

Figure 9. Variation of ratio of drive current to voltage near the resonance is shown for various resonator metals. The plasma is assumed lossess.

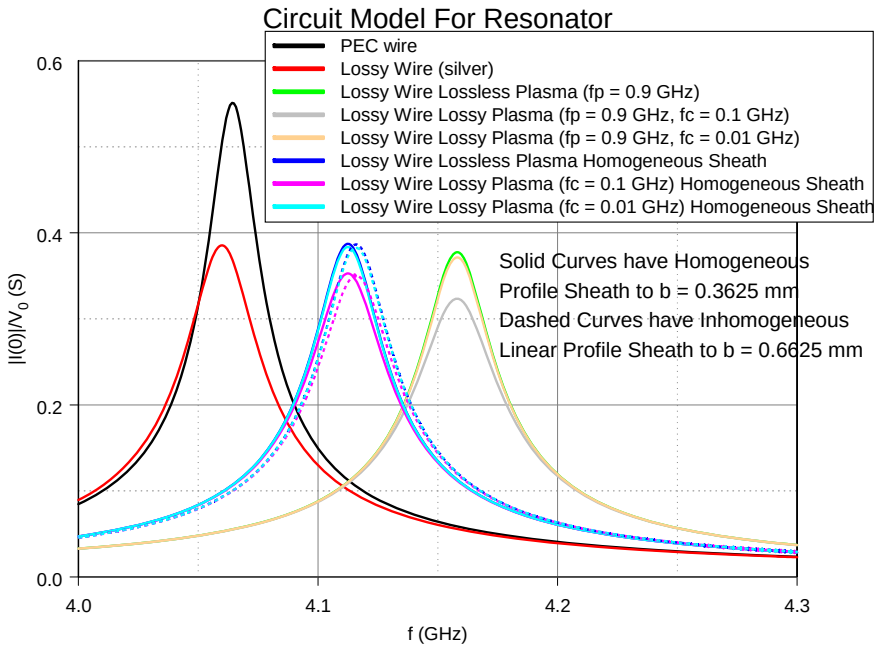

Figure 10. Variation of ratio of drive current to voltage near the resonance is shown for both homogeneous and linear profile plasma sheaths surrounding the silver resonator arms. The case of a perfectly conducting wire without a plasma and the case of a silver wire without a plasma are also shown.

The case of a plasma sheath is now treated. The homogeneous sheath uses

$$1/Y \approx \frac{\ln(h/b)}{-i\omega\pi\varepsilon} + \frac{\ln(b/a)}{-i\omega\pi\varepsilon_0}$$

$$\Omega' = 2\left[\ln(h/b) + \frac{\varepsilon'}{\varepsilon_0}\ln(b/a)\right]$$

$$Y_t \sim Y\frac{h}{\Omega'}\left[1 + 4\left(1 - \ln 2\right)/\Omega'\right]$$

The inhomogeneous linear sheath $\varepsilon(\rho) = \varepsilon_0 + \{\varepsilon(b) - \varepsilon_0\}(\rho - a)/(b - a)$ uses

$$1/Y = \frac{\ln(h/b)}{-i\omega\varepsilon(b)\pi} + 1/Y_b$$

$$1/Y_b = \frac{\ln(b/a) - \ln(b - a_s) + \ln(a - a_s)}{-i\omega\pi\{b\varepsilon_0 - a\varepsilon(b)\}/(b - a)}$$

where

$$a_s = \{b\varepsilon_0 - a\varepsilon(b)\}/\{\varepsilon_0 - \varepsilon(b)\}$$

As discussed above the slight shift to the right for the curves with the linear profile sheath as compared to the homogeneous sheath is caused by the fact that the equivalent radius of the linear profile 0.315 mm is slightly smaller than the homogeneous sheath 0.3625 mm.

10 SIMULATIONS

This section summarizes simulation results performed using the code EIGER which is part of the EMPHASIS code suite.

10.1 Thin Wire Algorithm

To handle inhomogeneous plasma sheaths, which are thin compared to the wire-to-wire spacing, we decided to use the thin wire algorithm. This algorithm takes the form

$$\underline{E}^{>}(a,s) + \Delta Z_C \frac{\partial^2}{\partial s^2}\underline{I} - \Delta Z_L \underline{I} = -\underline{E}^{inc}(s)$$

where s is a distance coordinate along the wire, a is the wire radius, the incident field at the wire center is $\underline{E}^{inc}$ and the scattered field is

$$\underline{E}^{>}(\rho,s) = \frac{i}{\omega\mu_0\varepsilon}\left(\nabla\nabla + \overline{k}^2\right)\cdot\int \frac{e^{i\overline{k}R}}{4\pi R}\underline{I}(s')\,ds'$$

with ρ the perpendicular distance from the wire

$$R = \sqrt{\rho^2 + (s-s')^2}$$

and complex wavenumber

$$\overline{k}^2 = \omega^2\mu_0\varepsilon$$

The vector current $\underline{I}$ is the scalar current times a unit vector along the wire direction $\underline{e}_s$. The parameters ΔZ_L and ΔZ_C describe the properties of the sheath around the wire as well as properties of the wire. The unknowns are the wire currents I_n at points along the wire (which are linearly interpolated between points).

10.2 Thin Wire Parameters

For a surface impedance Z_s on the wire (representing conductive losses) we take

$$\Delta Z_L = \frac{Z_s}{2\pi a}$$

For a homogeneous plasma sheath with permittivity ε_0 and radius b we take the correction to the capacitive impedance per unit length to be

$$\Delta Z_C = \frac{1}{2\pi}\left[\frac{1}{-i\omega\varepsilon_0} - \frac{1}{-i\omega\varepsilon(b)}\right]\ln(b/a)$$

Similarly for an inhomogeneous sheath

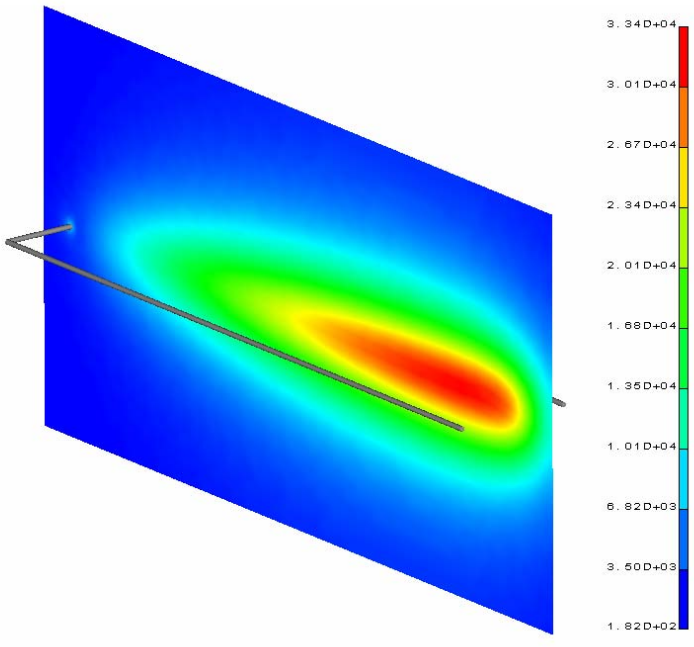

Figure 11. Magnitude of electric field in plane between resonator arms from EIGER simulation.

$$\Delta Z_C = \frac{1}{2}/Y_b - \frac{1}{2\pi}\frac{1}{-i\omega\varepsilon(b)}\ln(b/a)$$

where

$$1/Y_b = \frac{1}{\pi}\int_a^b \frac{d\rho/\rho}{-i\omega\varepsilon(\rho)}$$

A linear profile $\varepsilon(\rho) = \varepsilon_0 + \{\varepsilon(b) - \varepsilon_0\}(\rho - a)/(b - a)$ gives

$$1/Y_b = \frac{-1}{-i\omega\pi\{b\varepsilon_0 - a\varepsilon(b)\}/(b-a)} a_s \int_a^b \frac{d\rho/\rho}{\rho - a_s} = \frac{\ln(b/a) - \ln(b - a_s) + \ln(a - a_s)}{-i\omega\pi\{b\varepsilon_0 - a\varepsilon(b)\}/(b-a)}$$

where

$$a_s = \{b\varepsilon_0 - a\varepsilon(b)\}/\{\varepsilon_0 - \varepsilon(b)\}$$

and proper care must be taken about the branch of the logarithm when a_s is complex (absolute values can be used when a_s is real).

10.3 Examples

Several examples are compared here between the formulas in preceding sections of the report and the simulations discussed above. The length was taken to be $\ell = 17$ mm. The spacing was taken to be $h = 3$ mm. The wire diameter was taken to be $2a = 0.125$ mm.

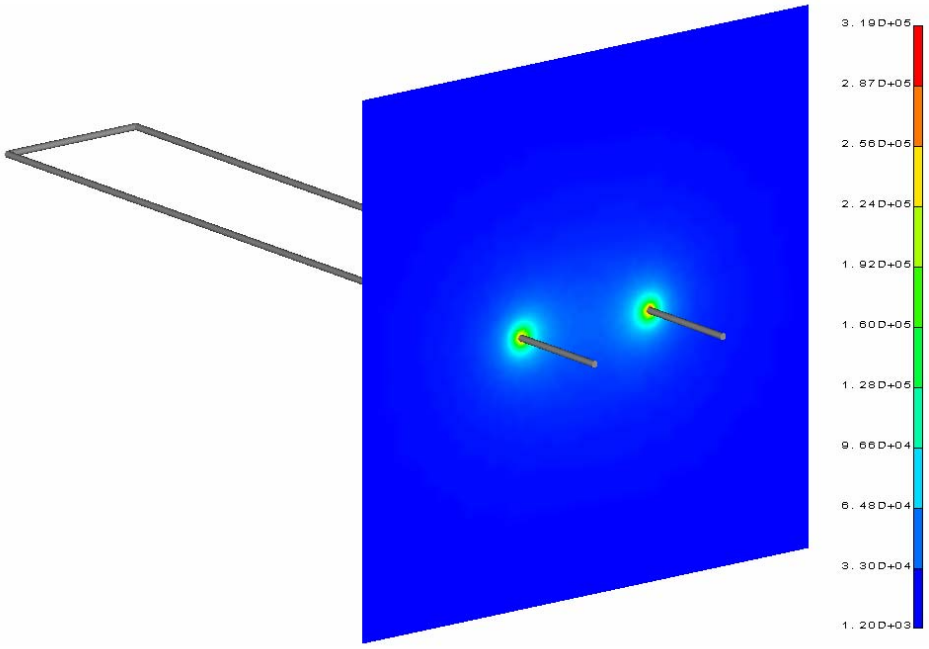

Figure 12. Magnitude of electric field in plane perpendicular to resonator arms from EIGER simulation.

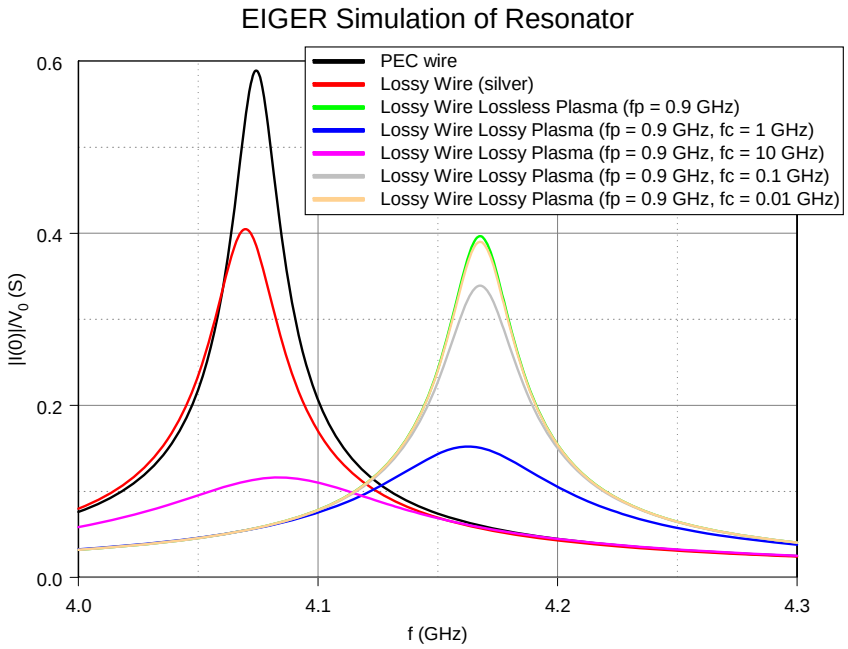

Figure 13. Variation of drive current divided by drive voltage from EIGER simulations with frequency near the resonance for various plasma collision frequencies and a silver resonator. The case of a perfectly conducting wire without a plasma and the case of a silver wire without a plasma are also shown.

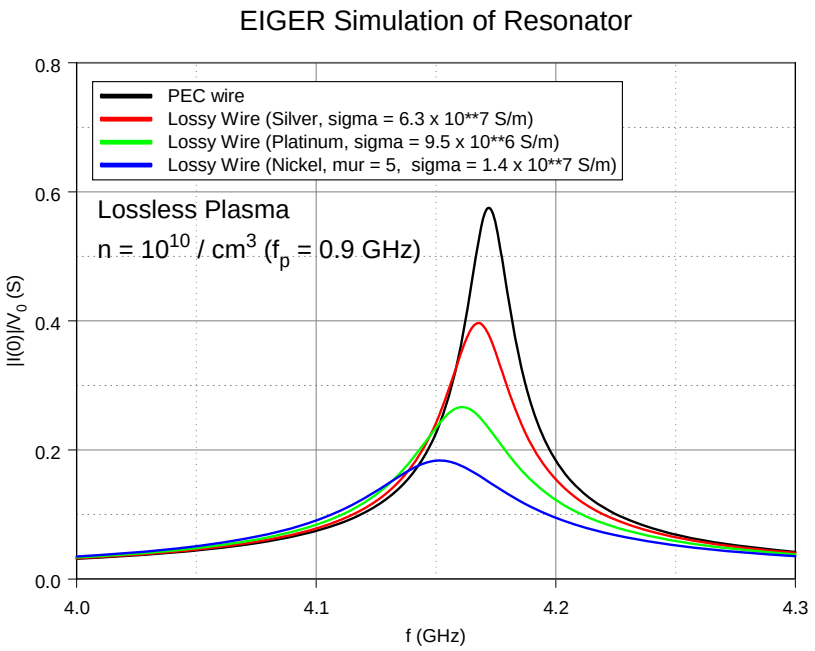

Figure 14. Variation of ratio of drive current to voltage from EIGER simulations near the resonance is shown for various resonator metals. The plasma is assumed lossess.

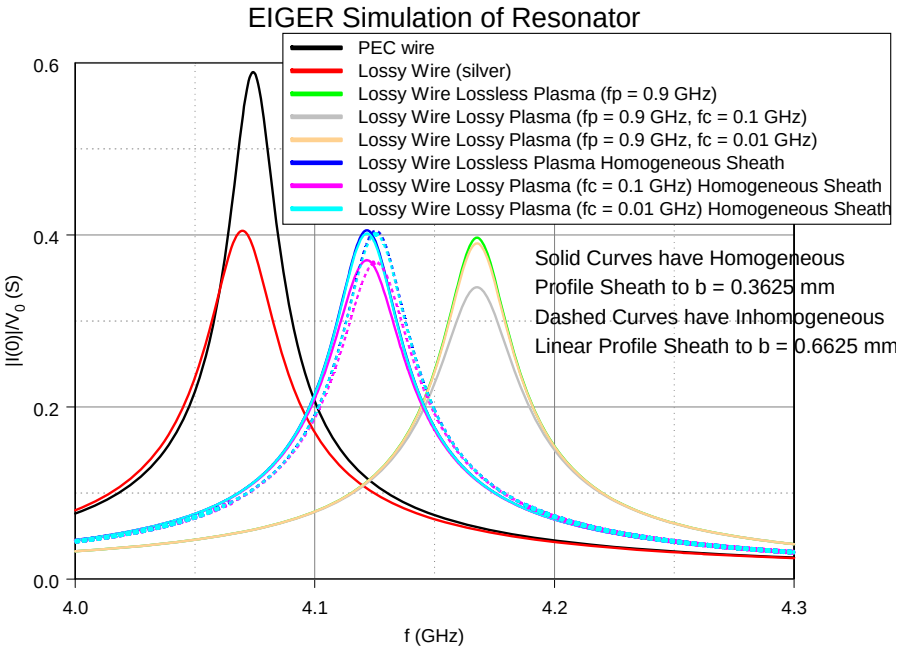

Figure 15. Variation of ratio of drive current to voltage from EIGER simulations near the resonance is shown for both homogeneous and linear profile plasma sheaths surrounding the silver resonator arms. The case of a perfectly conducting wire without a plasma and the case of a silver wire without a plasma are also shown. The sheath in these simulations was put into the EIGER code by means of the thin wire algorithm parameters.

10.3.1no plasma and perfectly conducting wire

The case where there is no plasma and the wire is perfectly conducting was run first. The resonant frequency formula

$$\omega_r \sqrt{\mu_0 \varepsilon_0} \approx \frac{\pi/2}{\ell + C_t/C + L_t/L}$$

gives $f_r = \omega_r/(2\pi) = 4.064$ GHz, where $L_t/L \approx [1 - 2(2 - \ln 2)/\Omega]\, h/2 \approx 1$ mm and $C_t/C \approx [1 + 4(1 - \ln 2)/\Omega]\, h/\Omega \approx 0.45$ mm, $\Omega = 2\ln(h/a)$. The simulation gave $f_r = 4.076$ GHz (a difference of 0.3%). Note that the $\lambda/4 = \ell$ frequency is 4.409 GHz (8.2% high), so that the two end elements C_t and L_t have corrected most of the frequency shift from this value.

The quality factor formula is

$$Q = \frac{\pi}{4} \frac{\sqrt{L/C}}{R_{rad}(\omega_r)}$$

Note that the transmission line characteristic impedance is

$$\sqrt{L/C} \approx \sqrt{\mu_0/\varepsilon_0} \frac{1}{\pi} \ln(h/a)$$

This formula gives $Q \approx 202$, where $R_{rad}(\omega_r) \sim \sqrt{\mu_0/\varepsilon_0}\,(kh/2)^2\,(2/\pi)\,k\ell/\pi \approx 1.804$ ohms, $\sqrt{L/C} \approx 464.23$ ohms. The simulation gave $Q = 214$.

10.3.2no plasma and lossy wire

The case of the lossy wire with the conductivity of silver $\sigma = 6.3 \times 10^7$ S/m (at 20^o C [6]) is now given. The surface resistance at the resonant frequency $R_s(\omega_r) = \sqrt{\omega_r \mu_0/(2\sigma)} \approx 0.01596$ ohms. The quality factor is then

$$Q = \frac{\frac{\pi}{4}\sqrt{L/C}}{R_s(\omega_r)\left(\frac{1}{4k_r a} + \frac{h}{\pi a}\right) + R_{rad}(\omega_r)}$$

This gives $Q \approx 130$. The simulation then gave $Q = 145$ and the resonant frequency shifted to $f_r = 4.0695$ GHz.

10.3.3lossless plasma and lossy wire

The case where a collisionless plasma is present with density $n = 10^{10}/\text{cm}^3$ and plasma frequency $\omega_p^2 = ne^2/(m\varepsilon_0)$ or $f_p = \omega_p/(2\pi) = 0.898$ GHz is now treated. The permittivity is $\varepsilon'/\varepsilon_0 = 1 - \omega_p^2/\omega^2$ and then the resonant frequency is

$$\omega_r \sqrt{\mu_0 \varepsilon'} = \sqrt{\left(\omega_r^2 - \omega_p^2\right)\mu_0 \varepsilon_0} \approx \frac{\pi/2}{\ell + C_t/C + L_t/L}$$

The formulas now give $f_r \approx 4.16$ GHz. The simulation gives $f_r = 4.1675$ GHz.

The quality factor is again

$$Q = \frac{\frac{\pi}{4}\sqrt{L/C}}{R_s(\omega_r)\left(\frac{1}{4k_r a} + \frac{h}{\pi a}\right) + R_{rad}(\omega_r)}$$

$$\sqrt{L/C} \approx \sqrt{\mu_0/\varepsilon'}\frac{1}{\pi}\ln(h/a)$$

This formula gives $Q \approx 131$, where $\varepsilon'/\varepsilon_0 \approx 0.9534$ and $R_{rad}(\omega_r) \sim \sqrt{\mu_0/\varepsilon'}(kh/2)^2(2/\pi)k\ell/\pi \approx 1.845$ ohms, $R_s(\omega_r) \approx 0.01615$ ohms, $\sqrt{L/C} \approx 475.44$ ohms, $k_r a \approx 0.005321$. The simulation gave $Q = 154$. The larger discrepancy in the quality factor here can be explained by the fact that the formula above fixed the permittivity of the plasma at the resonant frequency. The simulation allowed the permittivity to vary with frequency. At the 3dB point the variation in permittivity acted to detune the resonance further from the observation frequency (if the simulation is run with the permittivity fixed at the resonant value the discrepancies are similar to previous cases).

10.3.4lossless plasma and lossy wire with homogeneous sheath

Now we assume we have a free space ε_0 sheath of diameter $2b = 0.25$ mm. The resonant frequency is approximately

$$\omega_r\sqrt{LC} \approx \frac{\pi/2}{\ell + C_t/C + L_t/L}$$

The transmission line parameters with the sheath are

$$L \sim \frac{\mu_0}{\pi}\ln(h/a)\ ,\ h >> 2a$$

$$C \approx \frac{\pi\varepsilon'}{\ln(h/a) + (\varepsilon'/\varepsilon_0 - 1)\ln(b/a)}$$

The inductance end correction remains the same but the capacitance end correction is now slightly changed to

$$C_t/C \sim \frac{h}{\Omega'}\left[1 + 4(1 - \ln 2)/\Omega'\right]$$

$$\Omega' = 2\left[\ln(h/b) + \frac{\varepsilon'}{\varepsilon_0}\ln(b/a)\right]$$

To approximate the resonant frequency we first assume that C_t/C is unchanged.

$$\sqrt{\frac{\mu_0\varepsilon_0\omega_p^2(1/X - 1)\ln(h/a)}{\ln(h/a) - X\ln(b/a)}} \approx \frac{\pi/2}{\ell + C_t/C + L_t/L} = \omega_p\sqrt{c_1\mu_0\varepsilon_0}$$

$$1 - (1 + c_1)X + c_1X^2\ln(b/a)/\ln(h/a) = 0$$

$$X = \omega_p^2/\omega_r^2$$

We find $c_1 = 20.463$ and $1 - 21.463X + 3.664X^2 = 0$, and $X = 5.811, 0.04697$. Using only the smaller root (since the other would affect the value of C_t/C) $f_r = 4.14$ GHz. The simulation gave $f_r = 4.15$ GHz.

The quality factor is again

$$Q = \frac{\frac{\pi}{4}\sqrt{L/C}}{R_s(\omega_r)\left(\frac{1}{4k_r a} + \frac{h}{\pi a}\right) + R_{rad}(\omega_r)}$$

Using the above values $\varepsilon'/\varepsilon_0 \approx 0.953$, $k_r a \approx 0.005294$, $\sqrt{L/C} \approx 477.54$ ohms, $R_{rad}(\omega_r) \approx \sqrt{\mu_0/\varepsilon'}\,(kh/2)^2\,(2/\pi)\,k\ell/\pi \approx 1.818$ ohms, $R_s(\omega_r) \approx 0.01611$ ohms. Thus $Q \approx 133$. The simulation gave $Q = 153$.

10.3.5slightly lossy plasma and lossy wire

The case where there is collisional damping but not enough to distort the current distribution along the resonator is covered by the full quality factor formula

$$Q = \frac{\frac{\pi}{4}\sqrt{L/C}}{\frac{\pi}{4}\left\{\frac{R_s(\omega_r)}{\pi a k_r} + \frac{\varepsilon''}{\varepsilon'}\sqrt{L/C}\right\} + R_s(\omega_r)\frac{h}{\pi a} + R_{rad}(\omega_r)}$$

$$\varepsilon' = \varepsilon_0\left(1 - \frac{\omega_p^2}{\omega^2 + \omega_{eff}^2}\right)$$

$$\varepsilon'' = \varepsilon_0\left(\frac{\omega_p^2\omega_{eff}/\omega}{\omega^2 + \omega_{eff}^2}\right)$$

Suppose we take $n = 10^{10}/\text{cm}^3$ or $f_p = 0.898$ GHz and $f_{eff} = 1$ GHz. The resonant frequency

$$\omega_r\sqrt{\mu_0\varepsilon'} = \sqrt{\left(\omega_r^2 - \frac{\omega_r^2\omega_p^2}{\omega_r^2 + \omega_{eff}^2}\right)\mu_0\varepsilon_0} \approx \sqrt{\left(\omega_r^2 - \omega_p^2 + \omega_p^2\omega_{eff}^2/\omega_r^2\right)\mu_0\varepsilon_0} \approx \frac{\pi/2}{\ell + C_t/C + L_t/L}$$

We solve this approximately to find $f_r \approx 4.155$ GHz, $\varepsilon'/\varepsilon_0 \approx 0.956$, $R_s(\omega_r) \approx 0.01614$ ohms, $R_{rad}(\omega_r) \approx 1.844$ ohms, $\sqrt{L/C} \approx 474.79$ ohms, $k_r a \approx 0.005322$, $\varepsilon''/\varepsilon' \approx 0.0111$. Thus $Q \approx 53.4$. The simulation gave $Q = 58.6$ and resonant frequency $f_r = 4.163$ GHz.

10.3.6lossy plasma and lossy wire with homogeneous plasma sheath

The complex dielectric constant is

$$\varepsilon = \varepsilon_0\left[1 - \frac{\omega_p^2/\omega^2}{1 + i\omega_{eff}/\omega}\right]$$

The admittance per unit length is

$$1/Y \approx \frac{\ln(h/b)}{-i\omega\pi\varepsilon} + \frac{\ln(b/a)}{-i\omega\pi\varepsilon_0}$$

$$-i\omega\varepsilon_0\pi/Y \approx \ln(h/a) + \frac{\ln(h/b)\left(\omega_p^2/\omega^2\right)}{1 + i\omega_{eff}/\omega - \omega_p^2/\omega^2}$$

For small ω_p^2/ω^2

$$Y \approx -i\omega\varepsilon_0\pi/\ln(h/a)\left[1 - \frac{\ln(h/b)\left(\omega_p^2/\omega^2\right)/\ln(h/a)}{1 + i\omega_{eff}/\omega}\right]$$

which can be written as

$$Y = G - iB$$

If we take the parameters of the preceding example we see that $\ln(h/b)/\ln(h/a) \approx 0.82$ and we would not expect a large change in Q or resonant frequency from the preceding case. The simulation gave $Q = 57.4$ and $f_r = 4.147$ GHz.

11 PLASMA INHOMOGENEITIES ALONG RESONATOR LENGTH

We now perform a couple of modifications to see the effect of variations in plasma density along the resonator length. Let us take the plasma to exist in a cylindrical region of radius $\rho_p = 3$ mm, and length $\ell_p = 8.5$ mm.

11.1 Open End

We first consider the block to be centered at the open end of the resonator. We assume that the transmission line parameters are modified in this region to be those associated with the plasma and that the parasitic capacitance at the end is also associated with the plasma. Thus the transmission line has a discontinuity at $z = \ell_p/2$. The current at the open end region $z < \ell_p/2$

$$I(z) = I(0)\cos(\gamma z) + \frac{1}{\gamma}\frac{dI}{dz}(0)\sin(\gamma z)$$

$$\gamma = \sqrt{-ZY}$$

The condition at the "open" end (assuming the same complex permittivity, which accounts for the loss parameters G and G_t, is used in the region surrounding the transmission line and at the "open" end) is

$$\frac{dI}{dz}(0) = \frac{Y}{Y_t}I(0)$$

$$Y_t \sim hY\frac{1}{\Omega}\left[1 + 4\left(1 - \ln 2\right)/\Omega\right]$$

$$\Omega = 2\ln(2h/a)$$

The current near the shorted end is

$$I(z) = I(\ell)\cos(\gamma_0(z-\ell)) + \frac{1}{\gamma_0}\frac{dI}{dz}(\ell)\sin(\gamma_0(z-\ell))$$

$$\gamma_0 = \sqrt{Zi\omega C}$$

$$Z = Z_w - i\omega L$$

$$Z_w = Z_s/(\pi a)$$

$$L = \frac{\mu_0}{\pi}\text{Arccosh}\left(\frac{h}{2a}\right) \sim \frac{\mu_0}{\pi}\ln(h/a)\ ,\ h >> 2a$$

$$C = \frac{\pi\varepsilon_0}{\text{Arccosh}\left(\frac{h}{2a}\right)} \sim \frac{\pi\varepsilon_0}{\ln(h/a)}\ ,\ h >> 2a$$

$$Y = \frac{-i\omega\pi\varepsilon}{\text{Arccosh}\left(\frac{h}{2a}\right)} \sim \frac{-i\omega\pi\varepsilon}{\ln(h/a)}\ ,\ h >> 2a$$

The condition near the shorted end with voltage drive V_0 is

$$V(\ell) = \frac{1}{i\omega C}\frac{dI}{dz}(\ell) = V_0 + \left(R_{rad} + h\frac{Z_s}{2\pi a} - i\omega L_t\right)I(\ell)$$

where

$$L_t = h\frac{\mu_0}{2\pi}\left[\ln(2h/a) - 2\right]$$

$$Z_s = R_s(1-i)$$

Because the plasma permittivity is taken to be near that of free space we regard the radiation resistance to be unchanged from the free space value

$$R_{rad} \sim \frac{1}{\pi}\sqrt{\mu_0/\varepsilon_0}\,(kh/2)^2\,\frac{2}{\pi}k\ell$$

Continuity of the current at $z = \ell_p/2$ gives

$$I(\ell_p/2 - 0) = I(\ell_p/2 + 0)$$

or

$$I(0)\cos(\gamma\ell_p/2) + \frac{1}{\gamma}\frac{dI}{dz}(0)\sin(\gamma\ell_p/2) = I(\ell)\cos(\gamma_0(\ell_p/2-\ell)) + \frac{1}{\gamma_0}\frac{dI}{dz}(\ell)\sin(\gamma_0(\ell_p/2-\ell))$$

Continuity of voltage at this point gives

$$-\frac{1}{Y}\frac{dI}{dz}\left(\ell_p/2-0\right)=\frac{1}{i\omega C}\frac{dI}{dz}\left(\ell_p/2+0\right)$$

or

$$\frac{\gamma}{Y}I\left(0\right)\sin\left(\gamma\ell_p/2\right)-\frac{1}{Y}\frac{dI}{dz}\left(0\right)\cos\left(\gamma\ell_p/2\right)=-\frac{\gamma_0}{i\omega C}I\left(\ell\right)\sin\left(\gamma_0\left(\ell_p/2-\ell\right)\right)+\frac{1}{i\omega C}\frac{dI}{dz}\left(\ell\right)\cos\left(\gamma_0\left(\ell_p/2-\ell\right)\right)$$

The four equations have now been set up for the end currents and their derivatives. Eliminating the derivatives

$$\left[\cos\left(\gamma\ell_p/2\right)+\frac{1}{\gamma}\frac{Y}{Y_t}\sin\left(\gamma\ell_p/2\right)\right]I\left(0\right)=I\left(\ell\right)\cos\left(\gamma_0\left(\ell_p/2-\ell\right)\right)$$

$$+\frac{1}{\gamma_0}i\omega C\left[V_0+\left(R_{rad}+h\frac{Z_s}{2\pi a}-i\omega L_t\right)I\left(\ell\right)\right]\sin\left(\gamma_0\left(\ell_p/2-\ell\right)\right)$$

$$\left[\frac{\gamma}{Y}\sin\left(\gamma\ell_p/2\right)-\frac{1}{Y_t}\cos\left(\gamma\ell_p/2\right)\right]I\left(0\right)=-\frac{\gamma_0}{i\omega C}I\left(\ell\right)\sin\left(\gamma_0\left(\ell_p/2-\ell\right)\right)+V_0\cos\left(\gamma_0\left(\ell_p/2-\ell\right)\right)$$

$$+\left(R_{rad}+h\frac{Z_s}{2\pi a}-i\omega L_t\right)I\left(\ell\right)\cos\left(\gamma_0\left(\ell_p/2-\ell\right)\right)$$

Eliminating $I\left(0\right)$

$$\frac{\gamma}{Y}\left\{\sin\left(\gamma\ell_p/2\right)-\frac{1}{\gamma}\frac{Y}{Y_t}\cos\left(\gamma\ell_p/2\right)\right\}\left[\cos\left(\gamma_0\left(\ell_p/2-\ell\right)\right)+\frac{1}{\gamma_0}i\omega C\left(R_{rad}+h\frac{Z_s}{2\pi a}-i\omega L_t\right)\sin\left(\gamma_0\left(\ell_p/2-\ell\right)\right)\right]$$

$$+\frac{\gamma_0}{i\omega C}\left\{\cos\left(\gamma\ell_p/2\right)+\frac{1}{\gamma}\frac{Y}{Y_t}\sin\left(\gamma\ell_p/2\right)\right\}$$

$$\left[\sin\left(\gamma_0\left(\ell_p/2-\ell\right)\right)-\frac{1}{\gamma_0}i\omega C\left(R_{rad}+h\frac{Z_s}{2\pi a}-i\omega L_t\right)\cos\left(\gamma_0\left(\ell_p/2-\ell\right)\right)\right]=$$

$$\left[\left\{\cos\left(\gamma\ell_p/2\right)+\frac{1}{\gamma}\frac{Y}{Y_t}\sin\left(\gamma\ell_p/2\right)\right\}\cos\left(\gamma_0\left(\ell_p/2-\ell\right)\right)\right.$$

$$\left.-\left\{\sin\left(\gamma\ell_p/2\right)-\frac{1}{\gamma}\frac{Y}{Y_t}\cos\left(\gamma\ell_p/2\right)\right\}\frac{\gamma}{\gamma_0}\frac{i\omega C}{Y}\sin\left(\gamma_0\left(\ell_p/2-\ell\right)\right)\right]V_0/I\left(\ell\right)$$

Now taking the limit $C_t, L_t, Y_t, Z_s \to 0$ and $\gamma \to \gamma_0$

$$\frac{i\omega C}{\gamma_0}\sin\left(\gamma_0\ell\right)/\left[\cos\left(\gamma_0\ell\right)-\frac{1}{\gamma_0}i\omega CR_{rad}\sin\left(\gamma_0\ell\right)\right]=I\left(\ell\right)/V_0$$

11.2 Shorted End

Next we consider the block to be centered at the shorted end of the resonator. The transmission line

parameters have a discontinuity at $z = \ell - \ell_p/2$.

$$I(z) = I(0)\cos(\gamma_0 z) + \frac{1}{\gamma_0}\frac{dI}{dz}(0)\sin(\gamma_0 z)$$
$$\frac{dI}{dz}(0) = \frac{C}{C_t}I(0)$$

$$C_t \sim hC\frac{1}{\Omega}\left[1 + 4\left(1 - \ln 2\right)/\Omega\right]$$

$$\Omega = 2\ln(2h/a)$$

The current near the shorted end is

$$I(z) = I(\ell)\cos(\gamma(z-\ell)) + \frac{1}{\gamma}\frac{dI}{dz}(\ell)\sin(\gamma(z-\ell))$$

The condition near the shorted end with voltage drive V_0 is

$$V(\ell) = -\frac{1}{Y}\frac{dI}{dz}(\ell) = V_0 + \left(R_{rad} + h\frac{Z_s}{2\pi a} - i\omega L_t\right)I(\ell)$$

where

$$L_t = h\frac{\mu_0}{2\pi}\left[\ln(2h/a) - 2\right]$$

$$Z_s = R_s(1-i)$$

Because the plasma permittivity is taken to be near that of free space we regard the radiation resistance to be unchanged from the free space value

$$R_{rad} \sim \frac{1}{\pi}\sqrt{\mu_0/\varepsilon_0}\,(kh/2)^2\,\frac{2}{\pi}k\ell$$

Continuity of the current at $z = \ell - \ell_p/2$ gives

$$I(\ell - \ell_p/2 + 0) = I(\ell - \ell_p/2 - 0)$$

or

$$I(\ell)\cos(\gamma(-\ell_p/2)) + \frac{1}{\gamma}\frac{dI}{dz}(\ell)\sin(\gamma(-\ell_p/2)) = I(0)\cos(\gamma_0(\ell - \ell_p/2)) + \frac{1}{\gamma_0}\frac{dI}{dz}(0)\sin(\gamma_0(\ell - \ell_p/2))$$

Continuity of voltage at this point gives

$$-\frac{1}{Y}\frac{dI}{dz}(\ell - \ell_p/2 + 0) = \frac{1}{i\omega C}\frac{dI}{dz}(\ell - \ell_p/2 - 0)$$

or

$$\frac{\gamma}{Y}I\left(\ell\right)\sin\left(\gamma\left(-\ell_p/2\right)\right)-\frac{1}{Y}\frac{dI}{dz}\left(\ell\right)\cos\left(\gamma\left(-\ell_p/2\right)\right)=-\frac{\gamma_0}{i\omega C}I\left(0\right)\sin\left(\gamma_0\left(\ell-\ell_p/2\right)\right)+\frac{1}{i\omega C}\frac{dI}{dz}\left(0\right)\cos\left(\gamma_0\left(\ell-\ell_p/2\right)\right)$$

Eliminating the current derivatives gives

$$I\left(\ell\right)\cos\left(\gamma\left(-\ell_p/2\right)\right)-Y\frac{1}{\gamma}V_0\sin\left(\gamma\left(-\ell_p/2\right)\right)-Y\frac{1}{\gamma}\left(R_{rad}+h\frac{Z_s}{2\pi a}-i\omega L_t\right)I\left(\ell\right)\sin\left(\gamma\left(-\ell_p/2\right)\right)$$

$$=\left[\cos\left(\gamma_0\left(\ell-\ell_p/2\right)\right)+\frac{1}{\gamma_0}\frac{C}{C_t}\sin\left(\gamma_0\left(\ell-\ell_p/2\right)\right)\right]I\left(0\right)$$

$$I\left(\ell\right)\sin\left(\gamma\left(-\ell_p/2\right)\right)+\frac{1}{\gamma}YV_0\cos\left(\gamma\left(-\ell_p/2\right)\right)+\frac{1}{\gamma}Y\left(R_{rad}+h\frac{Z_s}{2\pi a}-i\omega L_t\right)I\left(\ell\right)\cos\left(\gamma\left(-\ell_p/2\right)\right)$$

$$=-\frac{\gamma_0}{\gamma}\frac{Y}{i\omega C}\left[\sin\left(\gamma_0\left(\ell-\ell_p/2\right)\right)-\frac{1}{\gamma_0}\frac{C}{C_t}\cos\left(\gamma_0\left(\ell-\ell_p/2\right)\right)\right]I\left(0\right)$$

Eliminating $I\left(0\right)$

$$\left\{\cos\left(\gamma_0\left(\ell-\ell_p/2\right)\right)+\frac{1}{\gamma_0}\frac{C}{C_t}\sin\left(\gamma_0\left(\ell-\ell_p/2\right)\right)\right\}$$

$$\left\{\sin\left(\gamma\left(-\ell_p/2\right)\right)+\frac{1}{\gamma}Y\left(R_{rad}+h\frac{Z_s}{2\pi a}-i\omega L_t\right)\cos\left(\gamma\left(-\ell_p/2\right)\right)\right\}$$

$$+\frac{\gamma_0}{\gamma}\frac{Y}{i\omega C}\left\{\sin\left(\gamma_0\left(\ell-\ell_p/2\right)\right)-\frac{1}{\gamma_0}\frac{C}{C_t}\cos\left(\gamma_0\left(\ell-\ell_p/2\right)\right)\right\}$$

$$\left\{\cos\left(\gamma\left(-\ell_p/2\right)\right)-\frac{1}{\gamma}Y\left(R_{rad}+h\frac{Z_s}{2\pi a}-i\omega L_t\right)\sin\left(\gamma\left(-\ell_p/2\right)\right)\right\}=$$

$$\left[\frac{\gamma_0}{\gamma}\frac{Y}{i\omega C}\left\{\sin\left(\gamma_0\left(\ell-\ell_p/2\right)\right)-\frac{1}{\gamma_0}\frac{C}{C_t}\cos\left(\gamma_0\left(\ell-\ell_p/2\right)\right)\right\}\sin\left(\gamma\left(-\ell_p/2\right)\right)\right.$$

$$\left.-\left\{\cos\left(\gamma_0\left(\ell-\ell_p/2\right)\right)+\frac{1}{\gamma_0}\frac{C}{C_t}\sin\left(\gamma_0\left(\ell-\ell_p/2\right)\right)\right\}\cos\left(\gamma\left(-\ell_p/2\right)\right)\right]\frac{1}{\gamma}YV_0/I\left(\ell\right)$$

If we take the limit $C_t, Y_t, L_t, Z_s \to 0$ and $\gamma \to \gamma_0, Y \to -i\omega C$

$$I\left(\ell\right)/V_0=\frac{i\omega C}{\gamma}\sin\left(\gamma_0\ell\right)/\left\{\cos\left(\gamma\ell\right)-\frac{i\omega C}{\gamma}R_{rad}\sin\left(\gamma\ell\right)\right\}$$

Figure 16 compares the open and short end plasma block results with the homogeneous plasma results and with the silver wire without a plasma present (the PEC wire is also shown). Notice that the plasma block at the shorted end (one quarter of the length of the resonator $\ell_p/2$ is immersed in the plasma) has little effect (it nearly overlays the no plasma curve). The plasma near the open end shows a significant shift. This is expected since the electric field is large at the open end of the resonator and small near the shorted end (it is only the electric field that interacts with the plasma dielectric constant).

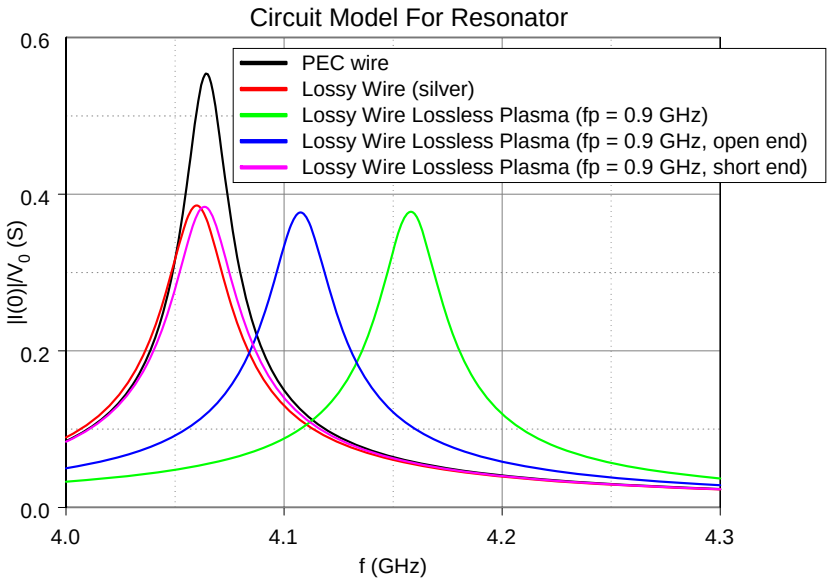

Figure 16. Variation of drive current divided by drive voltage with frequency near the resonance for a lossless cylindrical plasma block at various locations along.a silver resonator. The case of a perfectly conducting wire without a plasma and the case of a silver wire without a plasma are also shown.

12 DISC CAVITY

The cylindrical cavity has spacing $d = 25$ mm and radius $b = 200$ mm. Thus at $f_r \approx 4.1$ GHz the vertical electric field modes have the form (the half wavelength at this frequency is $\lambda/2 \approx 36.6$ mm, which is larger than the spacing d, and thus the TM mode with no half wave variations in the vertical will be the only propagating mode)

$$\frac{1}{r}\frac{\partial}{\partial r}\left(\frac{\partial}{\partial r} r E_z\right) + \frac{1}{r^2}\frac{\partial^2}{\partial \varphi^2} E_z + k_{mn}^2 E_z = 0$$

$$E_z = E_0 J_m\left(k_{mn} r\right)\cos\left(m\varphi\right)$$

$$i\omega\mu_0 H_\varphi = -\left(E_0 k_{mn}\right) J_m'\left(k_{mn} r\right)\cos\left(m\varphi\right)$$

12.1 Shorted Outer Radius

For a shorted condition at the outer periphery the boundary condition

$$E_z\left(r = b\right) = 0$$

gives

$$k_{mn} b = j_{m,n}$$

where

$$J_m\left(j_{m,n}\right) = 0\,,\; n = 1, 2, ...$$

We can also use other types of outer boundary conditions (for example, of the impedance type $E_z = -Z_s H_\varphi$) to represent radiation leakage at the periphery. Because we want to examine the case where $k_{mn} \to k \sim 85.9$ m^{-1} is fairly large so that $kb >> 1$ we use the asymptotic form

$$kb \approx 17.2 \to j_{m,n} \sim \left(n + m/2 - 1/4\right)\pi\,,\; n \to \infty$$

The modal spacing due to the variation in m is

$$\Delta k \sim \pi/\left(2b\right) \sim 7.85\ \ \mathrm{m}^{-1}$$

The modal spacing due to the variation in n is

$$\Delta k \sim \pi/b$$

These modal spacing implies a spacing quality factor in the range

$$k/\Delta k \approx 5.5 - 11$$

The energy stored in a mode is

$$W = \int_V \frac{1}{2}\varepsilon \left|\underline{E}\right|^2 dV = \frac{d}{\varepsilon_m}\int_0^b \frac{1}{2}\varepsilon \left|E_0 J_m\left(j_{m,n}r/b\right)\right|^2 2\pi r dr = \frac{1}{2\varepsilon_m}\varepsilon d\pi b^2 \left|E_0\right|^2 \left[J'_m\left(j_{m,n}\right)\right]^2$$

and we have used [9]

$$\int_0^1 \left[J_m\left(j_{m,n}r\right)\right]^2 r dr = \frac{1}{2}\left[J'_m\left(j_{m,n}\right)\right]^2 = \frac{1}{2}\left[J_{m+1}\left(j_{m,n}\right)\right]^2$$

where the Neumann number $\varepsilon_m = 1$ if $m = 0$ and $\varepsilon_m = 2$ otherwise. The power dissipated by the walls can be found as

$$P = \oint_S \frac{1}{2} R_s \left|\underline{K}\right|^2 dS$$

$$= \frac{2}{\varepsilon_m}\int_0^b \frac{1}{2} R_s \left|\left(\frac{iE_0}{\omega\mu_0} j_{m.n}/b\right) J'_m\left(j_{m,n}r/b\right)\right|^2 2\pi r dr + \frac{1}{2} R_s \left|\left(\frac{iE_0}{\omega\mu_0} j_{m.n}/b\right) J'_m\left(j_{m,n}\right)\right|^2 d2\pi b \frac{1}{\varepsilon_m}$$

$$= \frac{2}{\varepsilon_m} R_s \left(\frac{j_{m,n}}{\omega\mu_0 b}\right)^2 \left|E_0\right|^2 \pi b^2 \int_0^1 \left[J'_m\left(j_{m,n}r\right)\right]^2 r dr + \frac{1}{\varepsilon_m} R_s \left(\frac{j_{m,n}}{\omega\mu_0 b}\right)^2 \left|E_0\right|^2 \left[J'_m\left(j_{m,n}\right)\right]^2 d\pi b$$

where $\underline{K} = \underline{n} \times \underline{H}$ is the electric surface current density on the cavity walls. To carry out the integral we use the identities [9], [10]

$$\int \left[J'_m(x)\right]^2 x dx = \int \left[J_{m-1}(x) - \frac{m}{x} J_m(x)\right]^2 x dx = \int \left[J_{m-1}(x)\right]^2 x dx + m^2 \int \left[J_m(x)\right]^2 \frac{dx}{x}$$

$$-2m \int J_{m-1}(x) J_m(x) dx$$

$$\int \left[J_{m-1}(x)\right]^2 x dx = \frac{1}{2}\left[x J'_{m-1}(x)\right]^2 + \frac{1}{2}\left[x^2 - (m-1)^2\right] J^2_{m-1}(x)$$

$$\int \left[J_m(x)\right]^2 \frac{dx}{x} = \frac{1}{2m}\left[1 + J_0^2(x) + J_m^2(x) - 2\sum_{k=0}^{m} J_k^2(x)\right]$$

and

$$\int J_{m-1}(x) J_m(x) dx = \frac{1}{2} - \frac{1}{2} J_0^2(x) - \sum_{k=1}^{m-1} J_k^2(x)$$

where the final sum is dropped if $m = 1$. Next, collecting terms

$$\int \left[J'_m(x)\right]^2 x dx = \frac{1}{2}\left[x J'_{m-1}(x)\right]^2 + \frac{1}{2}\left[x^2 - (m-1)^2\right] J^2_{m-1}(x) + \frac{m}{2}\left[-1 - J_0^2(x) - J_m^2(x) + 2\sum_{k=0}^{m-1} J_k^2(x)\right]$$

Note that this also works for $m = 0$

$$\int \left[J_0'(x)\right]^2 x dx = \int \left[J_1(x)\right]^2 x dx = \frac{1}{2}\left[xJ_1'(x)\right]^2 + \frac{1}{2}\left(x^2-1\right)J_1^2(x)$$

Thus we can write

$$j_{m,n}^2 \int_0^1 \left[J_m'(j_{m,n}r)\right]^2 r dr = \int_0^{j_{m,n}} \left[J_m'(x)\right]^2 x dx =$$

$$\frac{1}{2}\left[j_{m,n}J_{m-1}'(j_{m,n})\right]^2 + \frac{1}{2}\left[j_{m,n}^2 - (m-1)^2\right]J_{m-1}^2(j_{m,n}) + \frac{m}{2}\left[-1 - J_0^2(j_{m,n}) - J_m^2(j_{m,n}) + 2\sum_{k=0}^{m-1} J_k^2(j_{m,n})\right]$$

Then we can write the power lost as

$$P = \frac{1}{\varepsilon_m} R_s \left(\frac{j_{m,n}}{\omega\mu_0 b}\right)^2 |E_0|^2 \pi b \left[J_m'(j_{m,n})\right]^2 \left[d + bF_m(j_{m,n})\right]$$

where we define

$$\left[J_m'(j_{m,n})\right]^2 F_m(j_{m,n}) =$$

$$\left[J_{m-1}'(j_{m,n})\right]^2 + \left[1 - (m-1)^2/j_{m,n}^2\right]J_{m-1}^2(j_{m,n}) + \frac{m}{j_{m,n}^2}\left[-1 - J_0^2(j_{m,n}) - J_m^2(j_{m,n}) + 2\sum_{k=0}^{m-1} J_k^2(j_{m,n})\right]$$

or

$$F_m(j_{m,n}) = 1 + \frac{m}{j_{m,n}^2 J_{m-1}^2(j_{m,n})}\left[-1 - J_0^2(j_{m,n}) + 2\sum_{k=0}^{m-1} J_k^2(j_{m,n})\right]$$

where we note that $F_0(j_{0,n}) = 1$.

The quality factor is then

$$Q_{m,n} = \frac{\omega W}{P} = \frac{\omega\varepsilon db\left(\omega\mu_0 b/j_{m,n}\right)^2}{2R_s\left[d + bF_m(j_{m,n})\right]}$$

Results for the quality factors from 3.5 GHz to 5 GHz are shown in Figure 17.

As a check we can construct an approximate formula for several half wave variations in the radial and azimuthal directions (and two vector field components) by writing approximately

$$W \approx \frac{1}{2}\mu_0 2H^2 \frac{1}{4}V$$

$$P \approx \frac{1}{2}R_s 2H^2 \frac{1}{4}S$$

$$Q = \frac{\omega W}{P} \approx \frac{\omega\mu_0 V}{R_s S} = \frac{2V}{\delta S}$$

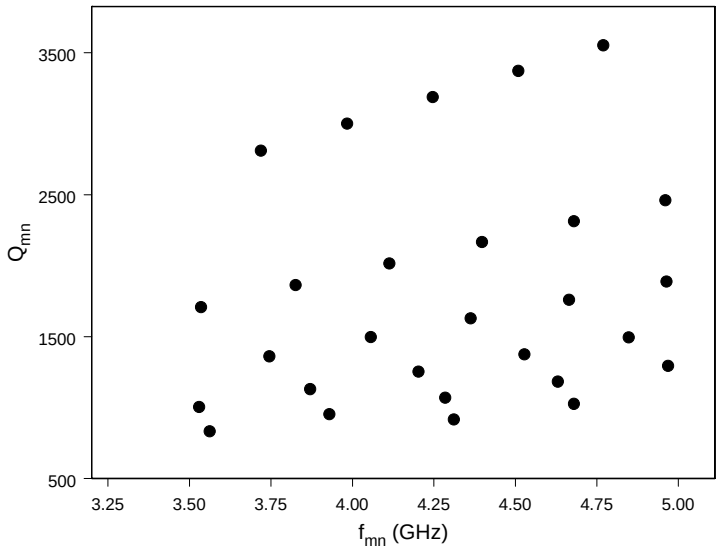

Figure 17. Quality factors versus resonant frequencies for cylindrical disc cavity resonator with shorted outer wall.

where (note that the final equality holds if the walls have free space permeability) the skin depth in the wall is

$$\delta = \sqrt{2/\left(\omega\mu\sigma\right)}$$

the volume is

$$V = d\pi b^2 \approx 3.14 \times 10^{-3} \text{ m}^3$$

and the surface area is

$$S = 2\pi b^2 + 2\pi bd \approx 0.283 \text{ m}^2$$

If we take the walls to be polysilicon with $\sigma \approx 10^5$ S/m then

$$\delta \approx 2.5 \times 10^{-5} \text{ m}$$

The quality factor is then

$$Q \approx 900$$

which is in the ballpark of the lower values in the figure.

The dimensions of the resonator we have been using are length $\ell = 17$ mm, spacing $h = 3$ mm, and wire diameter $2a = 0.125$ mm. Note that for $r < r_m$ where $kr_m \approx m$, there is very little field in the cavity mode. Thus a resonator located at the center of the resonator will not couple well into these modes with many high-order azimuthal variations.

To look at only two parallel walls we consider imaging the current elements of the resonator in the walls. The first subsection below considers the case where the resonator is oriented to be orthogonal to these resonant propagating modes.

12.2 Radiation at Outer Radius

We now consider the quality factor and modal frequencies when the outer periphery allows radiation from two thin walls that simply end at the outer periphery. Because the disc is electrically large in radius at the nominal resonant frequencies of the hairpin resonator we will use a boundary condition associated with a wave propagating between infinite planes and impinging on the ends of the planes. Also because the radiation loss is large compared to the wall loss we will take the walls to be perfectly conducting in this subsection.

The eigenmode frequency near the disc edge is taken as

$$k^2 \sim k_\varphi^2 + k_\rho^2$$

where for the mth azimuthal mode

$$k_\varphi = m/b$$

Thus

LINES RADIATING INTO SPACE

4·6a. Parallel-plate Guide into Space, E-plane.—A semi-infinite parallel-plate guide of zero wall thickness radiating into free space (plane wave in parallel-plate guide incident at angle α relative to normal of terminal plane).

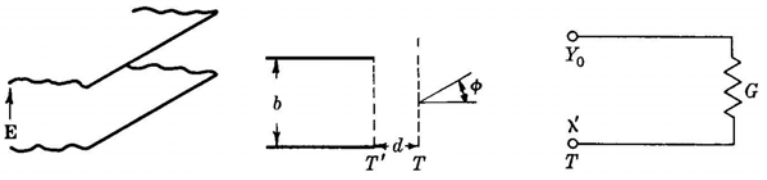

FIG. 4·6-1.

Equivalent-circuit Parameters.—At the reference plane T located at a distance d given by

$$\frac{2\pi d}{\lambda'} = x \ln \frac{2e}{\gamma x} - S_1(x;0,0), \tag{1}$$

the equivalent circuit is simply a conductance

$$\frac{G}{Y_0} = \tanh \frac{\pi x}{2}, \tag{2}$$

where

$$S_1(x;0,0) = \sum_{n=1}^{\infty} \left(\sin^{-1} \frac{x}{n} - \frac{x}{n} \right),$$

$$x = \frac{b}{\lambda'}, \qquad \theta = \frac{4\pi d}{\lambda'}, \qquad \lambda' = \frac{\lambda}{\cos \alpha},$$

$$e = 2.718, \qquad \gamma = 1.781.$$

At the reference plane T' an alternative equivalent circuit shown in Fig. 4·6-2 is characterized by

$$\frac{G'}{Y_0} = \frac{\sinh \pi x}{\cosh \pi x + \cos \theta}, \tag{3}$$

$$\frac{G'}{Y_0} \approx \frac{\pi b}{2\lambda'}, \qquad \text{for } \frac{b}{\lambda'} \ll 1, \tag{3a}$$

$$\frac{B'}{Y_0} = \frac{\sin \theta}{\cosh \pi x + \cos \theta}, \tag{4}$$

$$\frac{B'}{Y_0} \approx \frac{b}{\lambda'} \ln \frac{2e\lambda'}{\gamma b}, \qquad \text{for } \frac{b}{\lambda'} \ll 1. \tag{4a}$$

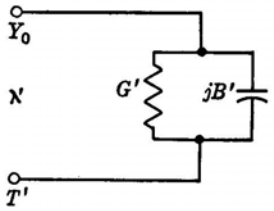

FIG. 4·6-2.

Figure 18. Page from the Waveguide Handbook [11] on circuit elements associated with a wave radiating into free space from between two infinite conducting planes. Note that to translate these results we take $b \to d$ and $b/\lambda' \to X$.

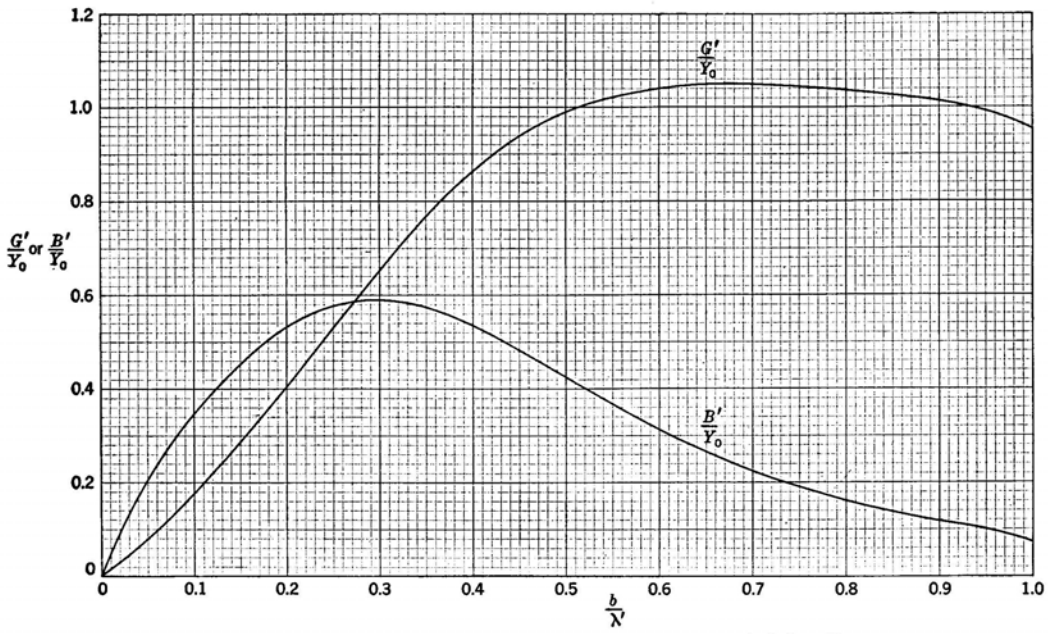

FIG. 4·6-4.—Radiating parallel plate guide, *E*-plane. Admittance at terminal plane T'.

Figure 19. Page from the Waveguide Handbook [11] on circuit elements associated with a wave radiating into free space from between two infinite conducting planes giving the effective circuit conductance and susceptance values. Note that to translate these results we take $b \to d$ and $b/\lambda' \to X$.

$$\cos\alpha = k_\rho/k \sim \sqrt{1-\left(\frac{m}{kb}\right)^2}$$

$$X = \frac{kd}{2\pi}\cos\alpha$$

$$\Theta/2 = X\left[\ln\left(2/X\right)+1-\gamma'\right] - \sum_{n=1}^{\infty}\left[\arcsin\left(X/n\right) - X/n\right]$$

$$\gamma' = 0.5772$$

$$G'/Y_0 = \frac{\sinh\left(\pi X\right)}{\cosh\left(\pi X\right)+\cos\Theta} \sim \frac{1}{4}kd\cos\alpha\,,\; X << 1$$

$$B'/Y_0 = \frac{\sin\Theta}{\cosh\left(\pi X\right)+\cos\Theta} \sim X\left[\ln\left(2/X\right)+1-\gamma'\right]\,,\; X << 1$$

where the admittance per unit width in the parallel plate guide is

$$Y_0 = \frac{1}{d}\sqrt{\varepsilon/\mu_0}$$

Setting the admittance per unit width to

$$Y' = G' - iB'$$

and the surface impedance to

$$Z_s = 1/\left(Y'd\right) = \frac{\sqrt{\mu_0/\varepsilon}}{G'/Y_0 - iB'/Y_0}$$

we then write the outer boundary condition as

$$E_z = -Z_s H_\varphi$$

If the outer boundary condition satisfies $Z_s/\sqrt{\mu_0/\varepsilon} << 1$ or if $Y' >> Y_0$ we can use the previous perturbation theory to find the quality factor. However from the figure for G'/Y_0 and B'/Y_0 if $X << 1$ an open circuit boundary condition is a more appropriate starting point for the perturbation calculation.

12.2.1high impedance load

In this case we write

$$H_\varphi\left(r=b\right) = 0$$

and thus the solution is

$$E_z = E_0 J_m\left(j'_{m,n}r/b\right)\cos\left(m\varphi\right)$$

$$i\omega\mu_0 H_\varphi = -\left(E_0 j_{m.n}/b\right) J'_m\left(j'_{m,n} r/b\right)\cos\left(m\varphi\right)$$

where

$$J'_m\left(j'_{m,n}\right) = 0$$

Note that

$$j'_{m,1} \sim m + 0.8086165m^{1/3} - 0.072490m^{-1/3} - 0.05097m^{-1} + 0.0094m^{-5/3} + \cdots$$

$$j'_{m,n} \sim \left(m + n/2 - 1/4\right)\pi\ ,\ n >> m$$

The energy stored is then

$$W = \int_V \frac{1}{2}\varepsilon\left|\underline{E}\right|^2 dV = \frac{d}{\varepsilon_m}\int_0^b \frac{1}{2}\varepsilon\left|E_0 J_m\left(j'_{m,n} r/b\right)\right|^2 2\pi r dr = \frac{1}{2\varepsilon_m}\varepsilon d\pi b^2\left|E_0\right|^2\left(1 - m^2/j'^2_{m,n}\right)\left[J_m\left(j'_{m,n}\right)\right]^2$$

The power lost is then

$$P = \frac{1}{2}d\,\mathrm{Re}\left(Y'd\right)\int_0^{2\pi}\left|E_z\left(b,\varphi\right)\right|^2 bd\varphi = \frac{1}{\varepsilon_m}\pi b d^2 G'\left|E_0\right|^2\left[J_m\left(j'_{m,n}\right)\right]^2$$

The quality factor is then ($j'_{15,1} \approx 16.961153$)

$$Q = \frac{\omega\varepsilon b\left(1 - m^2/j'^2_{m,n}\right)}{2dG'} \sim \frac{2b\left(1 - m^2/j'^2_{m,n}\right)}{d\sqrt{1 - \left(\frac{m}{kb}\right)^2}}$$

For $m = 15$, $n = 1$, $j'_{15,1} \approx 16.961153$, and $f = 4.1$ GHz

$$Q \approx 7$$

For $m = 0$, $n = 11$, $j'_{1,11} \approx 16.5$, and $f = 4.1$ GHz

$$Q \approx 16$$

12.2.2low impedance load

The short circuit perturbation theory gives

$$P = \frac{1}{2}d\,\mathrm{Re}\left(Z_s\right)\int_0^{2\pi}\left|H_\varphi\left(b,\varphi\right)\right|^2 bd\varphi = \frac{1}{\omega^2\mu_0^2\varepsilon_m}\pi b d\,\mathrm{Re}\left(Z_s\right)\left|E_0\right|^2\left(j_{m.n}/b\right)^2\left[J'_m\left(j_{m,n}\right)\right]^2$$

$$\mathrm{Re}\left(Z_s\right) = \frac{\sqrt{\mu_0/\varepsilon}G'/Y_0}{\left(G'/Y_0\right)^2 + \left(B'/Y_0\right)^2} \sim \frac{\left(\pi/2\right)\sqrt{\mu_0/\varepsilon}/X}{\pi^2/4 + \left[\ln\left(2/X\right) + 1 - \gamma'\right]^2}$$

$$X = \frac{kd}{2\pi}\sqrt{1 - \left(\frac{m}{kb}\right)^2}$$

Using the energy stored

$$W = \frac{1}{2\varepsilon_m}\varepsilon d\pi b^2 \left|E_0\right|^2 \left[J'_m\left(j_{m,n}\right)\right]^2$$

the quality factor is

$$Q = \frac{\left(kb\right)^3 \sqrt{\mu_0/\varepsilon}}{2\,\mathrm{Re}\left(Z_s\right) j_{m.n}^2}$$

If there are no large frequency shifts caused by the outer impedance boundary condition then $j_{mn} \sim kb$

$$Q \sim \frac{\left(kb\right)}{2\,\mathrm{Re}\left(Z_s/\sqrt{\mu_0/\varepsilon}\right)} \sim kb\frac{\pi^2/4 + \left[\ln\left(2/X\right) + 1 - \gamma'\right]^2}{\pi/X}$$

$$X = \frac{kd}{2\pi}\sqrt{1 - \left(\frac{m}{kb}\right)^2}$$

Now for $m = 15,\ f = 4.14$ GHz

$$X \approx 0.07$$

$$Q \sim 6.5$$

For $m = 1$ (in this case the perturbation theory may not be justified)

$$X \approx 0.35$$

$$Q \sim 13.8$$

12.2.3transmission line solution

Suppose we consider the region near $r = 0$ to provide a drive so that the general solution in the disc cavity is

$$E_z = E_0\left[J_m\left(kr\right) + RY_m\left(kr\right)\right]\cos\left(m\varphi\right)$$

$$i\omega\mu_0 H_\varphi = -\left(E_0 k\right)\left[J'_m\left(kr\right) + RY'_m\left(kr\right)\right]\cos\left(m\varphi\right)$$

The impedance boundary condition gives

$$Y' dE_z\left(b,\varphi\right) = -H_\varphi\left(b,\varphi\right)$$

or

$$R = -\frac{J'_m(kb) - i\sqrt{\mu_0/\varepsilon}Y'dJ_m(kb)}{Y'_m(kb) - i\sqrt{\mu_0/\varepsilon}Y'dY_m(kb)}$$

Then if we consider the normalized ratio of electric to magnetic fields (voltage to current) along the radial transmission line

$$-\frac{E_z(r,\varphi)/H_\varphi(r,\varphi)}{\sqrt{\mu_0/\varepsilon}} = i\frac{J_m(kr)\left[Y'_m(kb) - i\sqrt{\mu_0/\varepsilon}Y'dY_m(kb)\right] - Y_m(kr)\left[J'_m(kb) - i\sqrt{\mu_0/\varepsilon}Y'dJ_m(kb)\right]}{J'_m(kr)\left[Y'_m(kb) - i\sqrt{\mu_0/\varepsilon}Y'dY_m(kb)\right] - Y'_m(kr)\left[J'_m(kb) - i\sqrt{\mu_0/\varepsilon}Y'dJ_m(kb)\right]}$$

$$\sqrt{\mu_0/\varepsilon}Y'd = Y'/Y_0 = G'/T_0 - iB'/Y_0$$

$$G'/Y_0 = \frac{\sinh(\pi X)}{\cosh(\pi X) + \cos\Theta}$$

$$B'/Y_0 = \frac{\sin\Theta}{\cosh(\pi X) + \cos\Theta}$$

$$X = \frac{kd}{2\pi}\sqrt{1 - \left(\frac{m}{kb}\right)^2}$$

$$\Theta/2 = X\left[\ln(2/X) + 1 - \gamma'\right] - \sum_{n=1}^{\infty}\left[\arcsin(X/n) - X/n\right]$$

$$\gamma' = 0.5772$$

12.3 Two Wall Interaction with Horizontal Orientation

The two wall interaction will be investigated using images. Although we could include reflection coefficients at the walls to approximately account for losses, because the operating frequency will be below transverse resonance we can approximately use perfectly conducting images for this orientation. Here we are interested in the case where the resonator is centered to minimize quasistatic interaction with the walls and where it is oriented so that the walls are at $y = \pm d/2$, to minimize coupling to the E_y propagating modes (here we return to the notation where z is along the resonator arms and y is perpendicular to the cavity walls). Figure 23 shows the image summations with reversals of sign on each reflection.

The two components of the vector potential thus become

$$A_z(x,y,z) =$$

$$\frac{\mu_0}{4\pi}\int_0^\ell I(z')\sum_{n=-\infty}^{\infty}(-1)^n\left[\frac{e^{ik\sqrt{(x-h/2)^2+(y-nd)^2+(z-z')^2}}}{\sqrt{(x-h/2)^2+(y-nd)^2+(z-z')^2}} - \frac{e^{ik\sqrt{(x+h/2)^2+(y-nd)^2+(z-z')^2}}}{\sqrt{(x+h/2)^2+(y-nd)^2+(z-z')^2}}\right]dz'$$

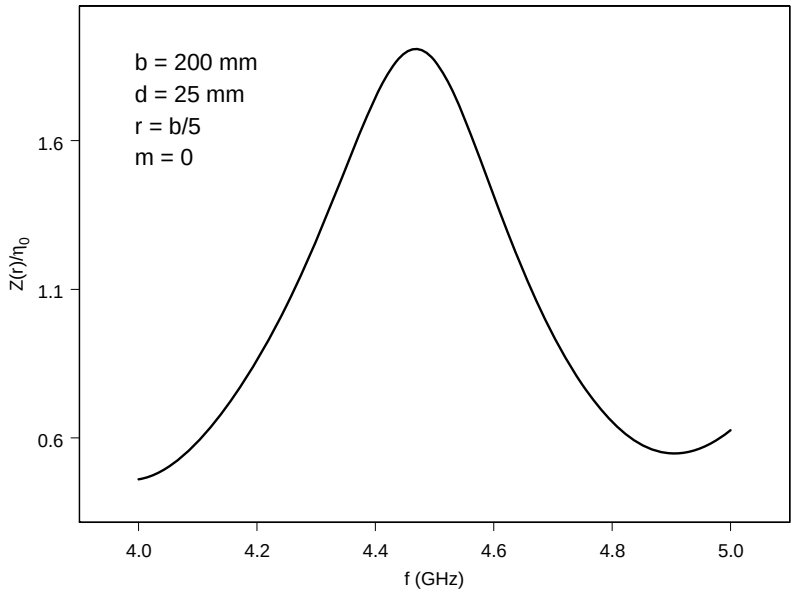

Figure 20. Impedance at $r = b/5$ for $m = 0$. The quality factor of the peak appears to be near 15.

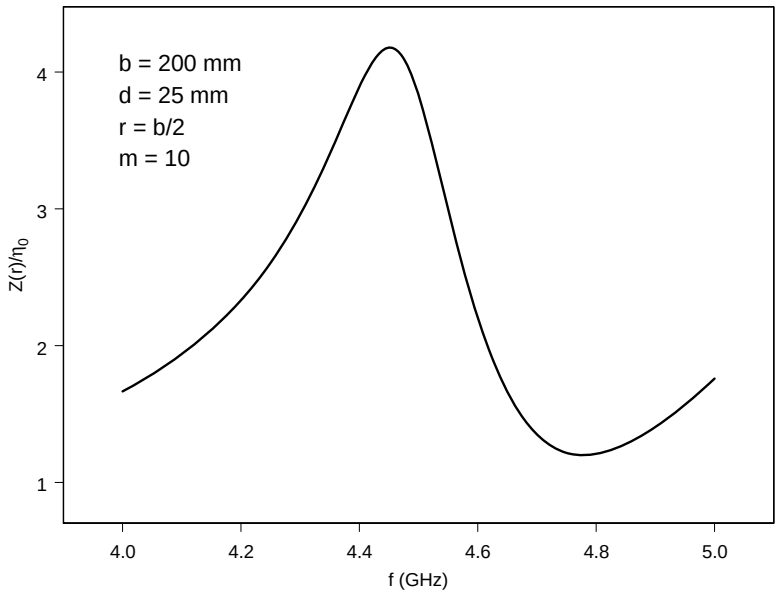

Figure 21. The quality factor of the peak appears to be near 18. It was necessary to move the obervation point out to $r = b/2$ because of the small size near $r = 0$ for $m = 10$.

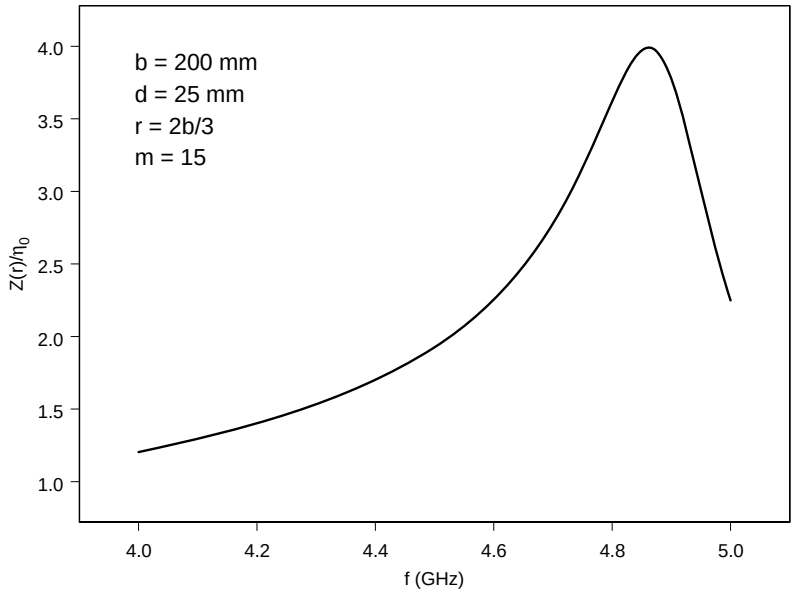

Figure 22. The quality factor of the peak appears to be near 19.

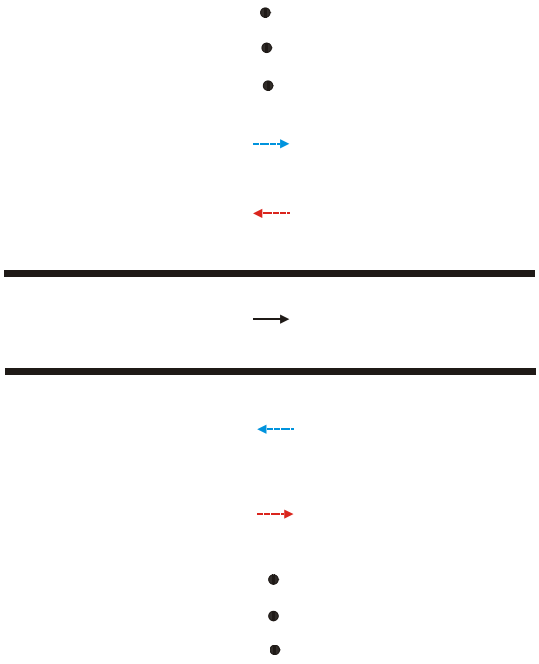

Figure 23. Set of images of resonator in walls of disc cavity when the normal to the plane of the resonator is also normal to the cylindrical disc cavity.

$$A_x(x,y,z) = -\frac{\mu_0}{4\pi} I(\ell) \sum_{n=-\infty}^{\infty} (-1)^n \int_{-h/2}^{h/2} \frac{e^{ik\sqrt{(x-x')^2+(y-nd)^2+(z-\ell)^2}}}{\sqrt{(x-x')^2+(y-nd)^2+(z-\ell)^2}} dx'$$

where we have approximated the "shorted" end as having constant current and taken the load current to be directed toward the $+x$ direction and the images are in the y direction, perpendicular to the cavity walls. Our interest here is in assessing the magnitude of the image response. Therefore let us take the scattered potential to be

$$A_z^s(x,0,z) =$$

$$\frac{\mu_0}{4\pi} \int_0^{\ell} I(z') \sum_{\substack{n=-\infty \\ n\neq 0}}^{\infty} (-1)^n \left[\frac{e^{ik\sqrt{(x-h/2)^2+(nd)^2+(z-z')^2}}}{\sqrt{(x-h/2)^2+(nd)^2+(z-z')^2}} - \frac{e^{ik\sqrt{(x+h/2)^2+(nd)^2+(z-z')^2}}}{\sqrt{(x+h/2)^2+(nd)^2+(z-z')^2}} \right] dz'$$

$$A_x^s(x,0,z) \approx -\frac{\mu_0}{4\pi} hI(\ell) \sum_{\substack{n=-\infty \\ n\neq 0}}^{\infty} (-1)^n \frac{e^{ik\sqrt{x^2+(nd)^2+(z-\ell)^2}}}{\sqrt{x^2+(nd)^2+(z-\ell)^2}}$$

We will also approximate the current distribution along the transmission line as the quarter wave form

$$I(z') \approx I(\ell) \sin(k_0 z') = I(\ell) \sin\left(\frac{\pi z'}{2\ell}\right)$$

The electric field is given by

$$\underline{E} = \frac{i}{\omega\varepsilon\mu_0} \nabla \times \nabla \times \underline{A} = \frac{i}{\omega\varepsilon\mu_0} \left[\nabla(\nabla \cdot \underline{A}) + k^2 \underline{A} \right]$$

or

$$E_z^s = \frac{i}{\omega\varepsilon\mu_0} \left(\frac{\partial^2}{\partial z \partial x} A_x^s + \frac{\partial^2}{\partial z^2} A_z^s + k^2 A_z^s \right)$$

and because the x segment is electrically short we can write

$$E_x^s \approx \frac{i}{\omega\varepsilon\mu_0} \left(\frac{\partial^2}{\partial x \partial z} A_z^s + \frac{\partial^2}{\partial x^2} A_x^s + k^2 A_x^s \right) \approx \frac{i}{\omega\varepsilon\mu_0} k^2 A_x^s$$

The open circuit voltage at the drive point due to the images can be found using reciprocity [5]. The result is

$$V_{oc}^s = -\frac{1}{I(\ell)} \int_C \underline{E}^s \cdot \underline{I} ds$$

This is still a rather complicated set of equations to implement. However because the resonator is operating near the relatively short quarter wave length, and because of the spacing between the images and the resonator, it is a reasonable approximation to use an average point current element for the z-directed current segments. We place the current elements at location

$$z' = \int_0^\ell z \sin\left(\frac{\pi z}{2\ell}\right) dz = \frac{2\ell}{\pi}\left[\frac{2\ell}{\pi}\sin\left(\frac{\pi z}{2\ell}\right) - z\cos\left(\frac{\pi z}{2\ell}\right)\right]_0^\ell = \frac{2}{\pi}\ell$$

with moments

$$I(\ell)\int_0^\ell \sin\left(\frac{\pi z}{2\ell}\right) dz = I(\ell)\left[-\frac{2\ell}{\pi}\cos\left(\frac{\pi z}{2\ell}\right)\right]_0^\ell = I(\ell)\,\ell\frac{2}{\pi}$$

Then

$$A_z^s(x,0,z) \approx$$

$$\frac{\mu_0}{4\pi} I(\ell)\,\ell\frac{2}{\pi}\sum_{\substack{n=-\infty\\ n\neq 0}}^{\infty}(-1)^n\left[\frac{e^{ik\sqrt{(x-h/2)^2+(nd)^2+(z-\ell 2/\pi)^2}}}{\sqrt{(x-h/2)^2+(nd)^2+(z-\ell 2/\pi)^2}} - \frac{e^{ik\sqrt{(x+h/2)^2+(nd)^2+(z-\ell 2/\pi)^2}}}{\sqrt{(x+h/2)^2+(nd)^2+(z-\ell 2/\pi)^2}}\right]$$

and the open circuit voltage from the images is

$$-V_{oc}^s \approx -E_x^s(0,0,\ell)\,h + \left[E_z^s(h/2,0,\ell 2/\pi) - E_z^s(-h/2,0,\ell 2/\pi)\right]\ell\frac{2}{\pi}$$

Inserting the above expressions gives

$$E_x^s \approx \frac{i}{\omega\varepsilon\mu_0}\frac{\mu_0}{4\pi} I(\ell)\,\ell\frac{2}{\pi}$$

$$\sum_{\substack{n=-\infty\\ n\neq 0}}^{\infty}(-1)^n\frac{\partial^2}{\partial x\partial z}\left[\frac{e^{ik\sqrt{(x-h/2)^2+(nd)^2+(z-\ell 2/\pi)^2}}}{\sqrt{(x-h/2)^2+(nd)^2+(z-\ell 2/\pi)^2}} - \frac{e^{ik\sqrt{(x+h/2)^2+(nd)^2+(z-\ell 2/\pi)^2}}}{\sqrt{(x+h/2)^2+(nd)^2+(z-\ell 2/\pi)^2}}\right]$$

$$-\frac{i}{\omega\varepsilon\mu_0}k^2\frac{\mu_0}{4\pi}hI(\ell)\sum_{\substack{n=-\infty\\ n\neq 0}}^{\infty}(-1)^n\frac{e^{ik\sqrt{x^2+(nd)^2+(z-\ell)^2}}}{\sqrt{x^2+(nd)^2+(z-\ell)^2}}$$

or

$$E_x^s(0,0,\ell) \approx -\frac{i}{\omega\varepsilon\mu_0}k^2\frac{\mu_0}{2\pi}hI(\ell)\sum_{n=1}^{\infty}(-1)^n\frac{e^{iknd}}{nd}$$

$$+\frac{i}{\omega\varepsilon\mu_0}\frac{\mu_0}{2\pi}I(\ell)\,\ell^2(1-2/\pi)\frac{2}{\pi}h\sum_{n=1}^{\infty}(-1)^n\frac{e^{ik\sqrt{(nd)^2+\ell^2(1-2/\pi)^2}}}{\left\{(nd)^2+\ell^2(1-2/\pi)^2\right\}^{3/2}}$$

$$\left[k^2 + \frac{i3k}{\left\{(nd)^2+\ell^2(1-2/\pi)^2\right\}^{1/2}} - \frac{3}{\left\{(nd)^2+\ell^2(1-2/\pi)^2\right\}}\right]$$

and

$$E_z^s = -\frac{i}{\omega\varepsilon\mu_0}\frac{\mu_0}{4\pi}hI\left(\ell\right)\sum_{\substack{n=-\infty\\n\neq 0}}^{\infty}\left(-1\right)^n\frac{\partial^2}{\partial z\partial x}\frac{e^{ik\sqrt{x^2+(nd)^2+(z-\ell)^2}}}{\sqrt{x^2+\left(nd\right)^2+\left(z-\ell\right)^2}}$$

$$+\frac{i}{\omega\varepsilon\mu_0}\frac{\mu_0}{4\pi}I\left(\ell\right)\ell\frac{2}{\pi}\sum_{\substack{n=-\infty\\n\neq 0}}^{\infty}\left(-1\right)^n\frac{\partial^2}{\partial z^2}\left[\frac{e^{ik\sqrt{(x-h/2)^2+(nd)^2+(z-\ell 2/\pi)^2}}}{\sqrt{\left(x-h/2\right)^2+\left(nd\right)^2+\left(z-\ell 2/\pi\right)^2}}-\frac{e^{ik\sqrt{(x+h/2)^2+(nd)^2+(z-\ell 2/\pi)^2}}}{\sqrt{\left(x+h/2\right)^2+\left(nd\right)^2+\left(z-\ell 2/\pi\right)^2}}\right]$$

$$+\frac{i}{\omega\varepsilon\mu_0}k^2\frac{\mu_0}{4\pi}I\left(\ell\right)\ell\frac{2}{\pi}\sum_{\substack{n=-\infty\\n\neq 0}}^{\infty}\left(-1\right)^n\left[\frac{e^{ik\sqrt{(x-h/2)^2+(nd)^2+(z-\ell 2/\pi)^2}}}{\sqrt{\left(x-h/2\right)^2+\left(nd\right)^2+\left(z-\ell 2/\pi\right)^2}}-\frac{e^{ik\sqrt{(x+h/2)^2+(nd)^2+(z-\ell 2/\pi)^2}}}{\sqrt{\left(x+h/2\right)^2+\left(nd\right)^2+\left(z-\ell 2/\pi\right)^2}}\right]$$

or

$$E_z^s\left(h/2,0,\ell 2/\pi\right)-E_z^s\left(-h/2,0,\ell 2/\pi\right)\approx\frac{i}{\omega\varepsilon\mu_0}\frac{\mu_0}{\pi}I\left(\ell\right)\ell\frac{2}{\pi}$$

$$\sum_{n=1}^{\infty}\left(-1\right)^n\left[k^2\left\{\frac{e^{iknd}}{nd}-\frac{e^{ik\sqrt{h^2+(nd)^2}}}{\sqrt{h^2+\left(nd\right)^2}}\right\}+ik\left\{\frac{e^{iknd}}{\left(nd\right)^2}-\frac{e^{ik\sqrt{h^2+(nd)^2}}}{h^2+\left(nd\right)^2}\right\}-\left\{\frac{e^{iknd}}{\left(nd\right)^3}-\frac{e^{ik\sqrt{h^2+(nd)^2}}}{\left\{h^2+\left(nd\right)^2\right\}^{3/2}}\right\}\right]$$

$$-\frac{i}{\omega\varepsilon\mu_0}\frac{\mu_0}{2\pi}h^2I\left(\ell\right)\ell\left(1-2/\pi\right)\sum_{n=1}^{\infty}\left(-1\right)^n\frac{e^{ik\sqrt{(nd)^2+\ell^2(1-2/\pi)^2}}}{\left\{\left(nd\right)^2+\ell^2\left(1-2/\pi\right)^2\right\}^{3/2}}$$

$$\left[k^2+\frac{i3k}{\left\{\left(nd\right)^2+\ell^2\left(1-2/\pi\right)^2\right\}^{1/2}}-\frac{3}{\left(nd\right)^2+\ell^2\left(1-2/\pi\right)^2}\right]$$

$$\approx\frac{i}{\omega\varepsilon\mu_0}\frac{\mu_0}{\pi}I\left(\ell\right)\ell\frac{2}{\pi}h^2\sum_{n=1}^{\infty}\left(-1\right)^n\frac{e^{iknd}}{\left(nd\right)^2}\left[k^2\left\{-ik/2+\frac{1}{\left(nd\right)}\right\}+\frac{i3k}{2\left(nd\right)^2}-\frac{3}{2\left(nd\right)^3}\right]$$

$$-\frac{i}{\omega\varepsilon\mu_0}\frac{\mu_0}{2\pi}h^2I\left(\ell\right)\ell\left(1-2/\pi\right)\sum_{n=1}^{\infty}\left(-1\right)^n\frac{e^{ik\sqrt{(nd)^2+\ell^2(1-2/\pi)^2}}}{\left\{\left(nd\right)^2+\ell^2\left(1-2/\pi\right)^2\right\}^{3/2}}$$

$$\left[k^2+\frac{i3k}{\left\{\left(nd\right)^2+\ell^2\left(1-2/\pi\right)^2\right\}^{1/2}}-\frac{3}{\left(nd\right)^2+\ell^2\left(1-2/\pi\right)^2}\right]$$

Therefore

$$\left[\pi i\omega\varepsilon/\left(k^3h^2\right)\right]V_{oc}^s/I\left(\ell\right)\approx\frac{1}{2}\sum_{n=1}^{\infty}\left(-1\right)^n\frac{e^{iknd}}{nkd}$$

$$+\left(k\ell\frac{2}{\pi}\right)^2\sum_{n=1}^{\infty}(-1)^n\frac{e^{iknd}}{(nkd)^2}\left[\left(-i/2+\frac{1}{nkd}\right)+\frac{i3}{2(nkd)^2}-\frac{3}{2(nkd)^3}\right]$$

$$-(k\ell)^2\frac{2}{\pi}(1-2/\pi)\sum_{n=1}^{\infty}(-1)^n\frac{e^{ik\sqrt{(nd)^2+\ell^2(1-2/\pi)^2}}}{\left\{(nkd)^2+(k\ell)^2(1-2/\pi)^2\right\}^{3/2}}$$

$$\left[1+\frac{i3}{\left\{(nkd)^2+(k\ell)^2(1-2/\pi)^2\right\}^{1/2}}-\frac{3}{(nkd)^2+(k\ell)^2(1-2/\pi)^2}\right]$$

Noting that

$$\sum_{n=1}^{\infty}(-1)^n\frac{e^{inx}}{n}=-\ln\left(1+e^{ix}\right)$$

gives (note that the other sums are rapidly convergent)

$$\left[\pi i\omega\varepsilon/\left(k^3h^2\right)\right]V_{oc}^s/I(\ell)\approx-\frac{1}{2kd}\ln\left(1+e^{ikd}\right)$$

$$+\left(k\ell\frac{2}{\pi}\right)^2\sum_{n=1}^{\infty}(-1)^n\frac{e^{iknd}}{(nkd)^2}\left[\left(-i/2+\frac{1}{nkd}\right)+\frac{i3}{2(nkd)^2}-\frac{3}{2(nkd)^3}\right]$$

$$-(k\ell)^2\frac{2}{\pi}(1-2/\pi)\sum_{n=1}^{\infty}(-1)^n\frac{e^{ik\sqrt{(nd)^2+\ell^2(1-2/\pi)^2}}}{\left\{(nkd)^2+(k\ell)^2(1-2/\pi)^2\right\}^{3/2}}$$

$$\left[1+\frac{i3}{\left\{(nkd)^2+(k\ell)^2(1-2/\pi)^2\right\}^{1/2}}-\frac{3}{(nkd)^2+(k\ell)^2(1-2/\pi)^2}\right]$$

We note that $kd\approx 2.1\approx 0.68\pi$ and therefore the argument of the logarithm is not near zero. Furthermore $k\ell\approx 1.46$ and $(kh)^2\approx 0.066$, $k/(\omega\varepsilon_0)=\sqrt{\mu_0/\varepsilon_0}\approx 120\pi$ ohms. Thus we find that $V_{oc}^s/I(\ell)$ is in the vicinity of an ohm. Away from resonance this is a small effect (see preceding graphs). However at resonance this can lead to a shift in frequency and in very little radiation damping. The figures show the real and imaginary parts. We have used the approximation

$$\left[\pi i\omega\varepsilon/\left(k^3h^2\right)\right]V_{oc}^s/I(\ell)\approx-\frac{1}{2kd}\ln\left(1+e^{ikd}\right)$$

These values of reactance indicate that we expect a very small shift in frequency (since the impedance at the 3 dB point of the resonance is a couple of ohms compared with tenths of an ohm reactance from the walls of the cavity). However, because the modes are cutoff for this polarization, the radiation quality factor would go to infinity (the polysilicon wall loss will make it finite, but because the Q of the cavity will be large there would be a large increase in the resonator Q). The real impedance from the walls cancels the real impedance of the resonator in free space since radiation is suppressed by the fact that the modes with projections on the resonator current are cutoff (the reason for the small difference in magnitude between

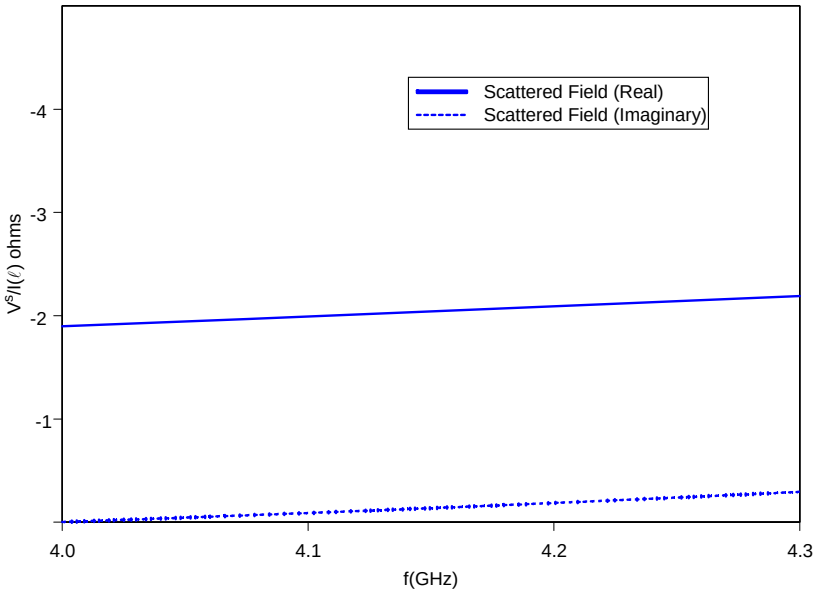

Figure 24. Real and imaginary parts of the scattered voltage at the drive point of the resonator (resulting from the image currents in the resonator walls) divided by the drive current. This is the horizontal orientation where the resonator does not couple into the propagating disc modes of the cavity. The suppression of resonator radiation by the perfectly conducting cavity walls leads to a negative real part in the scattered voltage. This means that the resonator quality factor is increased by operation in the cavity.

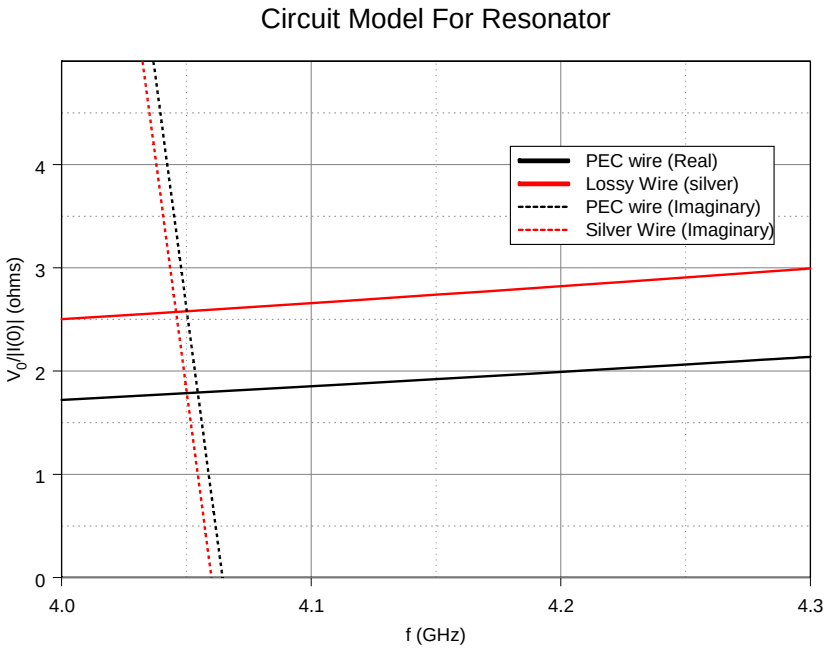

Figure 25. Real and imaginary parts of the ratio of drive voltage divided by drive current (without cavity wall effects present) for both a perfectly conducting and a silver wire resonator.

the two graphs is the approximations made in the scattered field). This effect therefore increases the Q of the resonator and it is then predominantly due to the wire loss.

The outer load at the edge of the resonator cavity did not come into the picture with this orientation because there was no coupling to the propagating modes in the disc region. The vertical orientation will couple to these modes.

12.4 Two Wall Interaction with Vertical Orientation

The propagating modes in the disc region are excited by the vertical orientation of the resonator. Because we expect that a better model for the disc cavity includes radiation at the open edges of the discs we will only treat this lower Q case.

A question impacting the size of the wall interaction is the balance of the two arms and drive geometry of the resonator. For example, if the drive is unbalanced with respect to the center line of the resonator, then common mode drives of the resonator arms will couple to the load, whereas the balanced case will not. We will look at the two wall interaction with a balanced resonator.

We again take the z axis along the longer arms of the resonator and the y axis perpendicular to the discs as well as along the short leg of the resonator.

The two components of the vector potential thus become (here there are no sign changes associated with the images as shown in Figure 26)

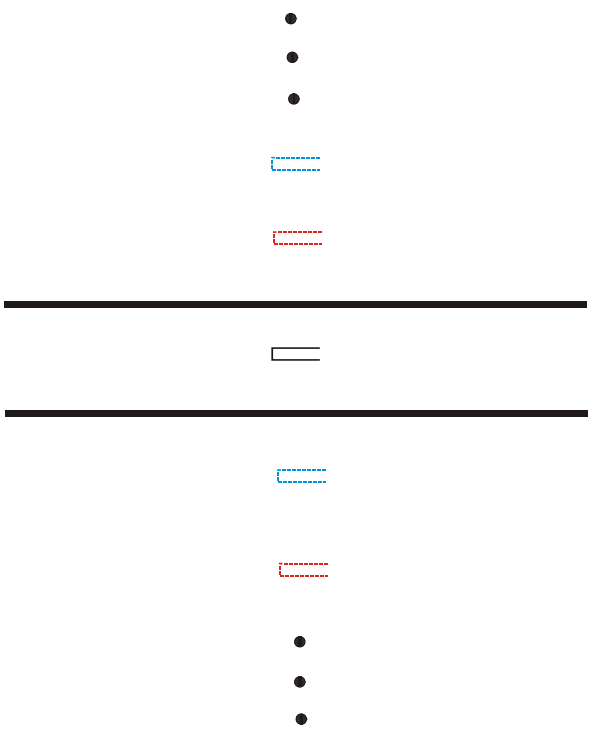

Figure 26. Set of images in cylindrcal walls of disc cavity when normal to the plane of the resonator is parallel to walls of disc cavity.

$$A_z(x,y,z) =$$

$$\frac{\mu_0}{4\pi}\int_0^\ell I(z')\sum_{n=-\infty}^{\infty}\left[\frac{e^{ik\sqrt{x^2+(y-nd-h/2)^2+(z-z')^2}}}{\sqrt{x^2+(y-nd-h/2)^2+(z-z')^2}}-\frac{e^{ik\sqrt{x^2+(y-nd+h/2)^2+(z-z')^2}}}{\sqrt{x^2+(y-nd+h/2)^2+(z-z')^2}}\right]dz'$$

$$A_y(x,y,z) = -\frac{\mu_0}{4\pi}I(\ell)\sum_{n=-\infty}^{\infty}\int_{-h/2}^{h/2}\frac{e^{ik\sqrt{x^2+(y-nd)^2+(z-\ell)^2}}}{\sqrt{x^2+(y-y'-nd)^2+(z-\ell)^2}}dy'$$

where we have approximated the "shorted" end as having constant current and taken the load current to be directed toward the $-y$ direction and the images are in the y direction, perpendicular to the cavity walls. Our interest here is in assessing the magnitude of the image response. Therefore let us take the scattered potential to be

$$A_z^s(x,y,z) =$$

$$\frac{\mu_0}{4\pi}\int_0^\ell I(z')\sum_{\substack{n=-\infty\\ n\neq 0}}^{\infty}\left[\frac{e^{ik\sqrt{x^2+(y-nd-h/2)^2+(z-z')^2}}}{\sqrt{x^2+(y-nd-h/2)^2+(z-z')^2}}-\frac{e^{ik\sqrt{x^2+(y-nd+h/2)^2+(z-z')^2}}}{\sqrt{x^2+(y-nd+h/2)^2+(z-z')^2}}\right]dz'$$

$$A_y^s(x,y,z) \approx -\frac{\mu_0}{4\pi}hI(\ell)\sum_{\substack{n=-\infty\\ n\neq 0}}^{\infty}\frac{e^{ik\sqrt{x^2+(y-nd)^2+(z-\ell)^2}}}{\sqrt{x^2+(y-nd)^2+(z-\ell)^2}}$$

We will also approximate the current distribution along the transmission line as the quarter wave form

$$I(z') \approx I(\ell)\sin(k_0 z') = I(\ell)\sin\left(\frac{\pi z'}{2\ell}\right)$$

The electric field is given by

$$\underline{E} = \frac{i}{\omega\varepsilon\mu_0}\nabla\times\nabla\times\underline{A} = \frac{i}{\omega\varepsilon\mu_0}\left[\nabla(\nabla\cdot\underline{A}) + k^2\underline{A}\right]$$

or

$$E_z^s = \frac{i}{\omega\varepsilon\mu_0}\left(\frac{\partial^2}{\partial z\partial y}A_y^s + \frac{\partial^2}{\partial z^2}A_z^s + k^2A_z^s\right)$$

and because the y segment is electrically short we can write

$$E_y^s \approx \frac{i}{\omega\varepsilon\mu_0}\left(\frac{\partial^2}{\partial y\partial z}A_z^s + \frac{\partial^2}{\partial y^2}A_y^s + k^2A_y^s\right) \approx \frac{i}{\omega\varepsilon\mu_0}\left(\frac{\partial^2}{\partial y^2} + k^2\right)A_y^s$$

The open circuit voltage at the drive point due to the images can be found using reciprocity [5]. The result is

$$V_{oc}^{s}=-\frac{1}{I\left(\ell\right)}\int_{C}\underline{E}^{s}\cdot\underline{I}ds$$

This is still a rather complicated set of equations to implement. However because the resonator is operating near the relatively short quarter wave length, and because of the spacing between the images and the resonator, it is a reasonable approximation to use an average point current element for the z-directed current segments. We place the current elements at location

$$z'\int_{0}^{\ell}\sin\left(\frac{\pi z}{2\ell}\right)dz=\int_{0}^{\ell}z\sin\left(\frac{\pi z}{2\ell}\right)dz=\left(\frac{2\ell}{\pi}\right)^{2}\int_{0}^{\pi/2}x\sin xdx=\left(\frac{2\ell}{\pi}\right)^{2}\left[\sin x-x\cos x\right]_{0}^{\pi/2}=\left(\frac{2\ell}{\pi}\right)^{2}$$

or

$$z'=\ell\frac{2}{\pi}$$

with moments

$$I\left(\ell\right)\int_{0}^{\ell}\sin\left(\frac{\pi z}{2\ell}\right)dz=I\left(\ell\right)\left[-\frac{2\ell}{\pi}\cos\left(\frac{\pi z}{2\ell}\right)\right]_{0}^{\ell}=I\left(\ell\right)\ell\frac{2}{\pi}$$

Then

$$A_{z}^{s}\left(x,y,z\right)\approx$$

$$\frac{\mu_{0}}{4\pi}I\left(\ell\right)\ell\frac{2}{\pi}\sum_{\substack{n=-\infty\\n\neq0}}^{\infty}\left[\frac{e^{ik\sqrt{x^{2}+\left(y-nd-h/2\right)^{2}+\left(z-\ell2/\pi\right)^{2}}}}{\sqrt{x^{2}+\left(y-nd-h/2\right)^{2}+\left(z-\ell2/\pi\right)^{2}}}-\frac{e^{ik\sqrt{x^{2}+\left(y-nd+h/2\right)^{2}+\left(z-\ell2/\pi\right)^{2}}}}{\sqrt{x^{2}+\left(y-nd+h/2\right)^{2}+\left(z-\ell2/\pi\right)^{2}}}\right]$$

and the open circuit voltage from the images is

$$-V_{oc}^{s}\approx-E_{y}^{s}\left(0,0,\ell\right)h+\left[E_{z}^{s}\left(0,h/2,\ell2/\pi\right)-E_{z}^{s}\left(0,-h/2,\ell2/\pi\right)\right]\ell\frac{2}{\pi}$$

Inserting the above expressions gives

$$E_{z}^{s}\left(0,\pm h/2,z\right)=\pm\frac{\mu_{0}}{4\pi}I\left(\ell\right)\ell\frac{2}{\pi}\frac{i}{\omega\varepsilon\mu_{0}}k^{2}\sum_{\substack{n=-\infty\\n\neq0}}^{\infty}\left[\frac{e^{ik\sqrt{\left(nd\right)^{2}+\left(z-\ell2/\pi\right)^{2}}}}{\sqrt{\left(nd\right)^{2}+\left(z-\ell2/\pi\right)^{2}}}-\frac{e^{ik\sqrt{\left(nd-h\right)^{2}+\left(z-\ell2/\pi\right)^{2}}}}{\sqrt{\left(nd-h\right)^{2}+\left(z-\ell2/\pi\right)^{2}}}\right]$$

$$\pm\frac{\mu_{0}}{4\pi}I\left(\ell\right)\ell\frac{2}{\pi}\frac{i}{\omega\varepsilon\mu_{0}}\frac{\partial^{2}}{\partial z^{2}}\sum_{\substack{n=-\infty\\n\neq0}}^{\infty}\left[\frac{e^{ik\sqrt{\left(nd\right)^{2}+\left(z-\ell2/\pi\right)^{2}}}}{\sqrt{\left(nd\right)^{2}+\left(z-\ell2/\pi\right)^{2}}}-\frac{e^{ik\sqrt{\left(nd-h\right)^{2}+\left(z-\ell2/\pi\right)^{2}}}}{\sqrt{\left(nd-h\right)^{2}+\left(z-\ell2/\pi\right)^{2}}}\right]$$

$$\pm\frac{\mu_{0}}{4\pi}hI\left(\ell\right)\frac{i}{\omega\varepsilon\mu_{0}}\frac{\partial}{\partial z}\sum_{\substack{n=-\infty\\n\neq0}}^{\infty}\frac{\left(nd-h/2\right)e^{ik\sqrt{\left(nd-h/2\right)^{2}+\left(z-\ell\right)^{2}}}}{\left(nd-h/2\right)^{2}+\left(z-\ell\right)^{2}}\left[ik-\frac{1}{\sqrt{\left(nd-h/2\right)^{2}+\left(z-\ell\right)^{2}}}\right]$$

or

$$E_z^s\left(0,\pm h/2,\ell 2/\pi\right)=$$

$$\pm\frac{\mu_0}{4\pi}I\left(\ell\right)\ell\frac{2}{\pi}\frac{i}{\omega\varepsilon\mu_0}\sum_{\substack{n=-\infty\\n\neq 0}}^{\infty}\left[\frac{e^{ik|nd|}}{|nd|}\left\{k^2+\frac{ik}{|nd|}-\frac{1}{(nd)^2}\right\}-\frac{e^{ik|nd-h|}}{|nd-h|}\left\{k^2+\frac{ik}{|nd-h|}-\frac{1}{(nd-h)^2}\right\}\right]$$

$$\pm\frac{\mu_0}{4\pi}hI\left(\ell\right)\ell\left(1-2/\pi\right)\frac{i}{\omega\varepsilon\mu_0}\sum_{\substack{n=-\infty\\n\neq 0}}^{\infty}\frac{\left(nd-h/2\right)e^{ik\sqrt{(nd-h/2)^2+\ell^2(1-2/\pi)^2}}}{\left\{\left(nd-h/2\right)^2+\ell^2\left(1-2/\pi\right)^2\right\}^{3/2}}$$

$$\left[k^2+\frac{i3k}{\sqrt{\left(nd-h/2\right)^2+\ell^2\left(1-2/\pi\right)^2}}-\frac{3}{\left(nd-h/2\right)^2+\ell^2\left(1-2/\pi\right)^2}\right]$$

or

$$E_z^s\left(0,\pm h/2,\ell 2/\pi\right)=\pm\frac{\mu_0}{4\pi}I\left(\ell\right)\ell\frac{2}{\pi}\frac{i}{\omega\varepsilon\mu_0}\sum_{n=1}^{\infty}\left[2\frac{e^{iknd}}{nd}\left\{k^2+\frac{ik}{nd}-\frac{1}{(nd)^2}\right\}\right.$$

$$\left.-\frac{e^{ik(nd-h)}}{nd-h}\left\{k^2+\frac{ik}{nd-h}-\frac{1}{(nd-h)^2}\right\}-\frac{e^{ik(nd+h)}}{nd+h}\left\{k^2+\frac{ik}{nd+h}-\frac{1}{(nd+h)^2}\right\}\right]$$

$$\pm\frac{\mu_0}{4\pi}hI\left(\ell\right)\ell\left(1-2/\pi\right)\frac{i}{\omega\varepsilon\mu_0}\sum_{n=1}^{\infty}\frac{\left(nd-h/2\right)e^{ik\sqrt{(nd-h/2)^2+\ell^2(1-2/\pi)^2}}}{\left\{\left(nd-h/2\right)^2+\ell^2\left(1-2/\pi\right)^2\right\}^{3/2}}$$

$$\left[k^2+\frac{i3k}{\sqrt{\left(nd-h/2\right)^2+\ell^2\left(1-2/\pi\right)^2}}-\frac{3}{\left(nd-h/2\right)^2+\ell^2\left(1-2/\pi\right)^2}\right]$$

$$\mp\frac{\mu_0}{4\pi}hI\left(\ell\right)\ell\left(1-2/\pi\right)\frac{i}{\omega\varepsilon\mu_0}\sum_{n=1}^{\infty}\frac{\left(nd+h/2\right)e^{ik\sqrt{(nd+h/2)^2+\ell^2(1-2/\pi)^2}}}{\left\{\left(nd+h/2\right)^2+\ell^2\left(1-2/\pi\right)^2\right\}^{3/2}}$$

$$\left[k^2+\frac{i3k}{\sqrt{\left(nd+h/2\right)^2+\ell^2\left(1-2/\pi\right)^2}}-\frac{3}{\left(nd+h/2\right)^2+\ell^2\left(1-2/\pi\right)^2}\right]$$

and

$$E_y^s\approx-\frac{i}{\omega\varepsilon\mu_0}\frac{\mu_0}{4\pi}hI\left(\ell\right)$$

$$\sum_{\substack{n=-\infty\\n\neq 0}}^{\infty}\frac{e^{ik\sqrt{x^2+(y-nd)^2+(z-\ell)^2}}}{\sqrt{x^2+\left(y-nd\right)^2+\left(z-\ell\right)^2}}\left[k^2-\frac{k^2\left(y-nd\right)^2}{x^2+\left(y-nd\right)^2+\left(z-\ell\right)^2}+\frac{ik}{\sqrt{x^2+\left(y-nd\right)^2+\left(z-\ell\right)^2}}\right.$$

$$-\frac{i2k\left(y-nd\right)^{2}}{\left\{x^{2}+\left(y-nd\right)^{2}+\left(z-\ell\right)^{2}\right\}^{3/2}}$$

$$-\frac{1}{\left\{x^{2}+\left(y-nd\right)^{2}+\left(z-\ell\right)^{2}\right\}}-\frac{ik\left(y-nd\right)^{2}}{\left\{x^{2}+\left(y-nd\right)^{2}+\left(z-\ell\right)^{2}\right\}^{3/2}}+\frac{3\left(y-nd\right)^{2}}{\left\{x^{2}+\left(y-nd\right)^{2}+\left(z-\ell\right)^{2}\right\}^{2}}\Bigg]$$

$$\approx-\frac{i}{\omega\varepsilon\mu_{0}}\frac{\mu_{0}}{4\pi}hI\left(\ell\right)\sum_{\substack{n=-\infty\\n\neq0}}^{\infty}\frac{e^{ik\sqrt{x^{2}+\left(y-nd\right)^{2}+\left(z-\ell\right)^{2}}}}{\sqrt{x^{2}+\left(y-nd\right)^{2}+\left(z-\ell\right)^{2}}}\Bigg[k^{2}-\frac{k^{2}\left(y-nd\right)^{2}+1}{x^{2}+\left(y-nd\right)^{2}+\left(z-\ell\right)^{2}}$$

$$+\frac{ik}{\sqrt{x^{2}+\left(y-nd\right)^{2}+\left(z-\ell\right)^{2}}}$$

$$-\frac{i3k\left(y-nd\right)^{2}}{\left\{x^{2}+\left(y-nd\right)^{2}+\left(z-\ell\right)^{2}\right\}^{3/2}}+\frac{3\left(y-nd\right)^{2}}{\left\{x^{2}+\left(y-nd\right)^{2}+\left(z-\ell\right)^{2}\right\}^{2}}\Bigg]$$

and if we take $r^{2}=x^{2}+\left(z-\ell\right)^{2}$

$$E_{y}^{s}\left(r,0\right)\approx-\frac{i}{\omega\varepsilon\mu_{0}}\frac{\mu_{0}}{4\pi}hI\left(\ell\right)\sum_{\substack{n=-\infty\\n\neq0}}^{\infty}\frac{e^{ik\sqrt{r^{2}+\left(nd\right)^{2}}}}{\sqrt{r^{2}+\left(nd\right)^{2}}}\Bigg[k^{2}-\frac{k^{2}\left(nd\right)^{2}+1}{r^{2}+\left(nd\right)^{2}}+\frac{ik}{\sqrt{r^{2}+\left(nd\right)^{2}}}$$

$$-\frac{i3k\left(nd\right)^{2}}{\left\{r^{2}+\left(nd\right)^{2}\right\}^{3/2}}+\frac{3\left(nd\right)^{2}}{\left\{r^{2}+\left(nd\right)^{2}\right\}^{2}}\Bigg]$$

If we take the limit $kr>>1$ in the brackets we find

$$E_{y}^{s}\left(r,0\right)\sim-\frac{i}{\omega\varepsilon\mu_{0}}\frac{\mu_{0}}{4\pi}k^{2}hI\left(\ell\right)\sum_{\substack{n=-\infty\\n\neq0}}^{\infty}\frac{e^{ik\sqrt{r^{2}+\left(nd\right)^{2}}}}{\sqrt{r^{2}+\left(nd\right)^{2}}}$$

At the current element

$$E_{y}^{s}\left(0,0,\ell\right)\approx\frac{i}{\omega\varepsilon\mu_{0}}\frac{\mu_{0}}{2\pi}hI\left(\ell\right)\sum_{\substack{n=-\infty\\n\neq0}}^{\infty}\frac{e^{ik|nd|}}{\left(nd\right)^{2}}\left(ik-\frac{1}{|nd|}\right)$$

Noting that we have an average vertical current

$$-I\left(\ell\right)h/d$$

we expect to have a propagating mode

$$E_z = \omega\mu_0 I(\ell)\frac{h}{d}\frac{1}{4}H_0^{(1)}(kr)$$

Using the following identities we can add and subtract this in image form

$$-\frac{i}{\pi}\int_{-d/2}^{d/2}\sum_{n=-\infty}^{\infty}\frac{e^{ik\sqrt{r^2+(z-nd)^2}}}{\sqrt{r^2+(z-nd)^2}}dz = -\frac{i}{\pi}\int_{-\infty}^{\infty}\frac{e^{ik\sqrt{r^2+z^2}}}{\sqrt{r^2+z^2}}dz = -i\frac{2}{\pi}\int_0^{\infty}\frac{e^{ik\sqrt{r^2+z^2}}}{\sqrt{r^2+z^2}}dz$$

$$= -i\frac{2}{\pi}\int_0^{\infty}e^{ikr\cosh\zeta}d\zeta = \frac{2}{\pi}\int_0^{\infty}\sin(kr\cosh\zeta)\,d\zeta - i\frac{2}{\pi}\int_0^{\infty}\cos(kr\cosh\zeta)\,d\zeta = J_0(kr)+iY_0(kr) = H_0^{(1)}(kr)$$

and the addition theorem if it is not centered

$$H_0^{(1)}\left(k\sqrt{y^2+(x-x_0)^2}\right) = \sum_{m=0}^{\infty}\varepsilon_m H_m^{(1)}(kr)\,J_m(kx_0)\cos(m\varphi)\ ,\ r=\sqrt{x^2+y^2} > |x_0|$$

We see from the above $kr >> 1$ limit that this Hankel function form is also expected from the average of the image series over the height. Then we have

$$E_y^s \approx -\frac{i}{\omega\varepsilon\mu_0}\frac{\mu_0}{4\pi}hI(\ell)\sum_{\substack{n=-\infty\\ n\neq 0}}^{\infty}\frac{e^{ik\sqrt{x^2+(y-nd)^2+(z-\ell)^2}}}{\sqrt{x^2+(y-nd)^2+(z-\ell)^2}}\left[k^2-\frac{k^2(y-nd)^2+1}{x^2+(y-nd)^2+(z-\ell)^2}\right.$$

$$+\frac{ik}{\sqrt{x^2+(y-nd)^2+(z-\ell)^2}}$$

$$\left.-\frac{i3k(y-nd)^2}{\left\{x^2+(y-nd)^2+(z-\ell)^2\right\}^{3/2}}+\frac{3(y-nd)^2}{\left\{x^2+(y-nd)^2+(z-\ell)^2\right\}^2}\right]$$

$$+\frac{i}{\omega\varepsilon\mu_0}k^2\frac{\mu_0}{4\pi}hI(\ell)\sum_{n=-\infty}^{\infty}\frac{1}{d}\int_{-d/2}^{d/2}\frac{e^{ik\sqrt{x^2+(y-nd)^2+(z-\ell)^2}}}{\sqrt{x^2+(y-nd)^2+(z-\ell)^2}}dz$$

$$+\frac{1}{\omega\varepsilon\mu_0}k^2\frac{\mu_0}{4d}hI(\ell)H_0^{(1)}\left(k\sqrt{x^2+(z-\ell)^2}\right)$$

or

$$H_0^{(1)}\left(k\sqrt{x^2+(z-\ell)^2}\right) = \sum_{m=0}^{\infty}\varepsilon_m H_m^{(1)}(kr)\,J_m(k\ell)\cos(m\varphi)$$

The final modal summation involves propagating terms which interact with the outer disc radius. Note that this addition theorem representation is only valid for $r > \ell$. If a reflection takes place at the outer disc radius, we expect a returning wave so that

$$H_0^{(1)}\left(k\sqrt{x^2+(z-\ell)^2}\right) = \sum_{m=0}^{\infty}\varepsilon_m H_m^{(1)}(kr)\,J_m(k\ell)\cos(m\varphi)$$

$$\rightarrow \sum_{m=0}^{\infty} \varepsilon_m \left[H_m^{(1)}(kr) + R_m J_m(kr) \right] J_m(k\ell) \cos(m\varphi)$$

The impedance boundary condition at the outer edge of the disc cavity gives

$$\cos\alpha = k_\rho / k \sim \sqrt{1 - \left(\frac{m}{kb}\right)^2}$$

$$X = \frac{kd}{2\pi} \cos\alpha$$

$$\Theta/2 = X\left[\ln(2/X) + 1 - \gamma'\right] - \sum_{n=1}^{\infty} \left[\arcsin(X/n) - X/n\right]$$

$$\gamma' = 0.5772$$

$$G'/Y_0 = \frac{\sinh(\pi X)}{\cosh(\pi X) + \cos\Theta} \sim \frac{1}{4} kd\cos\alpha\,,\; X << 1$$

$$B'/Y_0 = \frac{\sin\Theta}{\cosh(\pi X) + \cos\Theta} \sim X\left[\ln(2/X) + 1 - \gamma'\right]\,,\; X << 1$$

where the admittance per unit width in the parallel plate guide is

$$Y_0 = \frac{1}{d}\sqrt{\varepsilon/\mu_0}$$

Setting the admittance per unit width to

$$Y' = G' - iB'$$

the boundary condition to determine the reflection coefficient is

$$Y' dE_z(b,\varphi) = -H_\varphi(b,\varphi)$$

First let us simplify the problem by assuming the vertical leg of the resonator is centered in the disc cavity. Then we can write

$$E_y^s \approx -\frac{i}{\omega\varepsilon\mu_0}\frac{\mu_0}{4\pi} hI(\ell) \sum_{\substack{n=-\infty \\ n\neq 0}}^{\infty} \frac{e^{ik\sqrt{x^2+(y-nd)^2+(z-\ell)^2}}}{\sqrt{x^2+(y-nd)^2+(z-\ell)^2}} \left[k^2 - \frac{k^2(y-nd)^2 + 1}{x^2+(y-nd)^2+(z-\ell)^2} \right.$$

$$\left. + \frac{ik}{\sqrt{x^2+(y-nd)^2+(z-\ell)^2}} \right.$$

$$-\frac{i3k\left(y-nd\right)^{2}}{\left\{x^{2}+\left(y-nd\right)^{2}+\left(z-\ell\right)^{2}\right\}^{3/2}}+\frac{3\left(y-nd\right)^{2}}{\left\{x^{2}+\left(y-nd\right)^{2}+\left(z-\ell\right)^{2}\right\}^{2}}\Bigg]$$

$$+\frac{i}{\omega\varepsilon\mu_{0}}k^{2}\frac{\mu_{0}}{4\pi}hI\left(\ell\right)\sum_{\substack{n=-\infty\\n\neq0}}^{\infty}\frac{1}{d}\int_{-d/2}^{d/2}\frac{e^{ik\sqrt{x^{2}+\left(y-nd\right)^{2}+\left(z-\ell\right)^{2}}}}{\sqrt{x^{2}+\left(y-nd\right)^{2}+\left(z-\ell\right)^{2}}}dz$$

$$+\frac{i}{\omega\varepsilon\mu_{0}}k^{2}\frac{\mu_{0}}{4\pi}hI\left(\ell\right)\frac{1}{d}\int_{-d/2}^{d/2}\frac{e^{ik\sqrt{x^{2}+y^{2}+\left(z-\ell\right)^{2}}}}{\sqrt{x^{2}+y^{2}+\left(z-\ell\right)^{2}}}dz$$

$$+\frac{1}{\omega\varepsilon\mu_{0}}k^{2}\frac{\mu_{0}}{4d}hI\left(\ell\right)\left[H_{0}^{(1)}\left(k\sqrt{x^{2}+\left(z-\ell\right)^{2}}\right)+R_{0}J_{0}\left(k\sqrt{x^{2}+\left(z-\ell\right)^{2}}\right)\right]$$

The impedance boundary condition at the outer edge of the disc cavity then makes use of $\cos\alpha=1$ and field

$$E_{z}=\frac{1}{\omega\varepsilon\mu_{0}}k^{2}\frac{\mu_{0}}{4d}hI\left(\ell\right)\left[H_{0}^{(1)}\left(kr\right)+R_{0}J_{0}\left(kr\right)\right]$$

The boundary condition

$$Y'dE_{z}\left(b\right)=-H_{\varphi}\left(b\right)=\frac{1}{i\omega\mu_{0}}\frac{\partial E_{z}}{\partial\rho}$$

yields

$$i\eta Y'd\left[H_{0}^{(1)}\left(kb\right)+R_{0}J_{0}\left(kb\right)\right]=\left[H_{0}^{(1)\prime}\left(kb\right)+R_{0}J_{0}'\left(kb\right)\right]$$

$$R_{0}=-\frac{H_{0}^{(1)\prime}\left(kb\right)-i\eta Y'dH_{0}^{(1)}\left(kb\right)}{J_{0}'\left(kb\right)-i\eta Y'dJ_{0}\left(kb\right)}$$

The field is

$$E_{y}^{s}\left(0,0,\ell\right)\approx\frac{i}{\omega\varepsilon\mu_{0}}\frac{\mu_{0}}{2\pi}hI\left(\ell\right)\sum_{n=1}^{\infty}2\frac{e^{iknd}}{\left(nd\right)^{2}}\left(ik-\frac{1}{nd}\right)+\frac{i}{\omega\varepsilon\mu_{0}}k^{2}\frac{\mu_{0}}{2\pi}hI\left(\ell\right)\sum_{n=1}^{\infty}e^{iknd}\frac{1}{d}\int_{-d/2}^{d/2}\frac{e^{iky}}{\left(y+nd\right)}dy$$

$$+\frac{i}{\omega\varepsilon\mu_{0}}k^{2}\frac{\mu_{0}}{4\pi}hI\left(\ell\right)\frac{1}{d}\int_{-d/2}^{d/2}\frac{e^{ik\sqrt{r^{2}+y^{2}}}}{\sqrt{r^{2}+y^{2}}}dy$$

$$+\frac{1}{\omega\varepsilon\mu_{0}}k^{2}\frac{\mu_{0}}{4d}hI\left(\ell\right)\left[H_{0}^{(1)}\left(kr\right)+R_{0}J_{0}\left(kr\right)\right]$$

The open circuit voltage induced by this contribution (from the A_y potential to the E_y^s field) is

$$V_{oc}^{d}/I\left(\ell\right)=\frac{i}{\omega\varepsilon}k^{2}\frac{1}{2\pi}h^{2}\sum_{n=1}^{\infty}e^{iknd}\left[\frac{2}{\left(knd\right)^{2}}\left(ik-\frac{1}{nd}\right)+\frac{1}{d}\int_{-d/2}^{d/2}\frac{e^{iky}}{\left(y+nd\right)}dy\right]$$

$$+\frac{1}{\omega\varepsilon}k^{2}\frac{1}{4d}h^{2}\left[H_{0}^{(1)}\left(kr\right)+R_{0}J_{0}\left(kr\right)\right]+\frac{i}{\omega\varepsilon}k^{2}\frac{1}{4\pi}h^{2}\frac{1}{d}2\text{Arcsinh}\left(\frac{d}{2r}\right)+\frac{i}{\omega\varepsilon}k^{2}\frac{1}{4\pi}h^{2}\frac{1}{d}\int_{-d/2}^{d/2}\frac{e^{ik\sqrt{r^{2}+y^{2}}}-1}{\sqrt{r^{2}+y^{2}}}dy$$

$$=\frac{i}{\omega\varepsilon}k^{2}\frac{1}{2\pi}h^{2}\sum_{n=1}^{\infty}e^{iknd}\left[\frac{2}{\left(knd\right)^{2}}\left(ik-\frac{1}{nd}\right)+\frac{1}{d}e^{-iknd}\int_{nd-d/2}^{nd+d/2}\frac{dy}{y}-\frac{1}{d}e^{-iknd}\int_{nd-d/2}^{nd+d/2}\frac{1-e^{iky}}{y}dy\right]$$

$$+\frac{1}{\omega\varepsilon}k^{2}\frac{1}{4d}h^{2}\left[H_{0}^{(1)}\left(kr\right)+R_{0}J_{0}\left(kr\right)\right]+\frac{i}{\omega\varepsilon}k^{2}\frac{1}{4\pi}h^{2}\frac{1}{d}2\ln\left(d/r\right)-\frac{i}{\omega\varepsilon}k^{2}\frac{1}{4\pi}h^{2}\frac{2}{d}\int_{0}^{d/2}\frac{1-e^{iky}}{y}dy$$

$$=\frac{i}{\omega\varepsilon}k^{2}\frac{1}{2\pi}h^{2}\sum_{n=1}^{\infty}e^{iknd}\left[\frac{2}{\left(knd\right)^{2}}\left(ik-\frac{1}{nd}\right)+\frac{1}{d}e^{-iknd}\ln\left(\frac{nd+d/2}{nd-d/2}\right)\right.$$

$$\left.-\frac{1}{d}e^{-iknd}\left\{\text{Cin}\left(nkd+kd/2\right)-\text{Cin}\left(nkd-kd/2\right)\right\}+\frac{1}{d}e^{-iknd}i\left\{\text{Si}\left(nkd+kd/2\right)-\text{Si}\left(nkd-kd/2\right)\right\}\right]$$

$$+\frac{1}{\omega\varepsilon}k^{2}\frac{1}{4d}h^{2}\left[1+i\frac{2}{\pi}\left\{\ln\left(kd/2\right)+\gamma\right\}+R_{0}\right]-\frac{i}{\omega\varepsilon}k^{2}\frac{1}{4\pi}h^{2}\frac{2}{d}\left[\text{Cin}\left(kd/2\right)-i\,\text{Si}\left(kd/2\right)\right]$$

or

$$\left[4d\omega\varepsilon/\left(k^{2}h^{2}\right)\right]V_{oc}^{d}/I\left(\ell\right)=\left(1+R_{0}\right)-i\frac{2}{\pi}\left[\text{Cin}\left(kd/2\right)-i\,\text{Si}\left(kd/2\right)-\ln\left(kd/2\right)-\gamma\right]$$

$$+i\frac{2}{\pi}\sum_{n=1}^{\infty}\left[\frac{e^{iknd}}{n}\frac{2}{\left(knd\right)}\left(i-\frac{1}{knd}\right)+\ln\left(\frac{nd+d/2}{nd-d/2}\right)-\left\{\text{Cin}\left(knd+kd/2\right)-\text{Cin}\left(knd-kd/2\right)\right\}\right.$$

$$\left.+i\left\{\text{Si}\left(knd+kd/2\right)-\text{Si}\left(knd-kd/2\right)\right\}\right]$$

or

$$\left[4d\omega\varepsilon/\left(k^{2}h^{2}\right)\right]V_{oc}^{d}/I\left(\ell\right)=R_{0}+i\frac{2}{\pi}\sum_{n=1}^{\infty}\frac{e^{iknd}}{n}\frac{2}{\left(knd\right)}\left(i-\frac{1}{knd}\right)$$

Another contribution to this is from the A_z potential to the E_y^s field (this could be approximated for small h)

$$E_{y}^{s}\left(0,y,\ell\right)\approx\frac{i}{\omega\varepsilon\mu_{0}}\frac{\mu_{0}}{4\pi}I\left(\ell\right)\ell\frac{2}{\pi}$$

$$\frac{\partial}{\partial y}\sum_{\substack{n=-\infty\\ n\neq 0}}^{\infty}\left[\frac{\ell\left(1-2/\pi\right)e^{ik\sqrt{\left(y-nd-h/2\right)^2+\ell^2\left(1-2/\pi\right)^2}}}{\left\{\left(y-nd-h/2\right)^2+\ell^2\left(1-2/\pi\right)^2\right\}}\left\{ik-\frac{1}{\sqrt{\left(y-nd-h/2\right)^2+\ell^2\left(1-2/\pi\right)^2}}\right\}\right.$$

$$\left.-\frac{\ell\left(1-2/\pi\right)e^{ik\sqrt{\left(y-nd+h/2\right)^2+\ell^2\left(1-2/\pi\right)^2}}}{\left\{\left(y-nd+h/2\right)^2+\ell^2\left(1-2/\pi\right)^2\right\}}\left\{ik-\frac{1}{\sqrt{\left(y-nd+h/2\right)^2+\ell^2\left(1-2/\pi\right)^2}}\right\}\right]$$

$$E_y^s\left(0,0,\ell\right)\approx\frac{i}{\omega\varepsilon\mu_0}\frac{\mu_0}{2\pi}I\left(\ell\right)\ell\frac{2}{\pi}\sum_{n=1}^{\infty}\left[\frac{\ell\left(1-2/\pi\right)\left(nd+h/2\right)e^{ik\sqrt{\left(nd+h/2\right)^2+\ell^2\left(1-2/\pi\right)^2}}}{\left\{\left(nd+h/2\right)^2+\ell^2\left(1-2/\pi\right)^2\right\}^{3/2}}\right.$$

$$\left\{k^2+\frac{i3k}{\sqrt{\left(nd+h/2\right)^2+\ell^2\left(1-2/\pi\right)^2}}-\frac{3}{\left(nd+h/2\right)^2+\ell^2\left(1-2/\pi\right)^2}\right\}$$

$$-\frac{\ell\left(1-2/\pi\right)\left(nd-h/2\right)e^{ik\sqrt{\left(nd-h/2\right)^2+\ell^2\left(1-2/\pi\right)^2}}}{\left\{\left(nd-h/2\right)^2+\ell^2\left(1-2/\pi\right)^2\right\}^{3/2}}$$

$$\left.\left\{k^2+\frac{i3k}{\sqrt{\left(nd-h/2\right)^2+\ell^2\left(1-2/\pi\right)^2}}-\frac{3}{\left(nd-h/2\right)^2+\ell^2\left(1-2/\pi\right)^2}\right\}\right]$$

or

$$i2\pi\omega\varepsilon V_{oc}^s/I\left(\ell\right)=$$

$$-h\left(\ell\frac{2}{\pi}\right)\ell\left(1-2/\pi\right)\sum_{n=1}^{\infty}\left[\frac{\left(nd+h/2\right)e^{ik\sqrt{\left(nd+h/2\right)^2+\ell^2\left(1-2/\pi\right)^2}}}{\left\{\left(nd+h/2\right)^2+\ell^2\left(1-2/\pi\right)^2\right\}^{3/2}}\right.$$

$$\left\{k^2+\frac{i3k}{\sqrt{\left(nd+h/2\right)^2+\ell^2\left(1-2/\pi\right)^2}}-\frac{3}{\left(nd+h/2\right)^2+\ell^2\left(1-2/\pi\right)^2}\right\}$$

$$\left.-\frac{\left(nd-h/2\right)e^{ik\sqrt{\left(nd-h/2\right)^2+\ell^2\left(1-2/\pi\right)^2}}}{\left\{\left(nd-h/2\right)^2+\ell^2\left(1-2/\pi\right)^2\right\}^{3/2}}\left\{k^2+\frac{i3k}{\sqrt{\left(nd-h/2\right)^2+\ell^2\left(1-2/\pi\right)^2}}-\frac{3}{\left(nd-h/2\right)^2+\ell^2\left(1-2/\pi\right)^2}\right\}\right]$$

The other piece is (this could be approximated for small h) the contribution from the E_z^s field

$$i2\pi\omega\varepsilon\,\Delta V_{oc}^s/I\left(\ell\right)=\left(\ell\frac{2}{\pi}\right)^2\sum_{n=1}^{\infty}\left[2\frac{e^{iknd}}{nd}\left\{k^2+\frac{ik}{nd}-\frac{1}{\left(nd\right)^2}\right\}\right.$$

$$-\frac{e^{ik(nd-h)}}{nd-h}\left\{k^2+\frac{ik}{nd-h}-\frac{1}{(nd-h)^2}\right\}-\frac{e^{ik(nd+h)}}{nd+h}\left\{k^2+\frac{ik}{nd+h}-\frac{1}{(nd+h)^2}\right\}\Bigg]$$

$$+h\ell\,(1-2/\pi)\,\ell\frac{2}{\pi}\sum_{n=1}^{\infty}\frac{(nd-h/2)\,e^{ik\sqrt{(nd-h/2)^2+\ell^2(1-2/\pi)^2}}}{\left\{(nd-h/2)^2+\ell^2\,(1-2/\pi)^2\right\}^{3/2}}$$

$$\left[k^2+\frac{i3k}{\sqrt{(nd-h/2)^2+\ell^2\,(1-2/\pi)^2}}-\frac{3}{(nd-h/2)^2+\ell^2\,(1-2/\pi)^2}\right]$$

$$-h\ell\,(1-2/\pi)\,\ell\frac{2}{\pi}\sum_{n=1}^{\infty}\frac{(nd+h/2)\,e^{ik\sqrt{(nd+h/2)^2+\ell^2(1-2/\pi)^2}}}{\left\{(nd+h/2)^2+\ell^2\,(1-2/\pi)^2\right\}^{3/2}}$$

$$\left[k^2+\frac{i3k}{\sqrt{(nd+h/2)^2+\ell^2\,(1-2/\pi)^2}}-\frac{3}{(nd+h/2)^2+\ell^2\,(1-2/\pi)^2}\right]$$

Figure 28 shows the reflected impedance at the resonator drive point as in the previous orientation. Notice that the radiative load at the outer disc edge results in a reflected impedance which is negative over most of the range shown but is smaller in magnitude than the free space value (near +2 ohms). Thus there is net radiation and the influence on the resonator quality factor is not as large. However since it is varying in frequency, the effect of the disc cavity must be taken into account to establish the rigorous quality factor for the resonator.

As checks on the calculation the next two figures consider some modifications of the outer edge load. First we set the conductance G' to zero and find that the reflected impedance has a real part that cancels (to the level of approximation present) the free space real impedance of the resonator (with perfectly conducting wires). This makes sense since we have then eliminated radiative damping.

Finally we set the outer edge reflection coefficient to zero and observe that the reflected real part is now positive. This means that radiative damping is enhanced by the presence of the disc cavity. The direction of the change in real part seems reasonable because the resonator is electrically small and the close conducting walls would be expected to act as extensions of the radiating arms of the resonator, enhancing radiation.

13 CONCLUSIONS

This report constructs circuit models for a hairpin resonator probe used for detecting plasma properties such as plasma frequency (proportional to electron number density) and electron collision frequency. A transmission line model is used along the resonator length and lumped loads are used to capture the parasitic capacitance at the open end and the parasitic inductance at the drive or shorted end along with a lumped radiation resistance. The impact of a plasma sheath surrounding the resonator wires as well as the finite conductivity of the wires are addressed. Electromagnetic simulations using a frequency domain method of moments code are also included as comparisons to the circuit model results. The effects of nonsymmetric fields around the wires and the sheath due to interactions between the resonator arms are shown to be small by a multipole technique. Inhomogeneities in plasma density along the resonator length are examined briefly. Finally, the impact of the polysilicon disc cavity, which contains the resonator, is

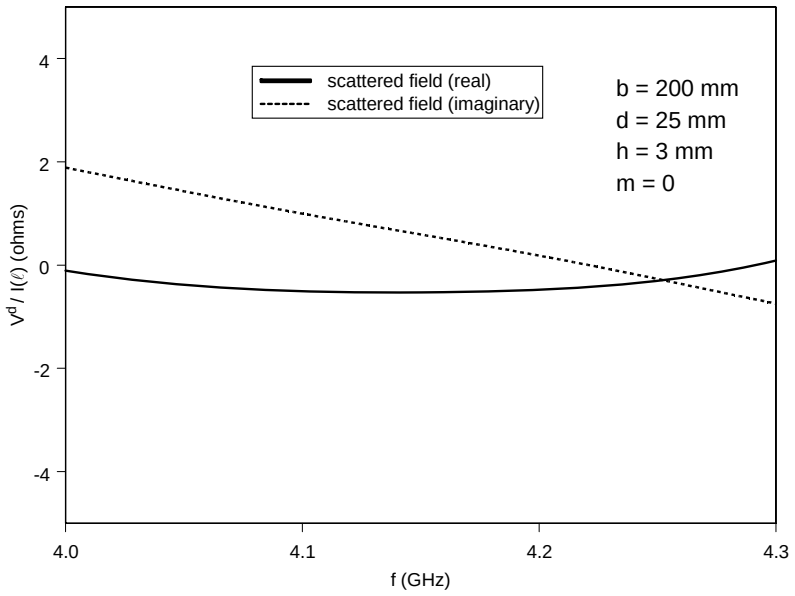

Figure 27. Real and imaginary parts of the scattered voltage at the drive point of the resonator (resulting from the image currents in the resonator walls) divided by the drive current. This is the vertical orientation where the resonator does couple into the propagating disc modes of the cavity. The propagating disc modes are reflected from open edges at the outer radius of the disc cavity. Although the real part of the scattered voltage is slightly negative over part of the range, the suppression of resonator radiation by the perfectly conducting cavity walls is not as signficant in this vertical orientation due to the radiation of the propagating disc modes at the outer cavity radius.

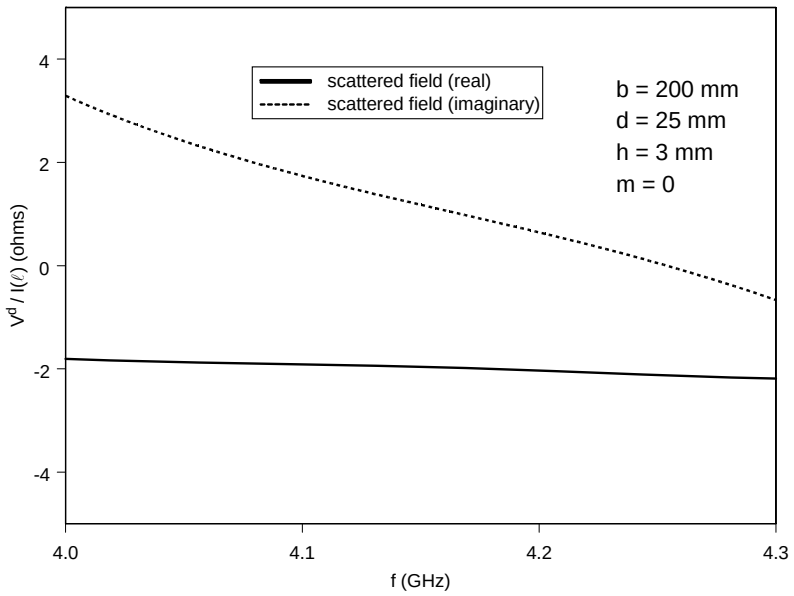

Figure 28. Real and imaginary parts of the scattered voltage at the drive point of the resonator (resulting from the image currents in the resonator walls) divided by the drive current. This is the vertical orientation where the resonator does couple into the propagating disc modes of the cavity. However in this plot the propagating disc modes are reflected from a short circuit at the outer radius of the disc cavity. The real part of the scattered voltage thus becomes negative similar to the horizontal orientation. The resonator quality factor will then be increased due to the suppression of resonator radiation by the perfectly conducting cavity walls similar to the horizontal resonator orientation.

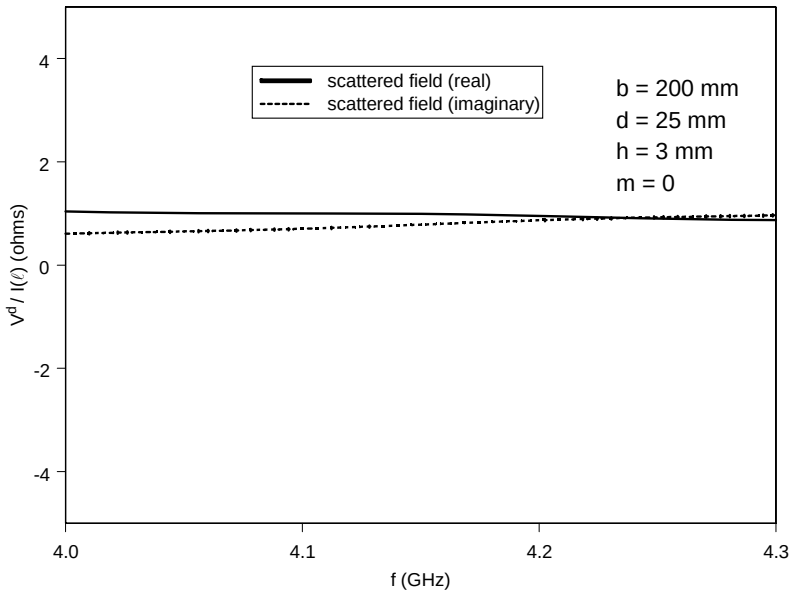

Figure 29. Real and imaginary parts of the scattered voltage at the drive point of the resonator (resulting from the image currents in the resonator walls) divided by the drive current. This is the vertical orientation where the resonator does couple into the propagating disc modes of the cavity. However in this plot the propagating disc modes are absorbed without reflection at the outer radius of the disc cavity. The real part of the scattered voltage then becomes positive, indicating that there is enhanced radiation damping relative to the case where the resonator is in free space. The cavity disc walls effectively help match the radiation properties of the resonator, leading to increased radiation damping and a reduced quality factor.

ascertained. The quality factor of the cavity is estimated using the properties of polysilicon as well as known approximations for the load admittance at the outer periphery of the disc. The resonator is operated at frequencies for which the only propagating modes in the disc cavity have a vertical electric field that is independent of vertical position. When the hairpin resonator is oriented with all wires parallel to the disc walls it does not couple effectively into these modes. However the presence of the disc cavity thereby suppresses radiation damping of the hairpin and increases its quality factor. When the hairpin resonator is oriented vertically it does couple into the propagating disc modes and the radiation characteristics are modified somewhat (but are not eliminated) by the disc resonances. Interestingly, if the disc edge were well matched to these modes, the radiation damping would actually be increased somewhat.

14 REFERENCES

[1] S. Ramo, J. R. Whinnery, and T. Van Duzer, **Fields and Waves in Communication Electronics**, New York: John Wiley & Sons, Inc., 1965, Ch. 1, Table 8.09.

[2] C. H. Papas, **Theory of Electromagnetic Wave Propagation**, New York: McGraw-Hill, 1965, p. 177.

[3] F. W. Grover, **Inductance Calculations**, New York: Dover Pub., Inc., 1946, p. 60.

[4] S. A. Schelkunoff, **Advanced Antenna Theory**, New York: John Wiley & Sons, Inc., 1952, pp. 142-143.

[5] E. C. Jordan and K. G. Balmain, **Electromagnetic Waves and Radiating Systems**, Englewood Cliffs, NJ: Prentice-Hall, Inc., 1968, Chapter 10, p. 485.

[6] G. W. C. Kaye and T. H. Laby, **Tables of Physical and Chemical Constants**, Essex: Longman Scientific & Technical, 1986, p. 118.

[7] R. M. Bozorth, **Ferromagnetism**, New York: IEEE Press, 1993, p. 800.

[8] L. K. Warne and K. C. Chen, "Long Line Coupling Models," SAND2004-0872, March 2004.

[9] M. Abramowitz and I. A. Stegun (editors), **Handbook of Mathematical Functions**, New York: Dover Pub., 1972, Inc., pp. 361, 485.

[10] A. P. Prudnikov, Yu. A. Brychkov, O. I. Marichev, **Integrals and Series Volume 2: Special Functions**, Amsterdam, The Netherlands: Gordon and Breach Science Pub., 1998, p. 41.

[11] N. Marcuvitz, **Waveguide Handbook**, London, UK: Peter Peregrinus, Ltd., 1986, pp. 179-181.

Distribution

25	MS1423	G. A. Hebner, 01128
1	MS1423	E. V. Barnat, 01128
1	MS1423	P. A. Miller, 01128
1	MS0492	K. C. Chen, 12332
1	MS1152	R. S. Coats, 01652
2	MS1152	W. A. Johnson, 01652
1	MS1152	R. E. Jorgenson, 01652
1	MS1152	M. L. Kiefer, 01652
1	MS1152	M. E. Morris, 01652
5	MS1152	L. K. Warne, 01652
2	MS9018	Central Technical Files, 8944
2	MS0899	Technical Library, 04536